CRCLEME
Cooperative Research Centre for
Landscape Evolution & Mineral Exploration

CSIRO
EXPLORATION
AND MINING

AMIRA
Australian Mineral Industries Research Association Limited ACN 004 448 266

OPEN FILE
REPORT
SERIES

HYDROGEOCHEMISTRY IN THE MOUNT GIBSON GOLD DISTRICT

D.J. Gray

CRC LEME OPEN FILE REPORT 21

October 1998

(CSIRO Division of Exploration Geoscience Report 120R, 1991.
Second impression 1998)

AMIRA
Australian Mineral Industries Research Association Limited ACN 004 448 266

CRCLEME
Cooperative Research Centre for Landscape Evolution & Mineral Exploration

CSIRO
EXPLORATION AND MINING

HYDROGEOCHEMISTRY IN THE MOUNT GIBSON GOLD DISTRICT

D.J. Gray

CRC LEME OPEN FILE REPORT 21

October 1998

(CSIRO Division of Exploration Geoscience Report 120R, 1991.
Second impression 1998)

CRC LEME is an unincorporated joint venture between The Australian National University, University of Canberra, Australian Geological Survey Organisation and CSIRO Exploration and Mining
Headquarters: CRC LEME c/o CSIRO Exploration and Mining, Private Bag, PO Wembley, Western Australia, 6014

RESEARCH ARISING FROM CSIRO/AMIRA REGOLITH GEOCHEMISTRY PROJECTS 1987-1993

In 1987, CSIRO commenced a series of multi-client research projects in regolith geology and geochemistry which were sponsored by companies in the Australian mining industry, through the Australian Mineral Industries Research Association Limited (AMIRA). The initial research program, "Exploration for concealed gold deposits, Yilgarn Block, Western Australia" (1987-1993) had the aim of developing improved geological, geochemical and geophysical methods for mineral exploration that would facilitate the location of blind, buried or deeply weathered gold deposits. The program included the following projects:

P240: Laterite geochemistry for detecting concealed mineral deposits (1987-1991). Leader: Dr R.E. Smith.
Its scope was development of methods for sampling and interpretation of multi-element laterite geochemistry data and application of multi-element techniques to gold and polymetallic mineral exploration in weathered terrain. The project emphasised viewing laterite geochemical dispersion patterns in their regolith-landform context at local and district scales. It was supported by 30 companies.

P241: Gold and associated elements in the regolith - dispersion processes and implications for exploration (1987-1991). Leader: Dr C.R.M. Butt.
The project investigated the distribution of ore and indicator elements in the regolith. It included studies of the mineralogical and geochemical characteristics of weathered ore deposits and wall rocks, and the chemical controls on element dispersion and concentration during regolith evolution. This was to increase the effectiveness of geochemical exploration in weathered terrain through improved understanding of weathering processes. It was supported by 26 companies.

These projects represented "an opportunity for the mineral industry to participate in a multi-disciplinary program of geoscience research aimed at developing new geological, geochemical and geophysical methods for exploration in deeply weathered Archaean terrains". This initiative recognised the unique opportunities, created by exploration and open-cut mining, to conduct detailed studies of the weathered zone, with particular emphasis on the near-surface expression of gold mineralisation. The skills of existing and specially recruited research staff from the Floreat Park and North Ryde laboratories (of the then Divisions of Minerals and Geochemistry, and Mineral Physics and Mineralogy, subsequently Exploration Geoscience and later Exploration and Mining) were integrated to form a task force with expertise in geology, mineralogy, geochemistry and geophysics. Several staff participated in more than one project. Following completion of the original projects, two continuation projects were developed.

P240A: Geochemical exploration in complex lateritic environments of the Yilgarn Craton, Western Australia (1991-1993). Leaders: Drs R.E. Smith and R.R. Anand.
The approach of viewing geochemical dispersion within a well-controlled and well-understood regolith-landform and bedrock framework at detailed and district scales continued. In this extension, focus was particularly on areas of transported cover and on more complex lateritic environments typified by the Kalgoorlie regional study. This was supported by 17 companies.

P241A: Gold and associated elements in the regolith - dispersion processes and implications for exploration. Leader: Dr. C.R.M. Butt.
The significance of gold mobilisation under present-day conditions, particularly the important relationship with pedogenic carbonate, was investigated further. In addition, attention was focussed on the recognition of primary lithologies from their weathered equivalents. This project was supported by 14 companies.

Although the confidentiality periods of the research reports have expired, the last in December 1994, they have not been made public until now. Publishing the reports through the CRC LEME Report Series is seen as an appropriate means of doing this. By making available the results of the research and the authors' interpretations, it is hoped that the reports will provide source data for future research and be useful for teaching. CRC LEME acknowledges the Australian Mineral Industries Research Association and CSIRO Division of Exploration and Mining for authorisation to publish these reports. It is intended that publication of the reports will be a substantial additional factor in transferring technology to aid the Australian Mineral Industry.

This report (CRC LEME Open File Report 21) is a Second impression (second printing) of CSIRO, Division of Exploration Geoscience Restricted Report 120R, first issued in 1991, which formed part of the CSIRO/AMIRA Project P240.

Copies of this publication can be obtained from:
The Publication Officer, c/- CRC LEME, CSIRO Exploration and Mining, PMB, Wembley, WA 6014, Australia. Information on other publications in this series may be obtained from the above or from http://leme.anu.edu.au/

Cataloguing-in-Publication:
Gray, D.J.
Hydrogeochemistry in the Mt. Gibson Gold District
ISBN 0 642 28249 8
1. Geochemistry 2. Gold - Western Australia.
I. Title
CRC LEME Open File Report 21.
ISSN 1329-4768

ABSTRACT

Research was conducted into the hydrogeochemistry of groundwaters within the Mt. Gibson mine area and in the surrounding district. This work involved determination of field parameters such as pH and Eh, laboratory analysis of water samples for major and trace elements, isotope determinations (D and O^{18}), computer speciation of analytical data, and statistical analysis of the water data.

The groundwater system is dominated by a northward saline drainage system. Groundwater flow along this drainage appears to be restrained by an underground sill about 7 km north of the mine area, resulting in highly saline groundwaters within the mine region. This saline groundwater appears to flow back, south into the mine area, at depth. Thus, the north section of the mine area has fresher waters (about 3% TDS) overlying hypersaline water (> 13% TDS).

Based on the major element and isotope analyses, the mine groundwaters were resolved into a number of hydrogeochemically distinct water masses. In particular, the waters from drill hole sample sites 600 m west of the major area of supergene Au mineralization at Midway were identified as probably originating from contact with granitic rocks. The other mine groundwaters appear to be associated with mafic or ultramafic systems.

Waters within the Midway area showed highly anomalous characteristics, being high in dissolved Au, Fe, Mn, Co, Cd, Ba and I, and having low HCO_3 concentrations. These observations are explained as being due to weathering of sulphide minerals. Downgradient of the Midway area, the groundwater becomes acidic, due to oxidation/hydrolysis of the dissolved Fe. This has led to major dissolution of many metals, particularly (in order from least to most enriched) Cd, Co, Ni, Zn, Cu, Cr, Al and Ag. This enrichment is related to the base affinity of the metals.

Soluble Au was only observed above the detection limit (0.05 μg/L) within the mineralized area. Two major anomalies were recognized: the first, within the Midway area, may represent dissolution of Au by thiosulphate; while a second, more localized anomaly, within the N2 pit area may represent dissolution by chloride.

On the basis of this work, soluble Au analyses could be used at this site to indicate areas of Au mineralization at both a district and a mine scale. Thus, measurements of dissolved Au may represent a useful adjunct to drilling during Au exploration, particularly with respect to buried mineralization.

TABLE OF CONTENTS

LIST OF FIGURES

LIST OF TABLES

1.0 PROJECT LEADER'S PREFACE

R.E. Smith, 6 March, 1991

The area containing the Mt. Gibson Au deposits and the surrounding district was chosen to be the focus of a substantial multidisciplinary orientation study, one of the four which form the foundations of the CSIRO/AMIRA Laterite Geochemistry Project. The other locations are Boddington, Bottle Creek and Lawlers. In each case geochemical dispersion arising from concealed Au deposits is studied by establishing an understanding of the regolith/landform and bedrock relationships not only of the immediate ore environments but also of the district within which the deposits lie.

The Mount Gibson district characterizes the complex lateritic sand plain terrain of the Perenjori/Ningham region where an essentially complete undulating lateritic peneplain, though extensively preserved, is undergoing dismantling by erosion. Burial of complete and partly truncated laterite profiles, by erosional detritus, has taken place on many of the slopes and in the low lying areas. These are important dynamic processes which are continuing.

As the mineralized regolith and bedrock units of the Mount Gibson Au district strike northwards, they pass from a near-ridge crest setting, through mid-slope, lower-slope and trend into a drainage sump. These changing settings, coupled with extensive exploration drilling, provides the opportunity for systematic study of changing environments: upland, well-drained, with relatively fresh groundwater at depth and infiltration by rainwater at one extreme to low-lying areas immersed in highly saline groundwaters at the other.

The Mt. Gibson research is being presented in several parts. The regolith relationships in the environs of the S, C and N lateritic ore pits were the topic of Report 20R (Anand *et al.*, 1989). That report also presented the geochemical dispersion haloes within the loose pisolitic and nodular lateritic gravels. The present report is a study of the main groundwater regimes from the various geomorphic environments, mentioned above, which are relevant to dispersion from ore systems in the bedrock sequence, formation of lateritic and saprolitic Au deposits, and the robustness or otherwise (with regard to leaching) of the multi-element geochemical target "signal" in the lateritic units. The report draws from the setting described in Report 20R and also uses knowledge arising from the project's regolith/landform study of the Mount Gibson district that is still underway.

2.0 OBJECTIVES AND SCOPE

This report presents the results of groundwater research conducted in the region of the Mt. Gibson Au mining deposit. The research is part of a CSIRO/AMIRA multi-disciplinary, regolith-based orientation study of geochemical dispersion about the Mt. Gibson Au deposits (Anand *et al.*, 1989) conducted within the Laterite Geochemistry Project. This report relates effects on the groundwater chemistry from the underlying geology, hydrology and regolith run-off and infiltration.

The objectives of the groundwater-hydrogeochemical study are as follows:

(i) To establish the groundwater levels in a network of drill holes, enabling flow paths for groundwaters in areas of interest to be generally established.

(ii) Investigate the gross characteristics of groundwaters in and about the geochemical dispersion halo in laterite and about the associated ore environments,following the flow path from uplands, to mid slope, lower slope and saline sump regimes.

(iii) Inquire into the role of Fe-cycling and ferrolysis in the regolith situations at Mt. Gibson and in the formation of the geochemical haloes. The role of Mn will also be considered because of its possible role in Au chloride mobility.

(iv) Based upon the observed relationship at Mt. Gibson between sources, transportation and deposition of carbonates, inquire into the role of carbonate in the geochemistry of Au in the regolith environments.

(v) Determine the groundwater concentration of Au and of other chalcophile elements. Additionally, the concentration of potentially important ligands (Cl^-, OH^-, I^-, and $S_2O_3^{2-}$) will be determined and the importance of the potential complexes of Au and other elements estimated.

(vi) Investigate the impact of differing groundwater regimes on the multi-element characteristics of the dispersion haloes.

(vii) Consider to what degree we can understand the past groundwater regimes at Mt. Gibson from our knowledge of today's conditions.

Additionally, this groundwater survey will ultimately be compared with other groundwater investigations conducted at a number of sites in the Yilgarn Block of Western Australia. A compilation of data for mineralized and unmineralized regions should significantly advance our knowledge of groundwater characteristics - particularly in reference to the formation of geochemical haloes in weathered zones and the use of groundwaters in exploration.

3.0 METHODOLOGY

3.1 Site Characteristics

The Mt. Gibson Gold Project, a joint venture between Forsayth (Gibson) Ltd and Reynolds Australia Mines Pty Ltd, is located (117°45'E 29°45'S) some 300 km northeast of Perth and some 200 km from the west coast (Fig. 1). The mine site is 100 km NE along the Great Northern Highway from Dalwallinu and then 10 km east via a formed gravel road. Maps of the general region and the mine area are shown in Figs. 2 and 3.

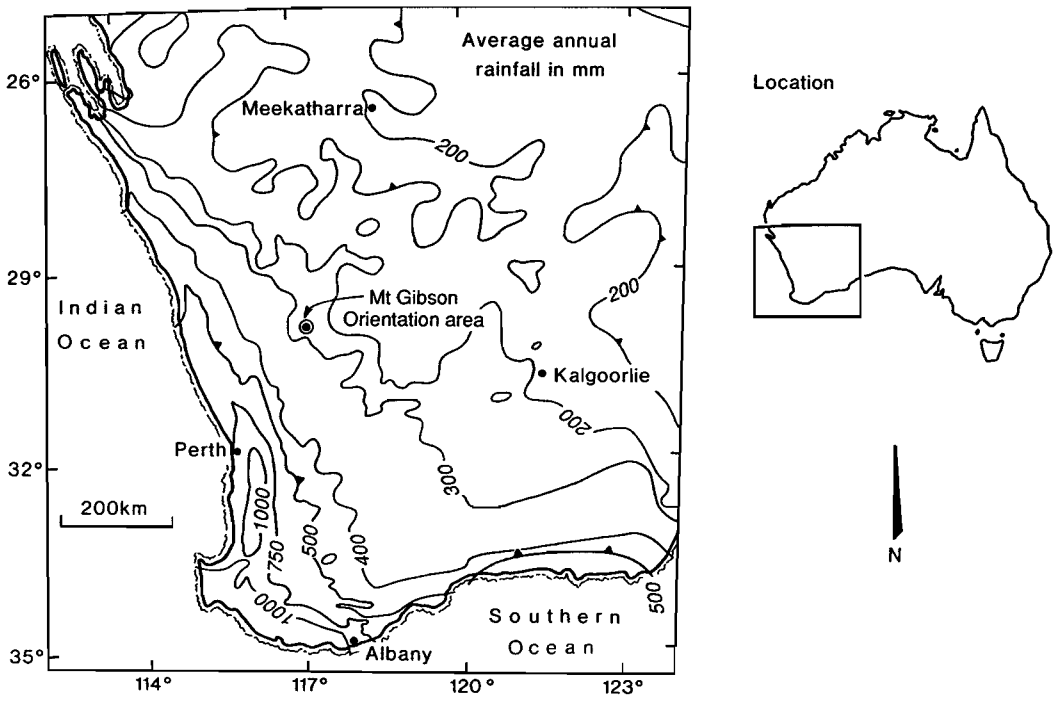

Figure 1. Area of study, with rainfall contours shown.

The area has a semi-arid to arid hot Mediterranean climate with a 250 mm average annual rainfall, most of which falls during the cooler months of May to August. However, there is a significant component of summer rainfall from erratic thunderstorms.

Deep lateritic weathering profiles are widespread in the region and there has been partial differential stripping. Outcrop of bedrock is only sporadic and detritus derived from partial erosion of the lateritic mantle is widely distributed. Reconnaissance scale (1:250,000) mapping of the Ninghan sheet by Lipple *et al.* (1983) indicates a great extent of yellow sand-plain with some lateritic gravel units. Alluvial and colluvial deposits are common in gentle sloping valleys of active or infilled drainage channels. Calcrete is common in the lower reaches of the drainage basins (particularly in the courses of paleodrainages). Many of these general features occur in the environs of the Mt. Gibson study area.

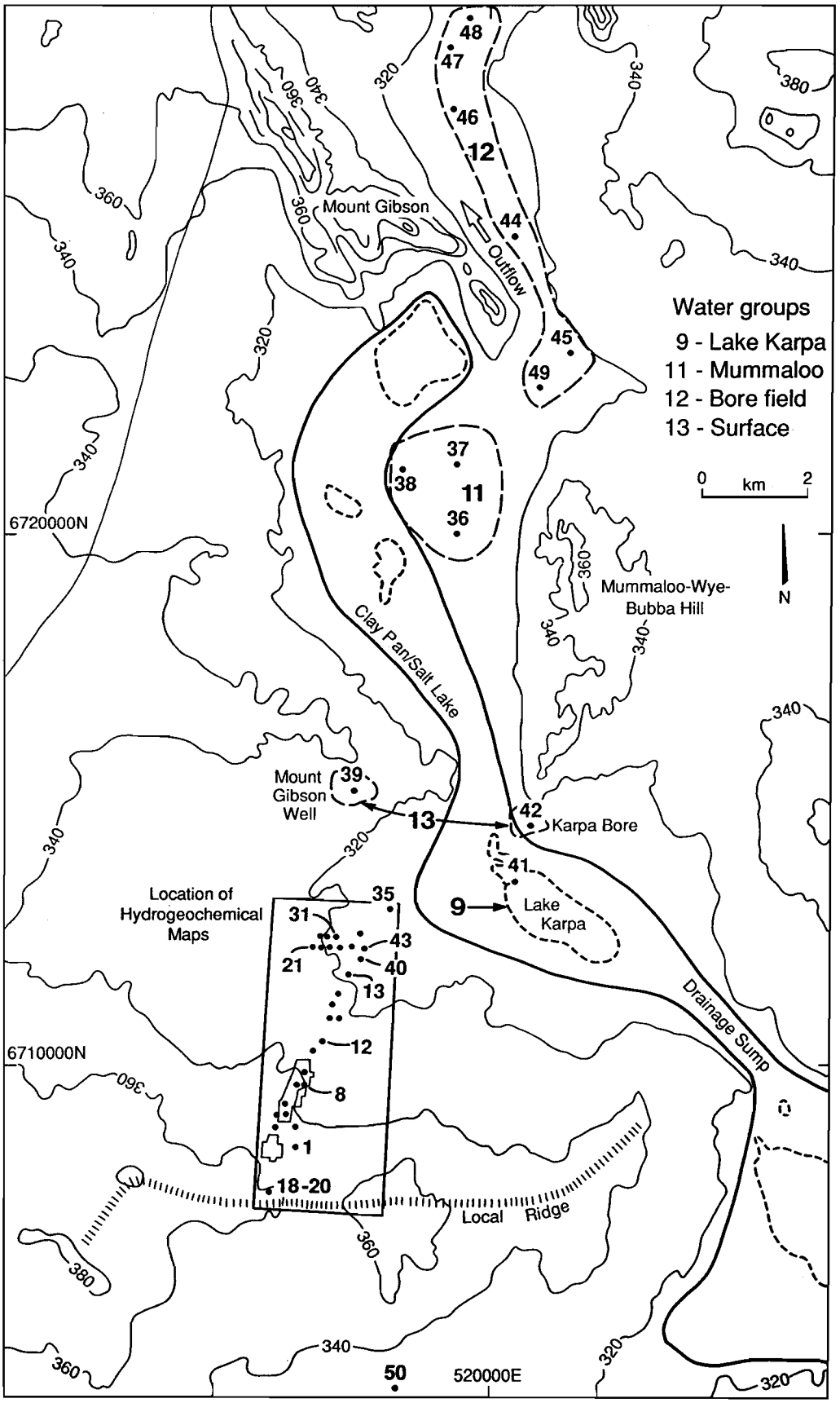

Figure 2. Topographical Map of the Mount Gibson Gold District, with Bore Hole Locations and Water Groups indicated.

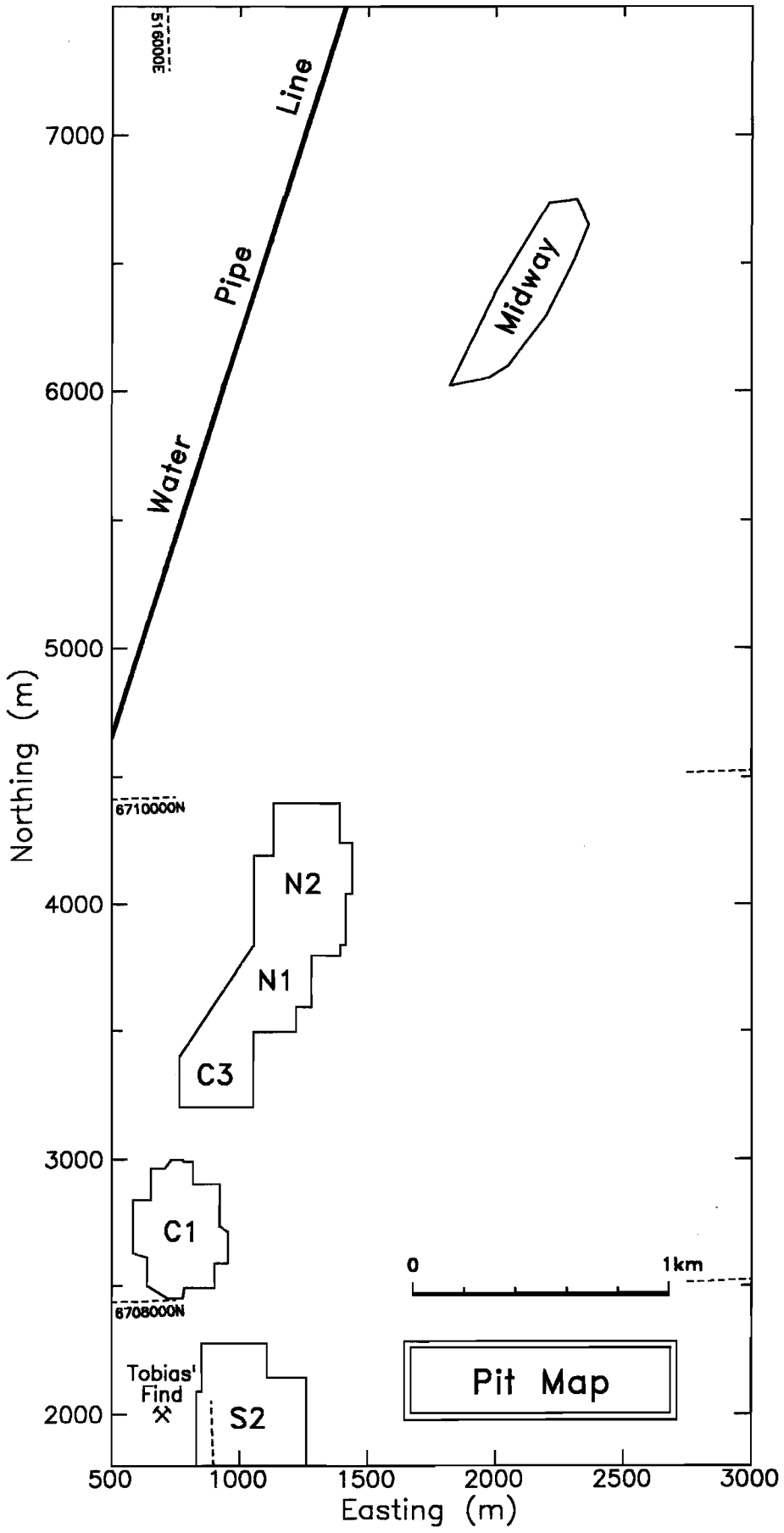

Figure 3. Map of the Mt. Gibson Au Mine Area Investigated in this Report.

Topographic and drainage details for the Mt. Gibson Mine area are shown in Fig. 4. The area lies at an elevation of 320 to 360 m above mean sea level on a broad divide between the extensive valley playas of Lakes Moore and Monger, both of which occur at levels of about 300 m. Much of the skyline has broadly convex local divides at 340 to 360 m, flanked by long gentle slopes which grade at 1 in 50 (2%) on the upper slopes to 1 in 200 overall (0.5%), leading to the local Lake Karpa drainage sump at 310 m (Fig. 2). Emergent above the general plateau skyline are a few prominent crests and monadnocks flanked by steep irregular slopes. The most prominent are Mount Gibson (the topographic feature, 480 m high, lying 18 km to the north and quite distinct from the Mt. Gibson Gold Project mining areas [1]) and Mt. Singleton (620 m), which are related to some of the more resistant geological strata of the supracrustal fold belts.

The current pits at the Mt. Gibson Mine, termed S1, S2, C1, C2, C3, N1, N2 and Midway, in sequence from south to north (Fig. 3), are arrayed along the upper flanks of a local ridge trending just east of north. Slight variations in this trend are associated with the heads of minor tributary valleys such as those between the S2 and C1 mine pits and between the C1 and C3 pits. Broad shallow elongate depressions occur on the ridge crests just west of the S2, N1, and N2 main pits.

The geological setting of the region is discussed in Anand *et al.* (1989). The primary Au mineralization appears to be developed in quartz veins along shears in a 400 to 500 m thick sequence of very poorly exposed interlayered volcaniclastic and epiclastic metasediments, felsic and mafic volcanic rocks, cherts and "quartz-eye" porphyries, and in the massive to weakly foliated amphibolite forming the structural footwall. The enclosing granitoids are gneissic to pegmatoidal in character and outcrop to the east, south, and west of the mine site. Amphibolites are exposed as rubble on upland areas to the west (Tobias' Find and west of N1 pit) and to the east of the mine site.

The supracrustal sequence and the granitoids are intruded by ENE-trending dolerite dykes.

Mining of lateritic Au commenced at Mt. Gibson in November 1986, resulting in production of 2300 kg of Au to November 1987. The pits are located in Fig. 3. The nature of the laterite and regolith material, and the geochemical associations, are discussed in detail in Anand *et al.* (1989).

At the Midway Pit (Hornet zone), 4.5 km north of the Mt. Gibson Mine plant, an *in situ* geological resource of 1.5 Mt @ 6.0 g/t Au, associated with Pb-Zn-Ag-Bi mineralization, has been reported from a plunging sequence of altered and sheared felsic and mafic volcanics with amphibolite (metabasalt) in the structural hangingwall and footwall of the orebodies (*Gold Gazette*, 1988). The geological setting appears similar to that hosting the auriferous quartz veins at the Mt. Gibson S, C, and N pit areas. Similar prospective volcanogenic/precious metal mineralization has been recognized in felsic volcanics in the Narndee complex (Marston, 1979).

---

[1] To avoid confusion the two features will be denoted in the text as:

(i) The topographic Mount Gibson;
(ii) Mt. Gibson, or the Mt. Gibson mine area.

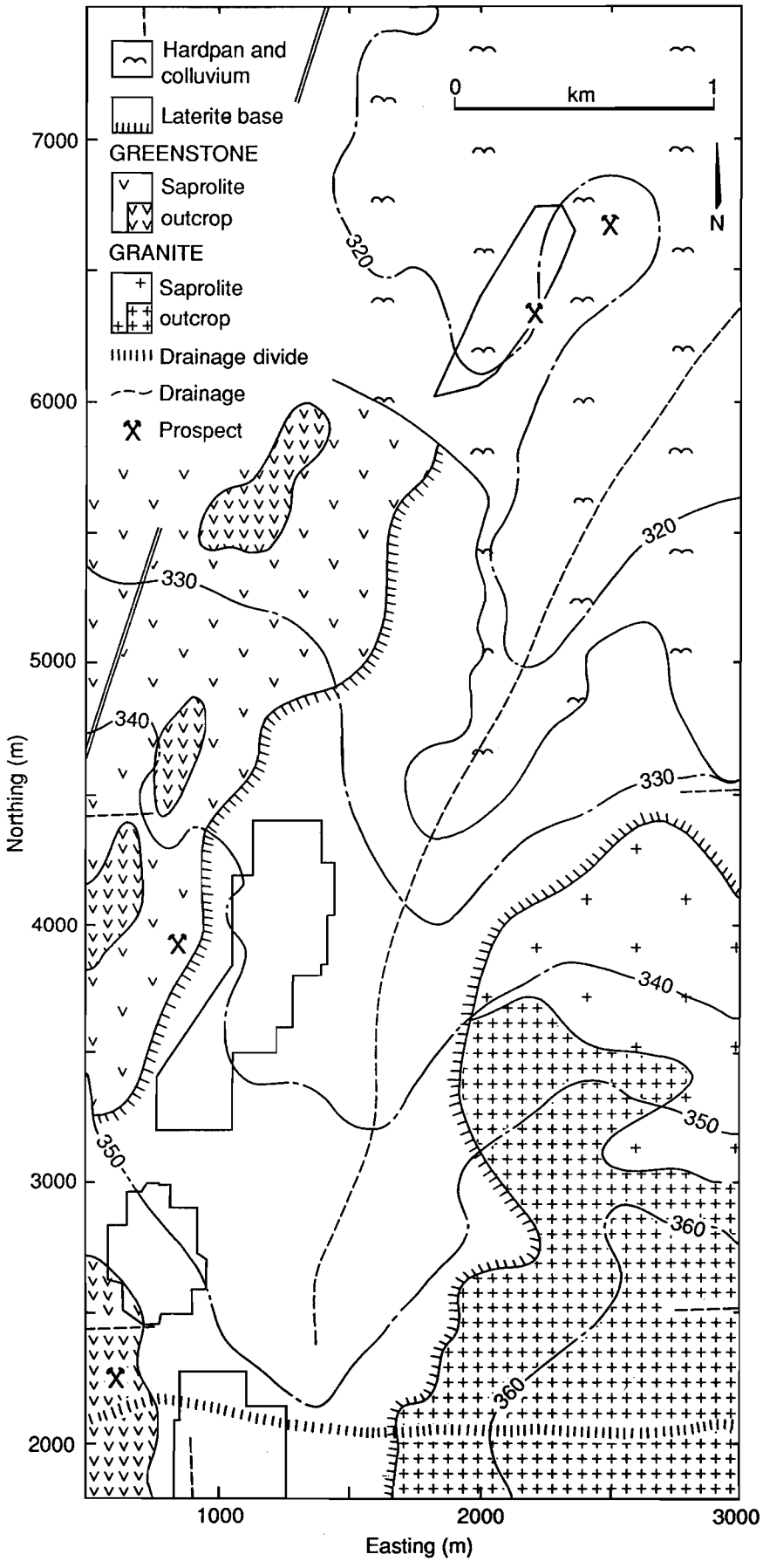

Figure 4. Topography, Drainage and Surficial Geology of the Mt. Gibson Au Mine Area.

3.2 Water Sampling

Sampling was done on established holes using a specially designed baler. Holes sampled are indicated in Figs. 2 and 5 and listed in Table 1.

In general, the sampling numbers will be used rather than the hole name, which can be determined from Table 1. Environments sampled are considered to lie in 13 Groups, as described in Table 2. While the classification is to some degree arbitrary, it is considered useful for an understanding of the hydrogeochemical processes occurring at this site. Justification of the Water Groups will be given in the text as the field and analytical data are discussed. The spatial distribution for these Water Groups is shown in Figs. 2 and 5. Data for seawater were also compiled from Weast *et al.* (1984) for comparison.

3.3 Water Analysis

The following information on waters was obtained in the field:

Depth to Watertable
Sampling depth
pH
Temperature
Conductivity
Oxidation Potential (Eh)
Ferrous ion (Fe^{2+}) concentration

A 500 mL water sample was collected for general chemical analysis. Twenty mL of the solution was analysed for HCO_3^-, by alkalinity titration. A further 250 mL was filtered to < 45μm in the laboratory. An acidified portion of the filtrate was analysed for Na and K by flame Atomic Absorption Spectrophotometry (AAS) on a Varian AA875 and for Mg, Ca, Al, Ba, Cr, Fe, Mn, Ni, Sr, Ag, Cd, Co, Cu, Pb, Zn and Si by Inductively Coupled Plasma torch optical emission (ICP) on a Hilger E-1000 ICP with a high solids torch. Matrix effects for the ICP analysis were removed by diluting with acid to a constant Na level and using matched standards.

An unacidified portion was analysed by Ion Chromatography, for Cl^-, Br^-, SO_4^{2-} and NO_3^- using a DIONEX AS4A column under standard eluent conditions and a conductivity detector, and for I^- and $S_2O_3^{2-}$ (thiosulphate) using a DIONEX AS5 column under standard eluent conditions and an electrochemical detector (Dionex, 1985). The $S_2O_3^{2-}$ analyses were performed on solutions that were frozen in the field and thawed in the laboratory prior to analysis, so as to avoid decomposition.

The accuracy of the total analyses was confirmed by measuring the cation/anion balance. Any waters with balances worse than 5% were rechecked.

Selected waters (MG2, MG5, MG11, MG13, MG14, MG24, MG31, MG34, MG40, and MG41) were analysed for hydrogen and oxygen isotope abundances, using a VG ISOGAS SIRA 9 Stable Isotope Gas Analyser, standardized for SMOW (Standard Mean Ocean Water).

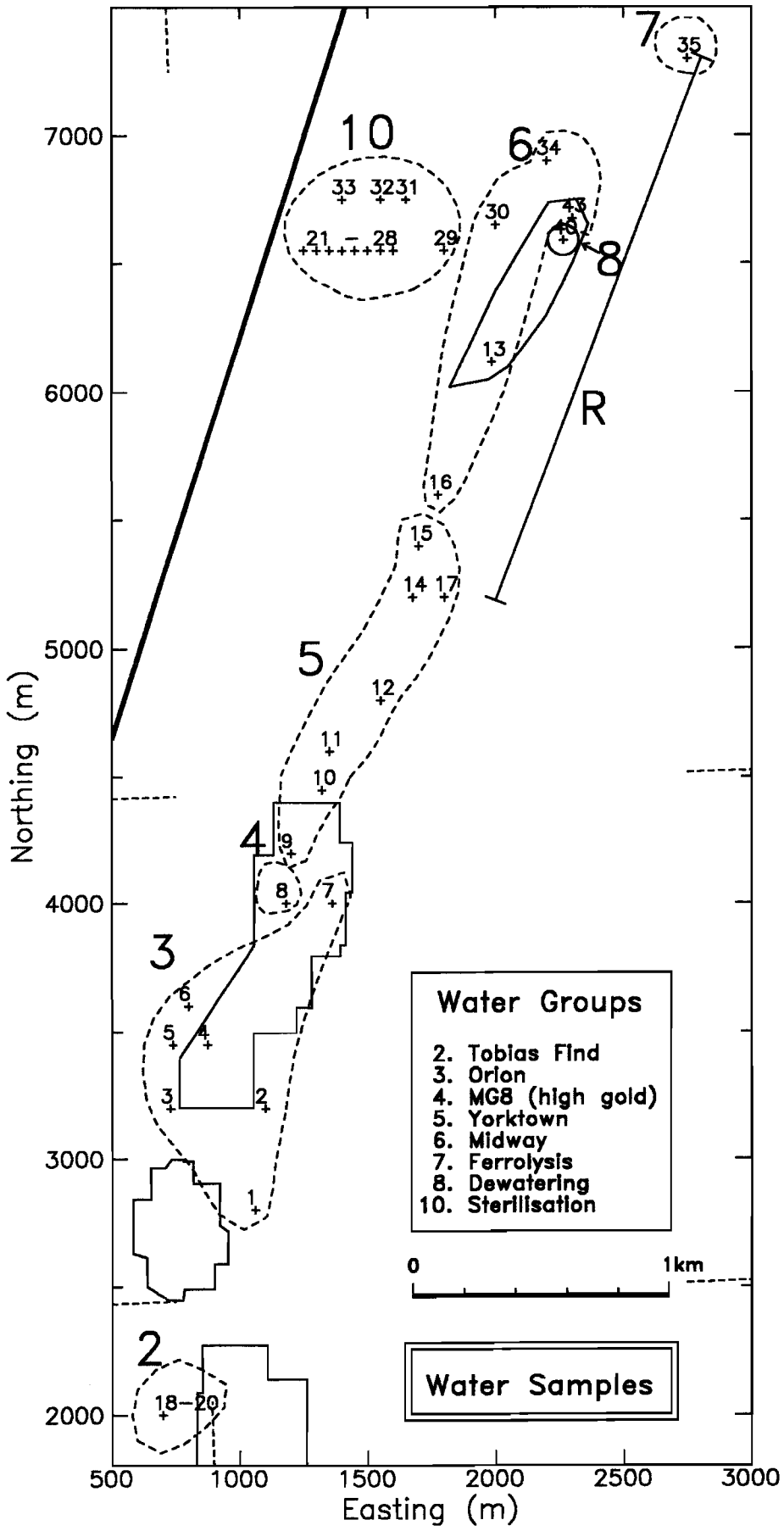

Figure 5. Bore Hole locations and Water Groups within the Mt. Gibson Au Mine Area.

Table 1. Drill Holes used for Water Samples at Mt. Gibson Au Mining Area and the Surrounding District.

Sample No.	Hole Name	Position (mine) East	Position (mine) North	Position (AMG*) East	Position (AMG*) North	Water Table (mRL)	Sample Depth (m below WT)	Group
1	1581	1060	2800	516236	6708372	313	3.5	3
2	1473	1100	3200	516287	6708771	312	5	3
3	1566	730	3200	515917	6708771	313	3.5	3
4	1605	875	3450	516068	6709027	314	1	3
5	1611	740	3450	515933	6709027	314	5	3
6	1472	800	3600	515997	6709179	nd	nd	3
7	1456	1360	4000	516568	6709564	312	5	3
8	1460	1180	4000	516388	6709569	311	5	4
9	1617	1200	4200	516413	6709768	313	5	5
10	1554	1320	4450	516539	6710015	312	5	5
11	1612	1350	4600	516573	6710164	312	1.5	5
12	1530	1550	4800	516778	6710359	312	5	5
13	PB6	1985	6120	517248	6711667	309	5	6
14	1491	1675	5200	516914	6710755	311	4	5
15	1590	1700	5400	516944	6710955	310	5	5
16	1478	1775	5600	517024	6711153	309	5	6
17	1489	1800	5200	517039	6710752	310	3	5
18	1591	700	2000	515855	6707582	318	30	2
19	"	"	"	"	"	"	17.5	2
20	"	"	"	"	"	"	5	2
21	44	1250	6550	516524	6712116	308	5	10
22	45	1300	6550	516574	6712115	308	5	10
23	46	1350	6550	516624	6712113	308	5	10
24	47	1400	6550	516674	6712112	308	5	10
25	48	1450	6550	516724	6712111	309	5	10
26	49	1500	6550	516774	6712109	309	5	10
27	50	1550	6550	516824	6712108	308	5	10
28	51	1600	6550	516874	6712107	309	5	10
29	MGH510	1800	6550	517074	6712102	309	5	10
30	-	2000	6650	517274	6712096	309	5	6
31	41	1650	6750	516929	6712305	309	5	10
32	39	1550	6750	516829	6712308	309	5	10
33	36	1400	3750	516679	6712312	308	5	10
34	-	2200	6900	517483	6712441	nd	3	6
35	MGR003	2750	7300	518043	6712826	308	2	7
36	-	3630	14440	519110	6719941	304#	1.8	11
37	-	3610	15680	519122	6721181	305#	5	11
38	-	2564	15600	518075	6721128	306#	5	11
39	MG@ Well	1950	9480	517301	6715027	nd	5	13
40	Dewater.	2265	6590	517540	6712129	nd	nd	8
41	Lake Karpa	5060	7735	520364	6713201	nd	0.2	9
42	Karpa Spring	5435	8885	520769	6714341	nd	0.5	13
43	-	2300	6675	517577	6712213	302	5	6
44	PB1	4310	19930	519933	6725411	nd	nd	12
45	OB7	5740	17730	521305	6723175	297#	5	12
46	OB11	3280	22160	518962	6727668	290#	5	12
47	OB10	3160	23360	518873	6728870	292#	5	12
48	OB6	3610	23930	519338	6729428	290#	5	12
49	OB9	5060	16980	520606	6722443	301#	5	12
50	Qtz Blow	3300	-750	511824	6706437	nd	5	1

*: Australian Map Grid
@: Mt. Gibson
#: Assuming Surface is at 310 mRL
nd: not determined

Table 2. Water Groups used in this Report.

Group	Description	Sample Nos.
1	"Quartz Blow" drilled through quartz rock	50
2	"Tobias' Find"	18-20
3	"Orion " drill holes north of Tobias' Find and south of hole MG8 (South Pit and Orion Areas)	1-7
4	"MG8 Anomaly"	8
5	"Yorktown" drill holes north of hole MG8 up to the Enterprise / Midway area (Orion North and Yorktown Areas)	9-12, 14, 15, 17
6	"Midway" Enterprise and Hornet Areas	13, 16, 30, 34, 43
7	"Ferrolysis" north of Hornet Pit	35
8	"Midway dewatering"	40
9	"Lake Karpa"	41
10	"Sterilisation" holes 300-500 m west of Hornet Pit	21-29, 31-33
11	"Mummaloo" holes north (about 10km) of the Mt. Gibson deposit and west of Mummaloo-Wye-Bubba Hill	36-38
12	"Bore Field" waters presently being used as the water source for the mine	44-49
13	"Surface" waters from the Southern Cross Windmill and the Karpa Bore	39, 42

A one litre sample, acidified with one mL concentrated nitric acid, was shaken for at least three days with one gram activated charcoal, enclosed in nylon mesh. The charcoal was then ashed, and the residue dissolved in concentrated hydrochloric/nitric acid. Vanadium, Bi and Sb were determined by ICP, using instrumentation as for other element analysis described above. Gold was analysed by AAS using a Varian AA-875 with a GTA-95 Graphite Tube Atomizer, following extraction into DIBK. Any matrix effect was checked by running two standard additions for each sample. Calibration of the method was obtained by shaking standards of varying concentrations, and in varying salinities, with activated carbon.

4.0 RESULTS AND DISCUSSION

4.1 Compilation of Data

Water data are listed in Appendix 1, and averaged data for each environment are summarized in Tables 3 and 4.

The Bore Field waters and waters from some holes in the mine area had been previously sampled and analysed for the major elements by commercial laboratories during exploration for a water supply for the mine site. TDS data derived from these analyses are used in Fig. 6.

4.2 Regional Description

The district-scale map is given in Fig. 2. The samples taken occur in a number of aquifer systems, from the fractured rock system in the Mt. Gibson Mine Area, to the north-south lying drainage system. The drainage system presumably represents a sediment aquifer, rather than a fractured rock aquifer as in the mine area. A current study of regolith/landform relationships over the Mount Gibson district is, in part, addressing the sedimentary stratigraphy of the drainage sump. Regional salinity values are shown in Fig. 6. Major attributes are described below.

The drainage system adjacent to the mine area is dominated by the saline sump (playa) system. The waters within the evaporative sumps are expected to be at or near halite saturation. Water taken from Lake Karpa (MG41) was measured at 31% total dissolved solids (TDS) and was saturated with respect to halite (Section 4.8.2). The Mummaloo waters, 1-2 km east of the surface saline system had high salinities (3.9 - 5.5%). However, the Bore Field waters were distinctly less saline. Bore holes MG44 and MG45, which lie just north of the narrow gap between the topographic Mount Gibson and Mummaloo-Wye-Bubba Hill, showed particularly low salinities (Fig. 6). These data suggest that this gap between the two hills represents a barrier to groundwater flow, and that the aquifer system just north of the barrier is presumably relatively freely draining and is receiving a significant contribution from recent runoff waters. The deeper, and presumably more saline, waters may therefore be retained in the aquifer system south of the topographic Mount Gibson. This proposal is also consistent with the extensive playa system developed in this aquifer system.

Topographic information is not available for the Bore Field waters. However, based on the topography as given in Fig. 2, and on the generally flat terrain, any variation in ground level is expected to be less than 5 m. The depth to water increases by more than 10 m from MG49 to MG48 along the south to north transect, indicating a large hydrological gradient across this transect, which is also consistent with the Bore Field waters representing an aquifer which is recharged with fresher water and is more freely draining than the playa groundwater system shown in Fig. 2.

4.3 Mine Region Description

Little information is available on the hydrogeology of the aquifers studied for this report. The mine area is dominantly a saprolitic and fractured rock system, though at the northern end it is probably at least partially continuous with the regional drainage, which is presumably more sedimentary in nature.

Table 3. Averaged data for Water Groups (Majors; data in mg/L unless otherwise stated)

	Water Group*													
	1 {1}	2 {3}	3 {7}	4 {1}	5 {7}	6 {5}	7 {1}	8 {1}	9 {1}	10 {12}	11 {3}	12 {6}	13 {2}	Sea Water
pH	5	6.9 (0.1)	6.4 (0.2)	6.6	6.6 (0.3)	6.2 (0.5)	3.5	6.5	7.4	6.2 (0.1)	6.8 (0.2)	7.1 (0.2)	8.0 (0.4)	nd
Eh	nd	0.23 (0.05)	0.36 (0.06)	0.45	0.35 (0.07)	0.23@ (0.17)	0.53	nd	0.32	0.36 (0.04)	0.25 (0.07)	nd	0.14@	nd
Fe^{2+}	0	1.3 (0.7)	0.2 (0.4)	0	0.2 (0.6)	21 (25)	0	5	0	0 (0)	1.7 (2.9)	0.7 (1.6)	0.5 (0.5)	0.01
DO#	6	4.5 (0.7)	4.5 (0.5)	5	5.2 (1.4)	3.2 (0.6)	6.4	5.7	2.1	5.6 (0.9)	4.4 (1.9)	6.0 (1.4)	3.8 (0.5)	nd
HCO_3	6	51 (6)	260 (40)	335	260 (50)	210 (210)	0	150	287	96 (8)	700 (600)	510 (100)	500 (90)	140
SO_4	11	207 (3)	1000 (400)	1390	1300 (600)	2100 (500)	3180	8790	26000	660 (80)	2800 (700)	1100 (500)	100 (130)	2210
Cl	195	985 (0)	6000 (3000)	7900	9000 (4000)	16000 (5000)	24600	72700	178000	5100 (500)	25000 (5000)	7000 (4000)	1000 (800)	19000
Br	0.78	3.8 (0.1)	21 (9)	28	29 (12)	50 (13)	70	170	600	17 (2)	62 (11)	23 (12)	3.2 (2.3)	65
I	0.013	0.51 (0.05)	0.26 (0.19)	0.15	0.3 (0.4)	1.1 (0.6)	0.39	0.95	1	0.09 (0.17)	1.6 (2.4)	0.9 (1.8)	0.38 (0.17)	0.06
NO_3	12	16.6 (0.8)	10 (10)	21	18 (15)	<2.4	<2.4	<7	<24	13 (4)	17 (21)	41 (21)	1.7 (2.1)	nd
Na	110	667 (6)	3900 (1700)	4740	5400 (2300)	9100 (2600)	12800	41200	90000	3110 (290)	14000 (3000)	4500 (2500)	500 (400)	10500
K	5.67	26.5 (0.2)	130 (50)	170	190 (70)	290 (80)	430	1110	5170	113 (9)	370 (90)	150 (80)	19 (14)	380
Mg	13	28 (0)	380 (190)	560	570 (260)	1000 (400)	1700	4900	13600	280 (50)	1580 (110)	470 (240)	110 (90)	1350
Ca	2	14 (2)	80 (50)	120	130 (60)	240 (140)	120	750	330	61 (11)	510 (190)	110 (50)	110 (60)	400
Sr	0	0.05 (0.08)	0.5 (0.7)	2.5	2.2 (1.6)	3.2 (0.6)	3.4	9.6	15.2	1.3 (0.4)	5.1 (1.3)	3.5 (2.2)	1.8 (2.3)	8.1
Si	17.6	29.0 (1.0)	28 (13)	25	24 (7)	23 (15)	44	13	13	40.4 (1.2)	21 (12)	33 (8)	27 (3)	3
TDS	375	2030 (2)	12000 (5000)	15000	17000 (7000)	29000 (9000)	43000	130000	314000	9500 (900)	45000 (9000)	14000 (8000)	2400 (1600)	34000

* : See Table 2 for Code
{}: Number of Samples
(): Standard Deviation

: Dissolved Oxygen
@ : Data Missing
nd: not determined

Table 4. Averaged data for Water Groups (Minors; data in mg/L unless otherwise stated)

	Water Group*													
	1 {1}	2 {3}	3 {7}	4 {1}	5 {7}	6 {5}	7 {1}	8 {1}	9 {1}	10 {12}	11 {3}	12 {6}	13 {2}	Sea Water
Al	0.26	0 (0)	0.001 (0.002)	0	0.001 (0.003)	0.2 (0.5)	14.5	0	0	0.001 (0.003)	0.012 (0.020)	0 (0)	0 (0)	0.01
Ba	0.060	0.065 (0.003)	0.018 (0.022)	0.019	0.025 (0.024)	0.06 (0.04)	0.039	0.017	0.027	0.023 (0.005)	0.11 (0.13)	0.06 (0.06)	0.5 (0.6)	0.03
Cr	0	0 (0)	0.001 (0.001)	0.013	0.001 (0.002)	0.001 (0.002)	0.026	0	0.15	0.000 (0.001)	0.002 (0.003)	0.008 (0.014)	0 (0)	0.000
Mn	0.07	0.46 (0.09)	0.17 (0.23)	0.028	0.09 (0.09)	2.7 (2.9)	3.8	1.4	27	0.03 (0.03)	1.6 (2.5)	0.8 (1.9)	1.6 (1.8)	0.002
Ni	0.017	0.026 (0.005)	0.010 (0.015)	0.021	0.003 (0.004)	0.028 (0.022)	0.28	0.029	0.24	0.008 (0.006)	0.010 (0.004)	0.003 (0.005)	0.015 (0.007)	0.005
Ag	0	0 (0)	0.009 (0.011)	0.021	0.007 (0.006)	0 (0)	0.022	0.070	0.15	0.006 (0.003)	0.002 (0.004)	0.002 (0.005)	0 (0)	0.0003
Cd	0	0.001 (0.002)	0.000 (0.001)	0.006	0.001@ (0.002)	0.005 (0.005)	0.013	0	0.063	0 (0)	0 (0)	0 (0)	0 (0)	0.0001
Co	0.006	0.011 (0.004)	0.001 (0.003)	0	0 (0)	0.04 (0.04)	0.22	0.03	0.21	0.002 (0.004)	0.007 (0.006)	0.003 (0.005)	0.010 (0.005)	0.0003
Cu	0.11	0 (0)	0.006 (0.005)	0.14	0.001 (0.001)	0.010 (0.022)	0.14	0	0.036	0.002 (0.003)	0 (0)	0 (0)	0 (0)	0.003
Pb	0.064	0.064 (0.000)	0.2 (0.4)	0.54	0.15 (0.19)	0.2 (0.4)	0.37	0	1.3	0 (0)	0.03 (0.05)	0.02 (0.04)	0.10 (0.05)	0.00003
Zn	0.13	0.13 (0.04)	0.11 (0.20)	0	0 (0)	0.06 (0.06)	0.62	0	0.90	0.001 (0.003)	0.16 (0.14)	0.04 (0.08)	0.09 (0.04)	0.01
Au (ppb)	<0.05	0.15 (0.12)	0.08 (0.04)	1.00	0.18 (0.12)	0.4@ (0.5)	<0.05	<0.05	<0.05	0.08 (0.08)	<0.05	<0.05	0.10 (0.11)	0.01
V	0.004	0.12 (0.04)	0.03 (0.02)	0.01	0.04 (0.02)	0.04 (0.04)	0.02	<0.002	<0.002	0.05 (0.03)	0.03 (0.04)	0.05 (0.02)	0.20 (0.23)	0.002
Bi	<0.002	0.004 (0.003)	0.002 (0.002)	<0.002	0.002 (0.002)	0.003 (0.003)	<0.002	0.002	0.002	0.002 (0.001)	0.003 (0.003)	0.002 (0.001)	0.002 (0.001)	0.00002
Sb	0.015	0.034 (0.017)	0.008 (0.003)	0.020	0.005 (0.005)	0.009 (0.005)	0.010	<0.005	<0.005	0.008 (0.004)	0.009 (0.011)	0.009 (0.002)	0.009 (0.003)	0.0003

* : See Table 2 for Code
{}: Number of Samples
(): Standard Deviation

@ : Data missing
nd: not determined

Lateritic gravels of the upper part of the weathering profile and sandy quartz-rich sediments, which can bury the weathering profile, provide relatively permeable aquifers. In the S, C and N pit areas these are near surface, tens of metres above the standing watertable, and would provide aquifers to infiltration from rainwater. However, for the area of holes west of Midway up to 20 m of quartz-rich sandy clay, probably derived by erosion from granitic saprolite, overlie lateritic gravel, duricrust and the saprolitic weathering profile. The watertable is within 8 to 10 m of surface and the sandy sediments and lateritic gravels would be relatively permeable aquifers to groundwaters.

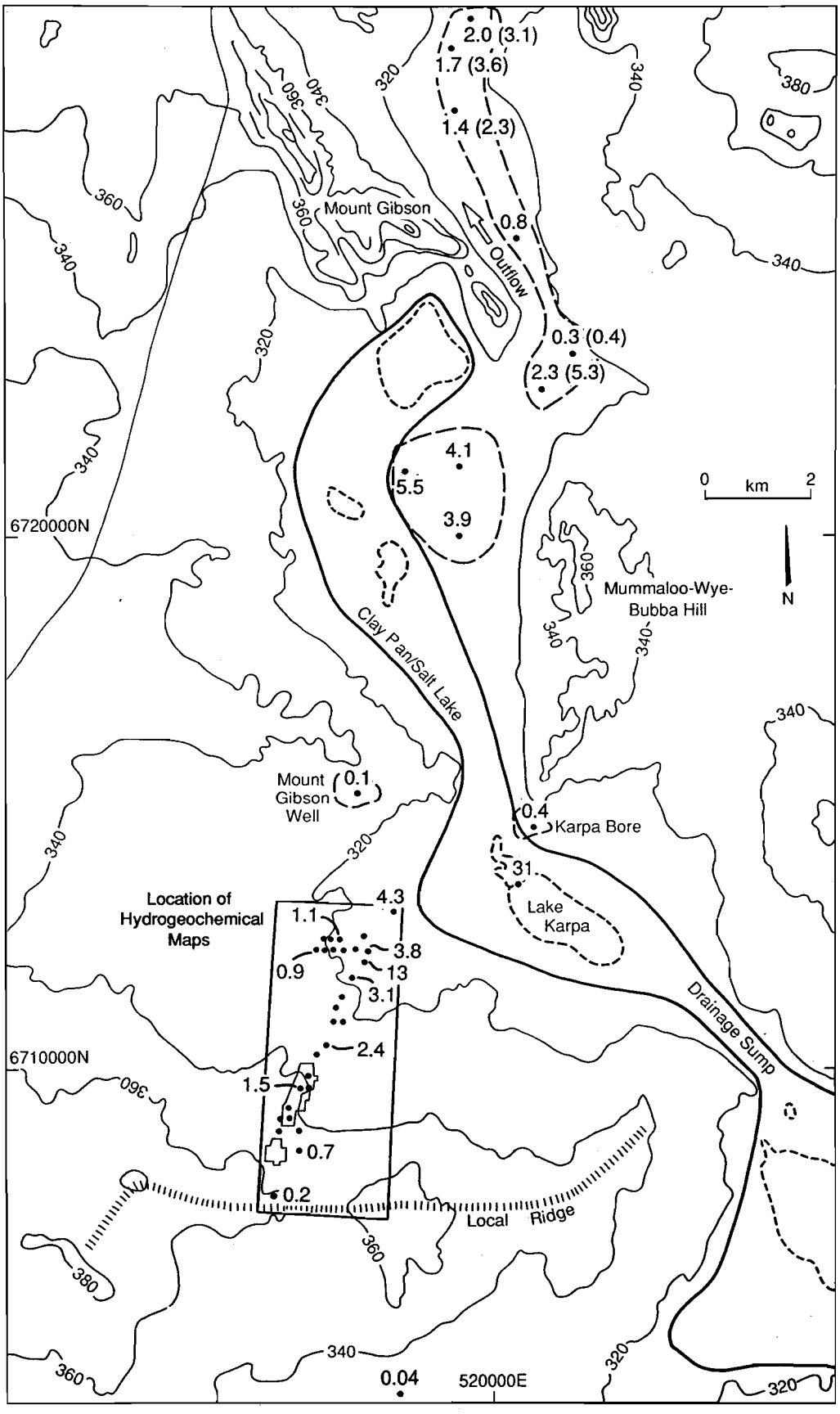

Figure 6. Regional Salinity Values (TDS in g/100mL). Note that numbers in brackets represent Data derived from commercial analyses during exploration for a water supply for the mine site.

The computer generated watertable contours for the Mt. Gibson deposit are shown in Fig. 7. As can be observed, the watertable data show a gentle downward slope from 318 m at Tobias' Find, which is at a topographical high and represents a groundwater divide (Fig. 4), to 308 m at hole MG35 past Midway, representing a flow length of about 5700 m. This is in contrast with the surface contours, which change in height by over 40 m over the same interval. Groundwater is suggested to originate at Tobias' Find and northwards, via rainfall, and then travel in a north - northeast direction before reaching the drainage sump system about 2000 to 3000 m to the north-east of Midway. The aquifer system may be discontinuous, as suggested by the lower salinity waters centered on hole MG14 at about 5300N (Fig. 8). Alternatively, the contours of groundwater salinity, as intersected by the distribution of drill holes may be irregularly shaped, perhaps due to local lateral flow.

At Midway the effect of dewatering can be observed with a sharp fall in the watertable (Fig. 7). It is not known what effects, if any, pumping may have had on the groundwater chemistry at this site.

The TDS of the Hornet dewatering borehole below Midway (MG40) is over three times the TDS of the surface waters (i.e. TDS of MG40 = 130,000 mg/L compared with MG43 at 38,000 mg/L). This is explained by the presence of two aquifer systems: a shallow system of recent origin of "low" salinity (TDS < 43,000 mg/L) and a deeper system of higher salinity (TDS > 127,000 mg/L). The waters sampled by baler are sampling the shallow aquifer system whereas the dewatering hole is pumping out water more representative of the deeper aquifer. This situation is demonstrated in Fig. 9, as modified from Smith (1987). The Midway area lies in a region where saline waters from the regional system are backflowing at depth. In comparison, the deepest water sample taken at Tobias' Find (MG18) was at 292 m, almost 20 m below the level of Lake Karpa, and was of low salinity (2000 mg/L). This suggest some major impediments to the backflow of the Lake Karpa brine, again as depicted in Fig. 9.

Thus, the general shallow aquifer system(s) at Mt. Gibson are discussed separately from the dewatering hole (MG40). The TDS data for the mine region (Fig. 8) demonstrate a general increase in TDS along the northward flow direction. A major exception is the area of holes MG14, MG15 and MG17, which may represent an influx of fresher water from another source. Of interest is the very sharp increase in TDS (from 11,000 mg/L to 37,000 mg/L in less than 500 m) going from the Sterilization holes east into Midway. This suggests a hydrodynamic boundary between the two sites with only limited mixing between the two aquifer systems.

4.4 Major Element Hydrogeochemistry

The major soluble elements [2] are HCO_3, SO_4, Cl, NO_3, Br, Na, K, Mg, Ca, Sr and Si. The waters are dominated by Na and Cl and most of the major ions show a very strong correlation with TDS (Section 4.9). Exceptions to this are HCO_3, Si, and to a lesser degree Ca and Sr.

[2] In general elements will be denoted by symbol, without valence information: i.e., Cl rather than Cl^-.

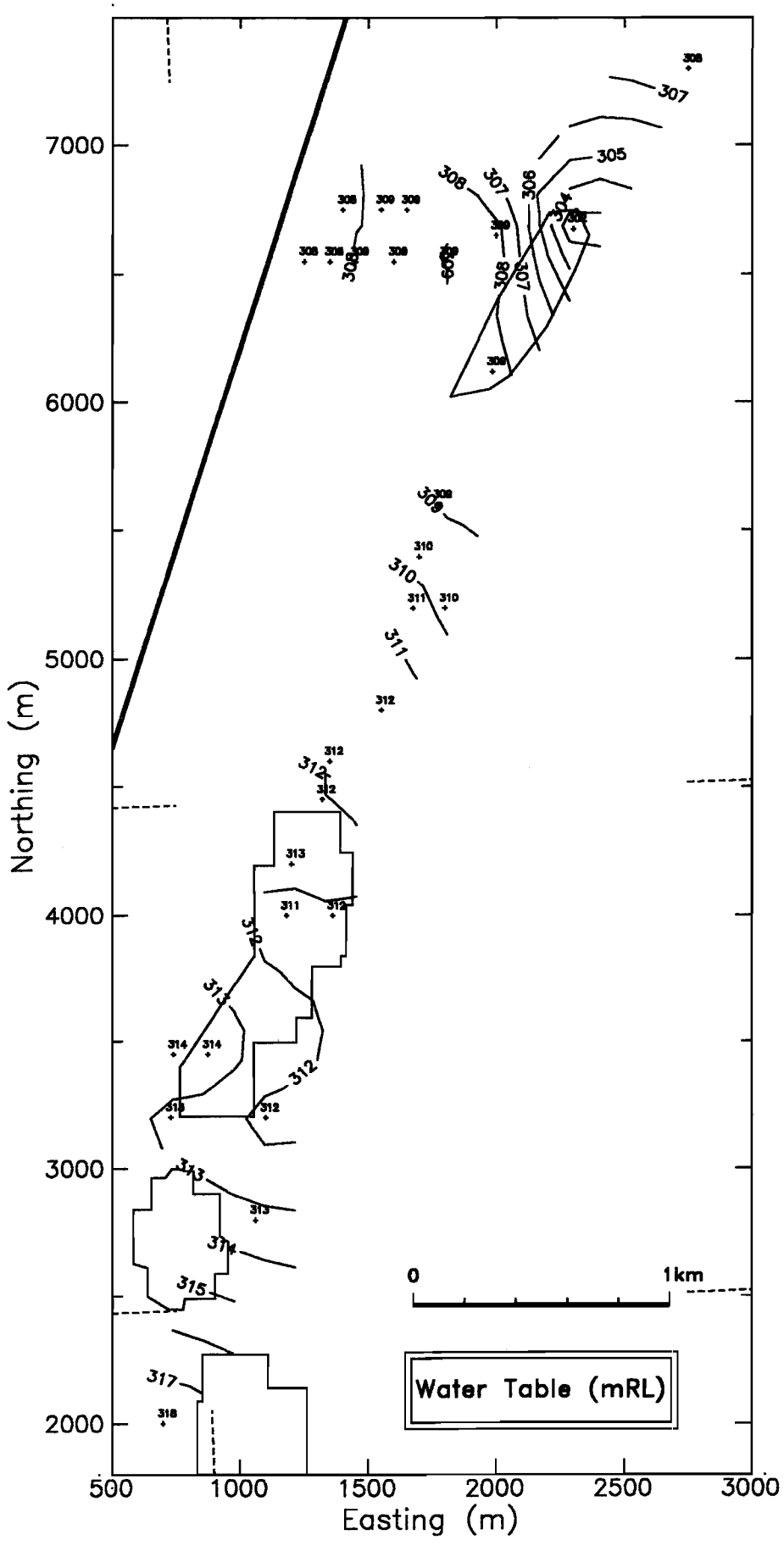

Figure 7. Watertable Contours for the Mt. Gibson Mine Area (in mRL).

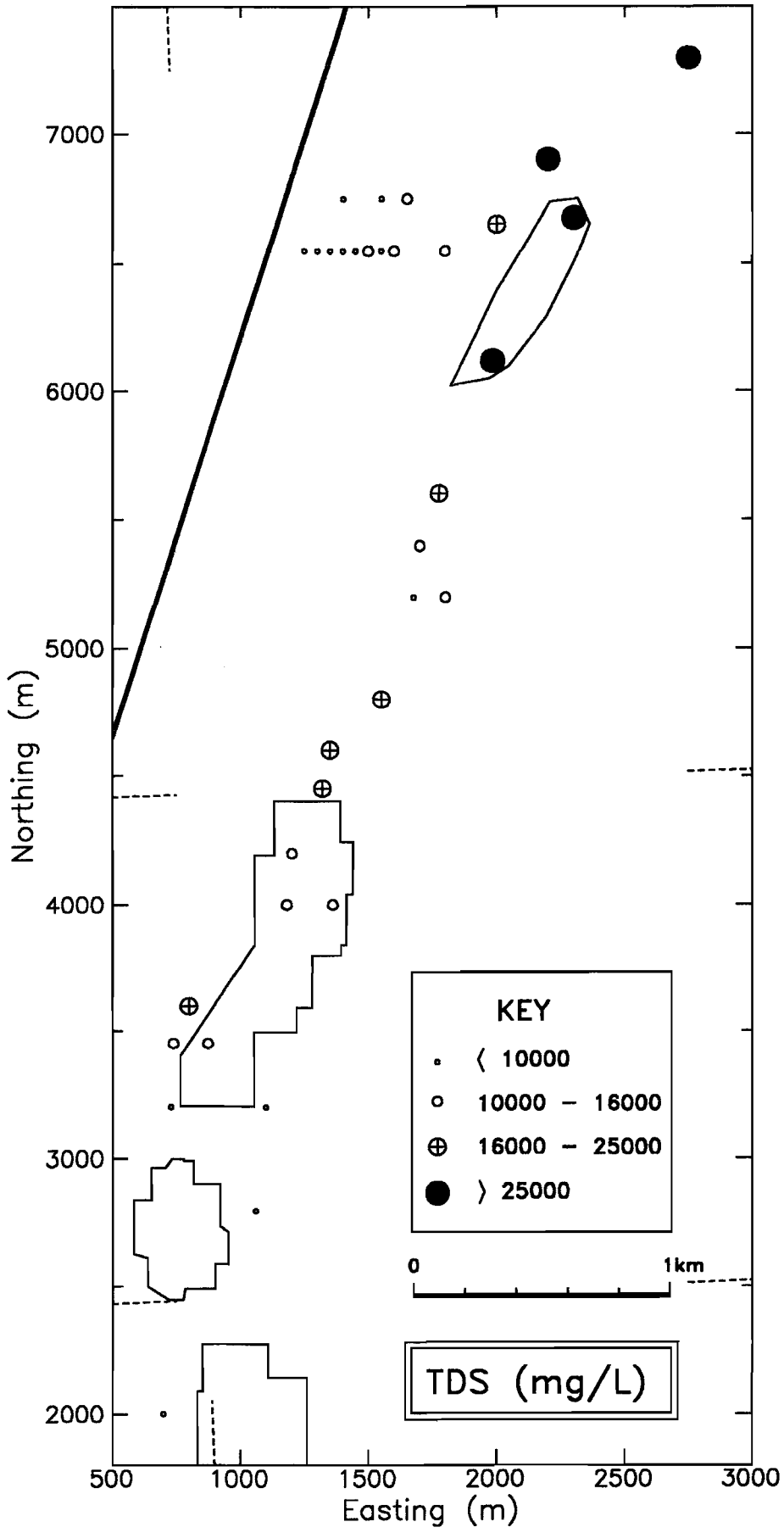

Figure 8. Total Dissolved Solids (in mg/L) for the Mt. Gibson Mine Area.

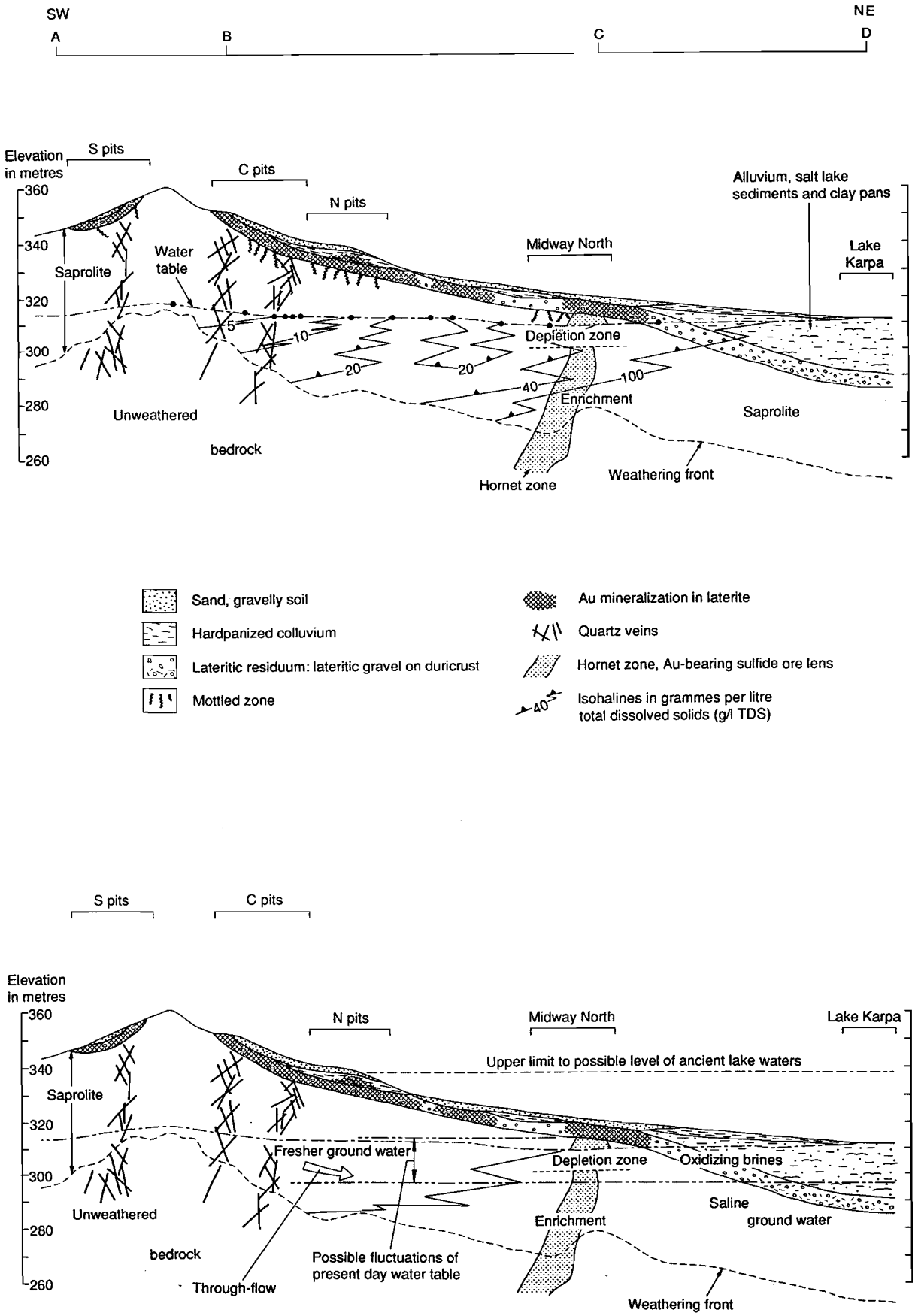

Figure 9. Longitudinal section from the Ridge west in the vicinity of the S Pits to the Saline Sump at Lake Karpa, based upon topographical contours and groundwaters from drill holes. Upper diagram observational, lower diagram is interpretational, modified from Smith (1987).

The plot of HCO_3 vs. TDS for the various waters is shown in Fig. 10. (Note that the TDS scale is split so as to show the MG40 and MG41 waters without losing detail). The samples are plotted in terms of Group numbers (Table 2) and the dashed line [3] represents the seawater dilution/evaporation line (i.e. the expected value if HCO_3 concentration was in the same proportion to total salinity as for seawater). This plot shows very clear distinctions between most of the groundwater Groups:

(i) Group 1 (quartz blow) is a low salinity water, and also had a low HCO_3 level, as would be expected for a water equilibrated with quartz rock;

(ii) Group 2 (Tobias' Find) has a salinity of about 2000mg/L and HCO_3 concentrations of 50mg/L;

(iii) Group 10 (Sterilization) waters had HCO_3 concentrations of about 100mg/L and plotted closely together;

(iv) Group 3 (Orion), Group 5 (Yorktown), and holes MG16 and MG30 from the Midway region all showed variable, though roughly similar, HCO_3 concentrations (200 - 300 mg/L), showing no correlation with salinity;

(v) Group 4 (MG8 anomaly) had a HCO_3 concentration greater than any Orion or Yorktown water. This water was distinguished on the basis of its high soluble Au (Section 4.7.5). However, as described below, many other major and minor elements show this water to differ significantly from other samples;

(vi) the other Midway holes MG13 and MG43 had anomalously low HCO_3;

(vii) the Ferrolysis hole MG35 was highly acidic (pH 3.5) and had no observable HCO_3;

(viii) the Bore Field waters (Group 12) were clearly distinguished from the mineralized waters on the basis of their higher HCO_3 levels.

The distinction between the various Groups using Si concentrations (Fig. 11) was not as clear as for HCO_3, though several characteristics could still be observed. In particular, Group 10 (Sterilization) waters were distinct from the Orion, Yorktown and Midway waters by virtue of their higher Si values.

Ca values (Fig. 12) are lowered in samples MG43, MG35, MG40 (Midway dewatering) and MG41 (Lake Karpa). This is possibly due to precipitation as calcite ($CaCO_3$) and/or gypsum ($CaSO_4 \cdot 2H_2O$). A similar, though weaker, effect is seen for Sr, which can precipitate as strontianite ($SrCO_3$) and/or celestine ($SrSO_4$).

NO_3 values within the mine area show no clear patterns. However, they provide an additional distinction between the Mine waters and the Bore Field waters, which are very high in NO_3 (41 ± 21 mg/L; Table 3).

---

[3] In all element concentration plots the position for sea water will be shown as "SW" and the seawater dilution/evaporation line as a dashed line

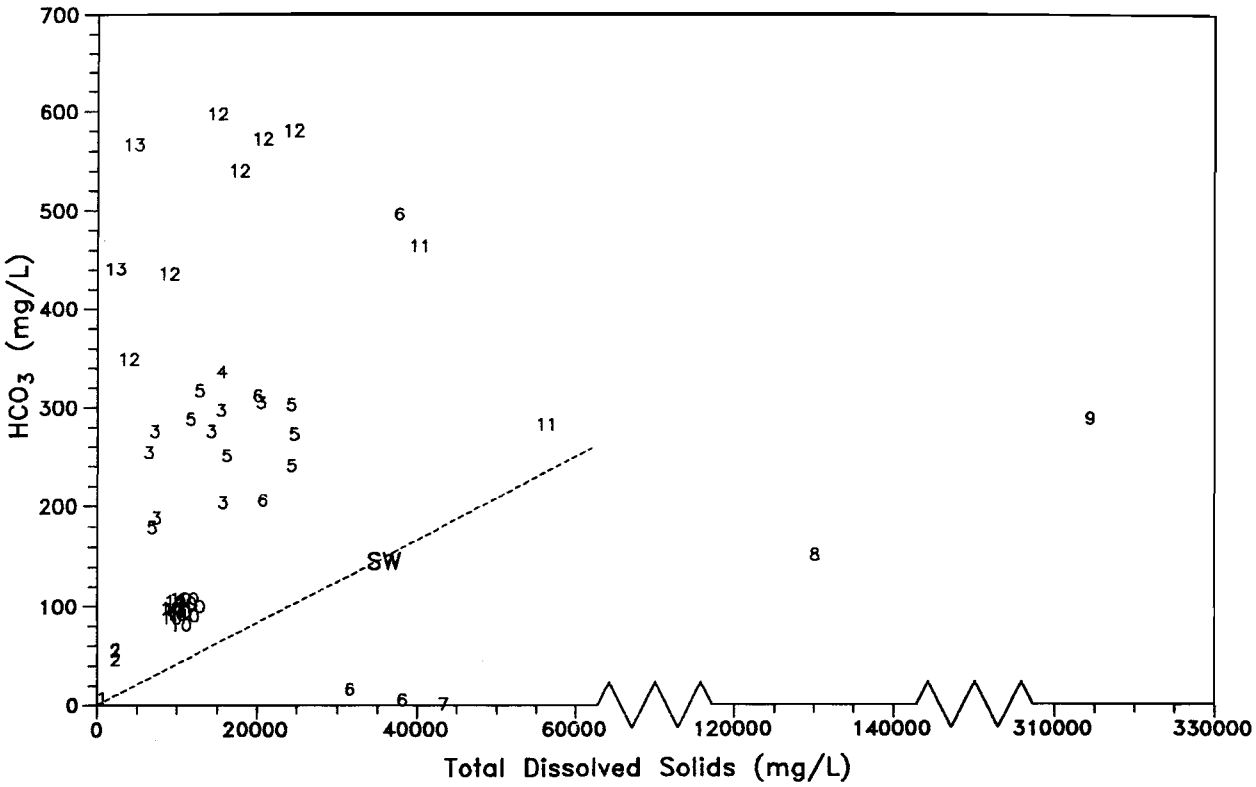

Figure 10. HCO_3 vs. TDS for Mount Gibson Waters.

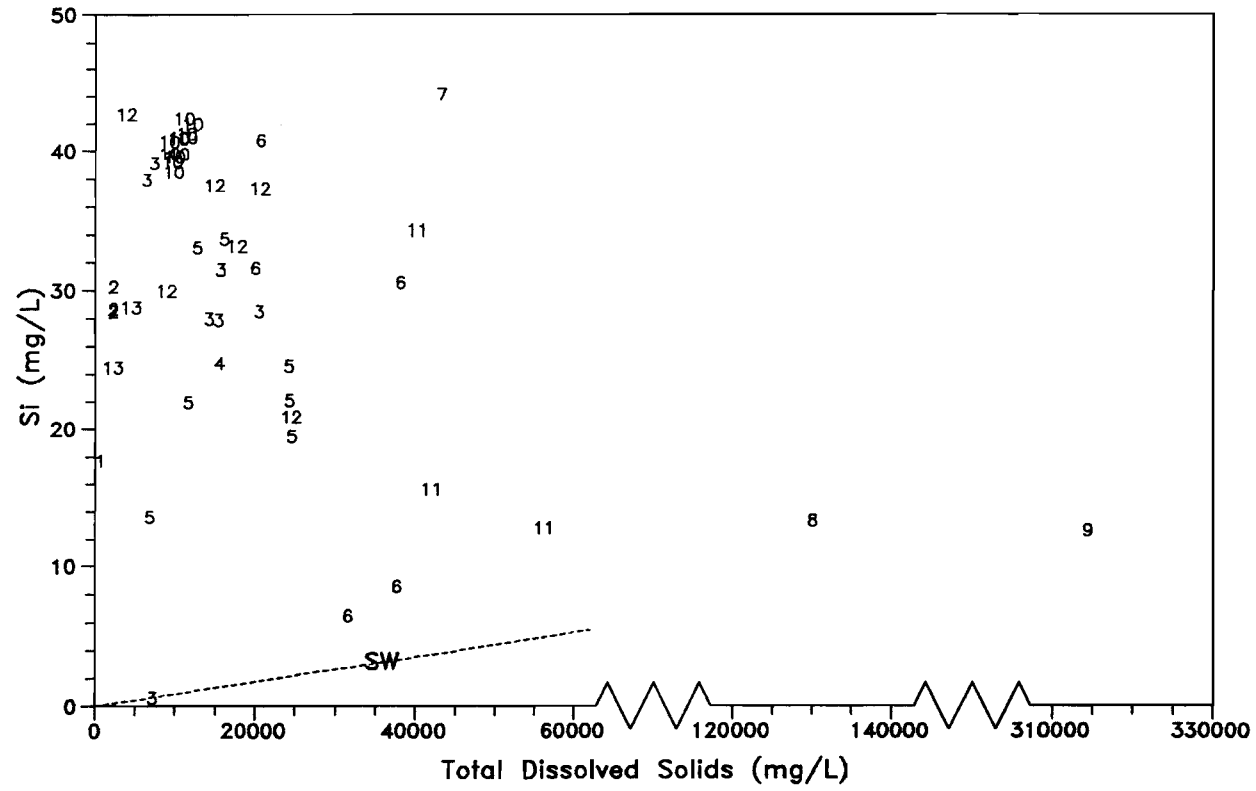

Figure 11. Si vs. TDS for Mount Gibson Waters.

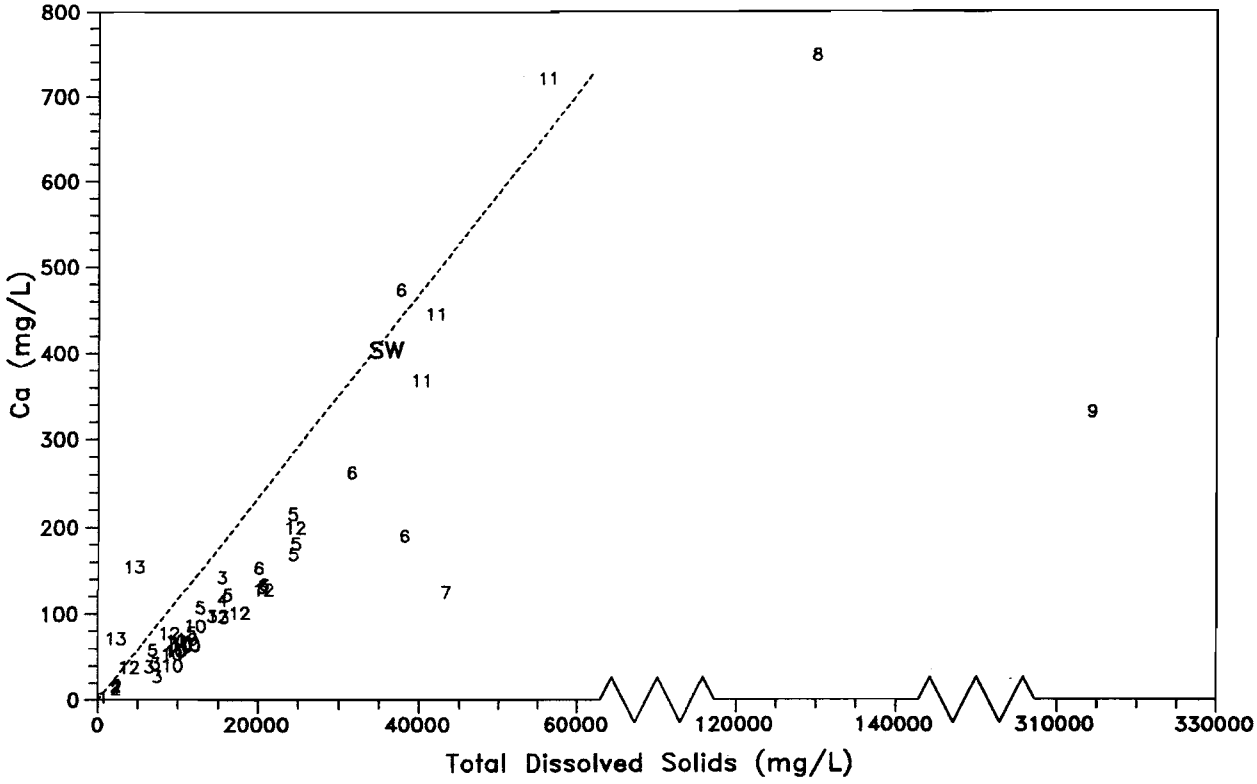

Figure 12. Ca vs. TDS for Mount Gibson Waters.

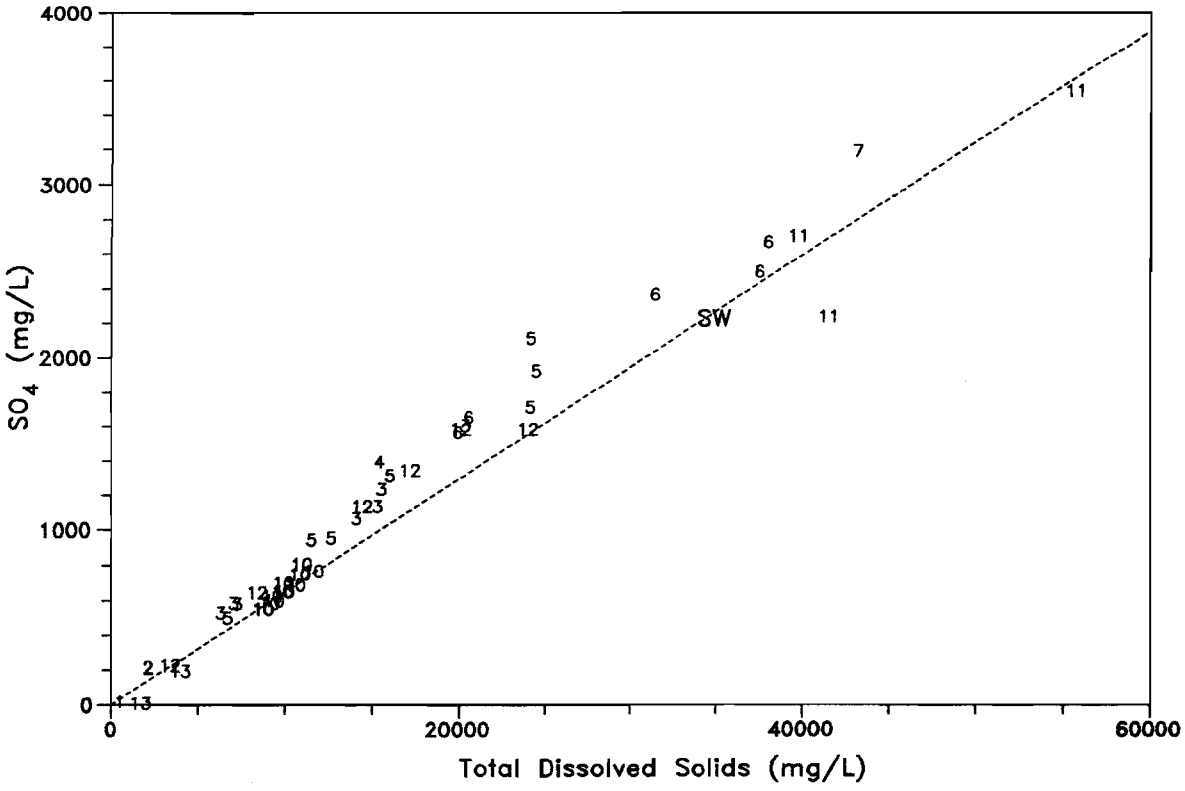

Figure 13. SO_4 vs. TDS for Mount Gibson Waters.

Any subtle patterns in element distributions for the major elements Na, K, Mg, Cl, SO_4, and Br are likely to be masked by the predominant effect of the high variation in salinity. Thus, a plot of SO_4 contentration vs. TDS (Fig. 13) is likely to show a close linear correlation. However, a plot of SO_4/Br [4] vs. TDS (Fig. 14) reveals additional information. If the waters are similar, only differing in terms of evaporation or dilution, then this ratio should be invariate (Eugster and Jones, 1979). This is not observed. Instead there is a major variation in the SO_4/Br ratio, from 36 (slightly above the sea water value) to about 52. Such a trend is NOT explained by evaporation or dilution of a particular groundwater which would result in a CONSTANT ratio, but rather reflects some change in the water chemistry, such as the dissolution or precipitation of ions, or the mixing of two differing waters (Eugster and Jones, 1979).

On examination of the data, the changes in ion ratios, illustrated for SO_4/Br, Cl/Br, Na/Br, Mg/Br and Sr/Br (Figs. 14-18), were modelled as TWO different mixing regimes. The first regime is suggested to represent waters within the mine area (i.e. Groups 3, 4, 5, 6 and 7). The mixing curves (shown as the solid lines in Figs. 14-18) are calculated using samples MG9 (a typical Orion or Yorktown water) and MG35 as end-members. Note that there is only weak agreement between measured and calculated ratios.

The second water regime represents waters within the drainage sump (i.e. Groups 8, 11, 12). The mixing curves (shown as the broken lines in Figs. 14-18) are calculated using samples MG46 and MG40 as end-members. With the exception of SO_4, which may be affected by gypsum precipitation, the samples plot closely to that expected by the theoretical mixing curve.

In addition, the Sterilization waters (Group 10) plot in a different region to the other waters - suggesting these groundwaters have a different origin and/or differing water-rock interactions have occurred. The Group 10 waters can be seen to form a rough linear trend in the SO_4/Br ratio (Fig. 14), which is strongly related to the position of the borehole: holes close to Midway such as MG28 or MG31 (Fig. 5) have a higher SO_4/Br ratio (> 40), while holes further east such as MG21 or MG33 show a lower ratio (about 36). A similar trend was observed for Mg/Br data, with this ratio being reduced in the Sterilization waters furthest out from Midway. These differences are greater than any analytical uncertainties. This effect is due to the Sterilization waters having lower sulphate and magnesium concentrations, suggesting less rock sulphide weathering, possibly indicating granitic rather than mafic rocks in the source area with which these waters have equilibrated.

4.5 Isotopic Investigations

The hypothesis of the different water systems in the mine area was tested by isotope [5] measurements on ten samples (Figs. 19 and 20). Isotope methods are a very useful corollary to the ion ratio determinations. The isotope ratios are a property of the water itself, and will be unaffected by any dissolution or precipitation reactions which could conceivably cause the ion ratio effects described above. Fig. 19 shows the plot of $‰\delta D$ vs. $‰\delta O^{18}$ (SMOW; see Section 3.3 for details). In general, a higher $‰\delta D$ indicates enrichment of the water in deuterium, the heavy isotope of hydrogen, and a higher $‰\delta O^{18}$ indicates

[4] Br is conventionally used in ratio plots as it is normally not affected by precipitation reactions.

[5] The methodology and theoretical basis of such measurements is given in many standard texts (e.g. Gat and Gonfiantini, 1981).

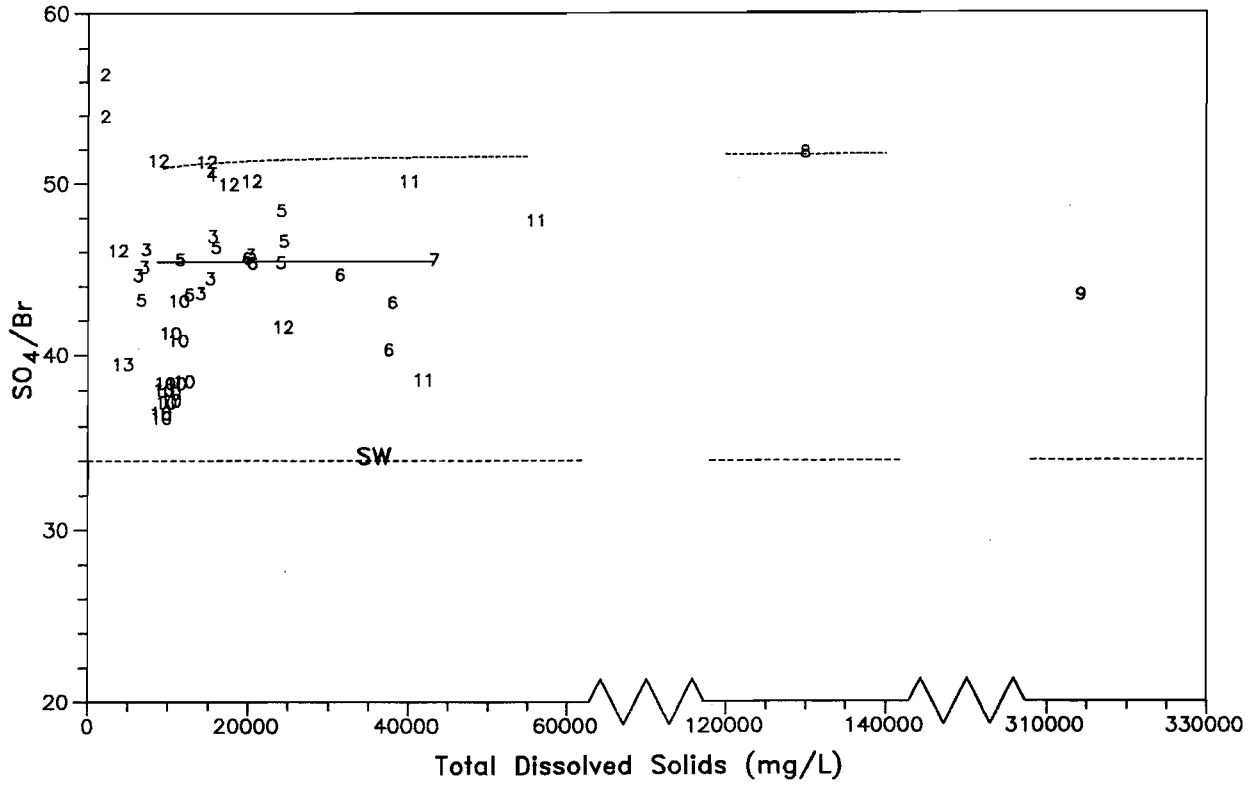

Figure 14. SO_4/Br vs. TDS for Mount Gibson Waters.

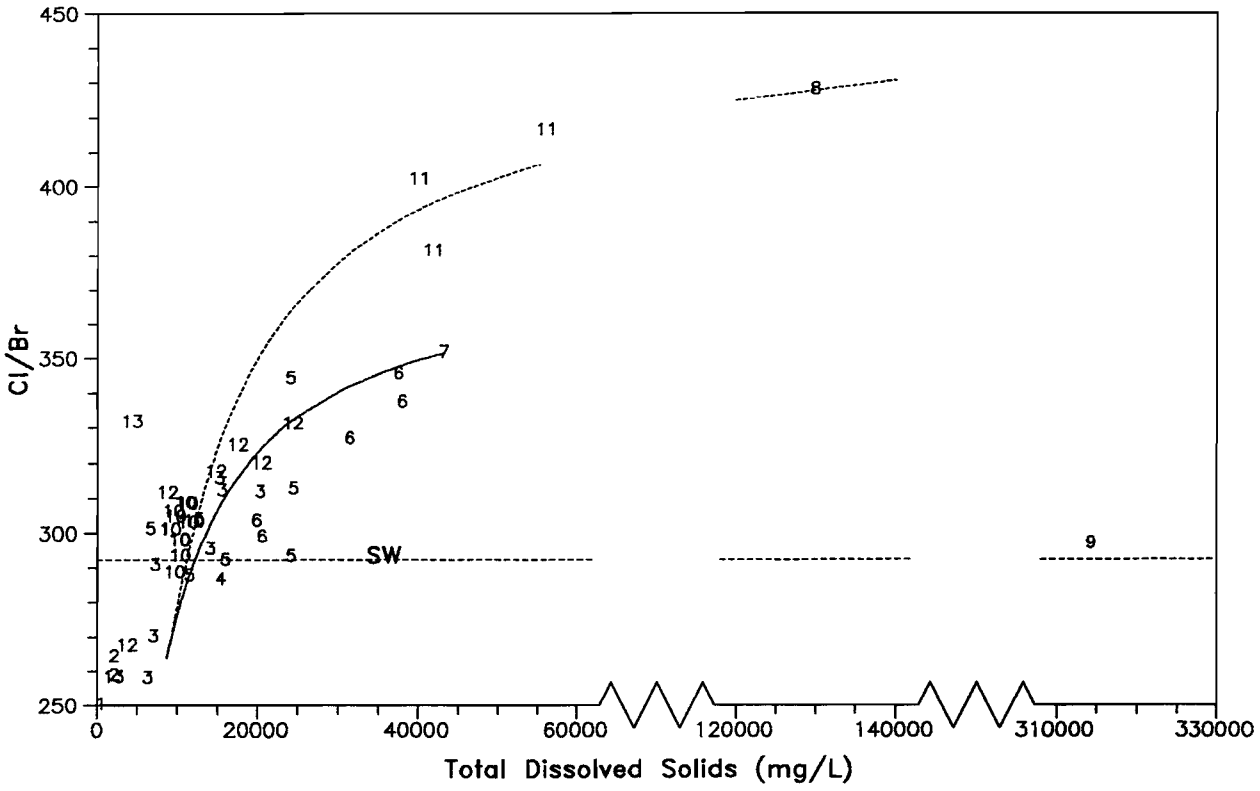

Figure 15. Cl/Br vs. TDS for Mount Gibson Waters.

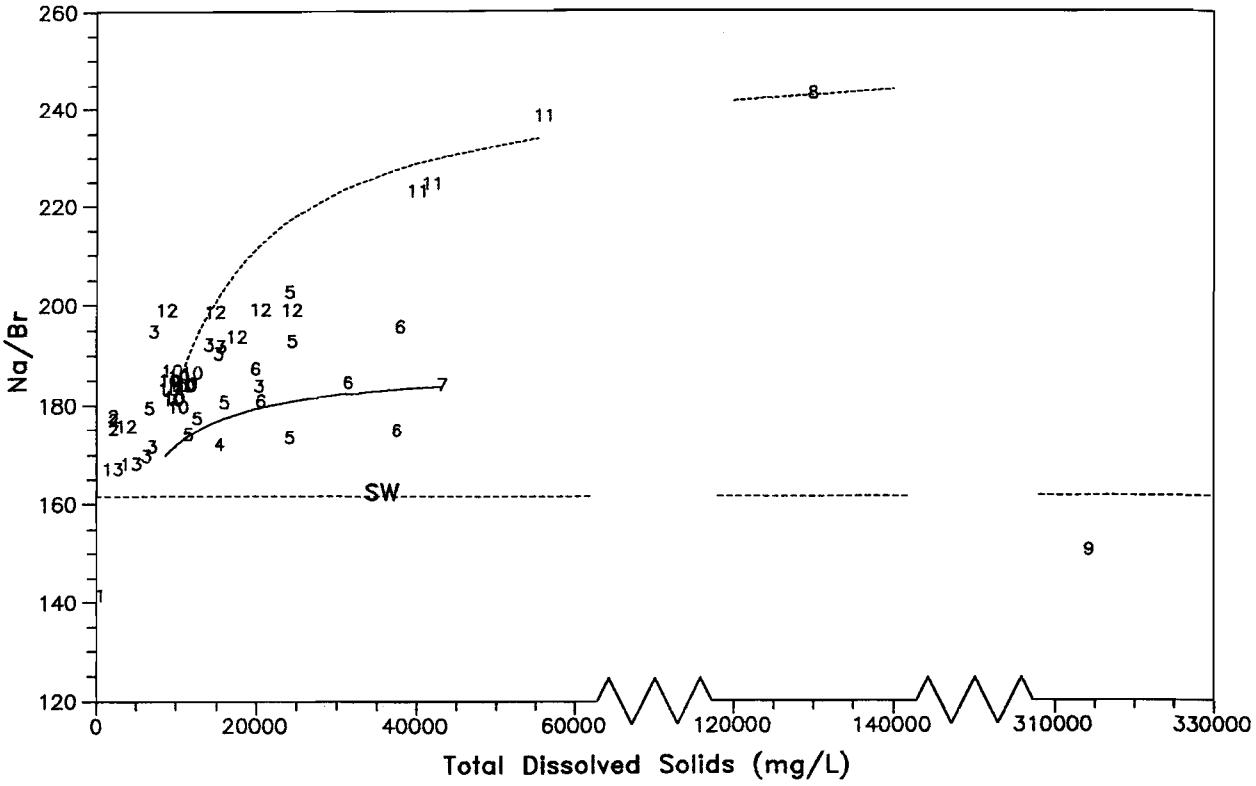

Figure 16. Na/Br vs. TDS for Mount Gibson Waters.

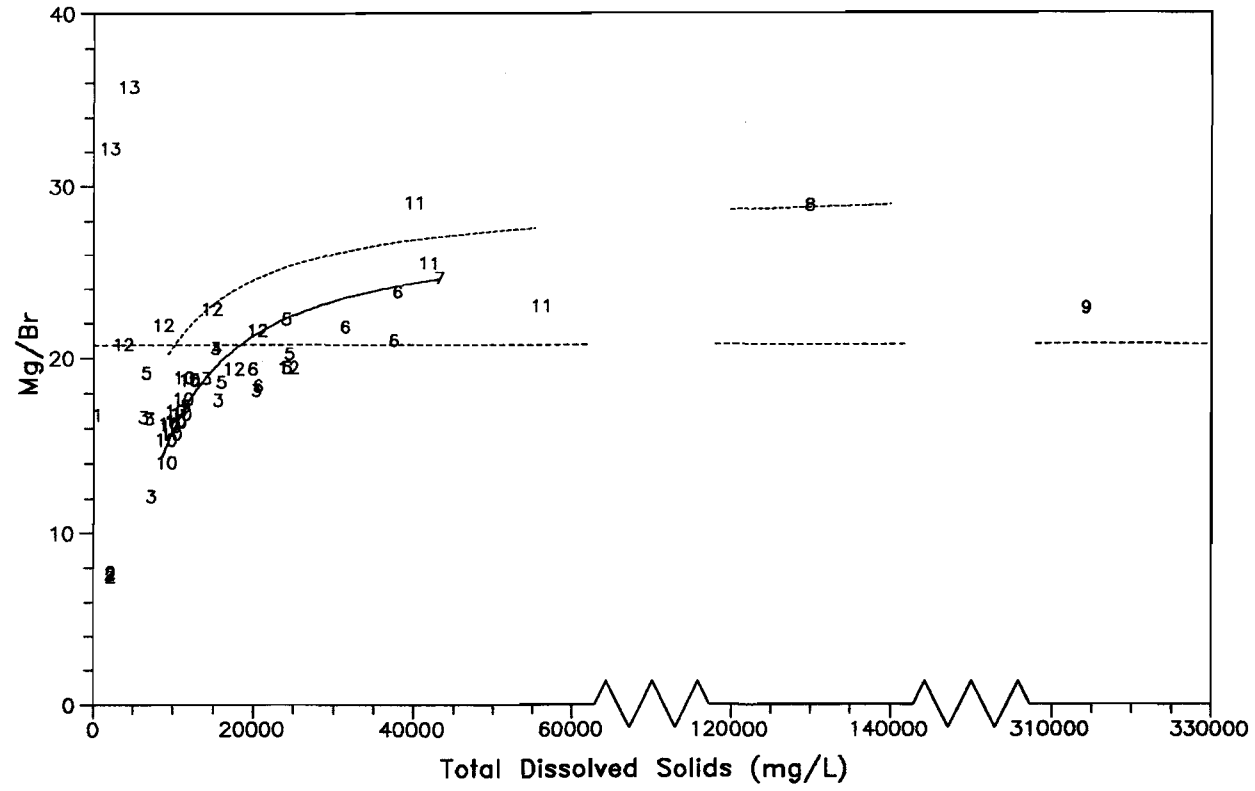

Figure 17. Mg/Br vs. TDS for Mount Gibson Waters.

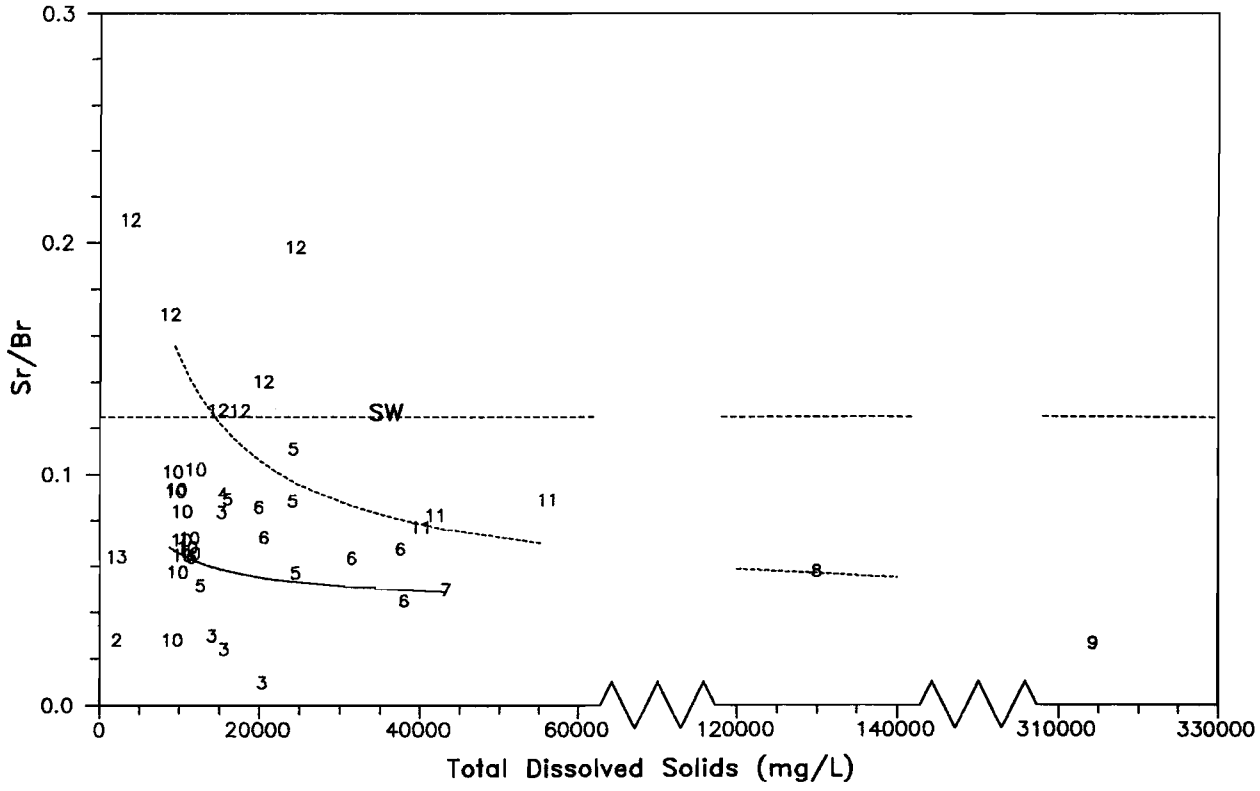

Figure 18. Sr/Br vs. TDS for Mount Gibson Waters.

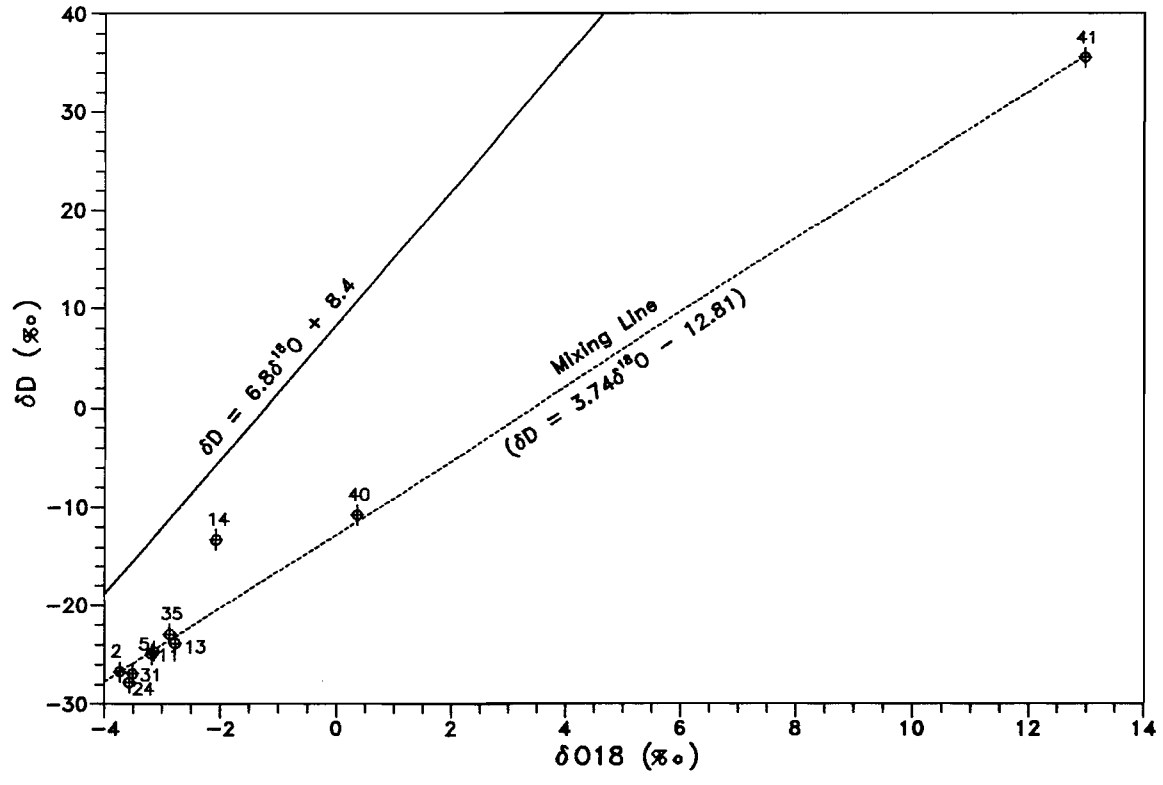

Figure 19. ‰δD (SMOW) vs. ‰dO^{18} (SMOW) for ten Mount Gibson Waters.

enrichment in O^{18}, the heavier isotope of oxygen. Such isotopic enrichments are generally caused by evaporation. Rain water at any site will generally show a linear relationship between ‰δD and ‰δO^{18}, which differs only slightly from site to site (Gat and Gonfiantini, 1981; Craig, 1961).

The relationship observed for meteoric waters at Perth is shown as the solid line in Fig. 19. The groundwaters plot away from this line. The Mine waters (MG2, MG5, MG11, MG13, MG35), the dewatering sample (MG40) and the Lake Karpa water (MG41) all plot on the same line (shown as the dotted line in Fig. 19). This isotopic enrichment is strongly correlated with salinity (Fig. 20). Such a line is similar to that for evaporation of a water under conditions of low relative humidity. Such a circumstance is unlikely for these groundwaters, which are 5 to 50 m below ground level. Thus, the dotted line in Fig. 19 is more likely to represent mixing of two separate waters: the first of low salinity with low heavy isotope abundance; and the second being highly saline with a high heavy isotope abundance (i.e. a highly evaporated water such as a saline sump or salt lake water).

The two Sterilization waters (MG24, MG31) appear to plot slightly off the line of best fit for the Mine waters (dotted line in Fig. 19). This is consistent with the hypothesis that the Sterilization waters are of a different origin than the Mine waters.

The major outlier from the mixing line is MG14. This sample was taken from the area between the N pits and Midway and, along with the adjacent samples MG15 and MG17 (Fig. 5), was considerably fresher than waters to the north or south (Fig. 8). This suggests that these waters represent an infiltration of fresher water into the groundwater system. Such a discontinuity in groundwater flow is not unexpected for a fractured rock aquifer, particularly where the bedrock sequence is highly folded and the weathering front irregular, and there may be hydrological barriers to uni-directional flow.

The highly linear isotope trend, involving both Mine and Drainage waters, is in stark contrast with the ion ratio data (see above) in which the Mine waters plot distinctly from the drainage waters. These data are explained by assuming the dotted mixing curves shown in Figs. 14 - 18 to be correct, and that the deviation of the Mine waters from this mixing curve to be due to dissolution of various ions with weathering of minerals in the fractured rock.

On the basis of the watertable, major ion, and isotope data, the system can be modelled in terms of a number of distinct water masses:

(i) a medium salinity (< 45,000 mg/L) water system, arising from movement of water through the aquifer in the main mine region (Groups 3 - 7), through which significant dissolution of minerals is occurring, resulting in high Mg and SO_4 concentrations;

(ii) a low salinity (< 12,000 mg/L) water system, represented by the Sterilization Waters (Group 10). This system differs from the former water in having lower SO_4/Br and Mg/Br ion ratios relative to former water system - i.e. they are depleted in SO_4 and Mg. The Sterilization waters possibly lie on the west side of a drainage divide (Fig. 4) from the other Mine waters and may be granitic in origin;

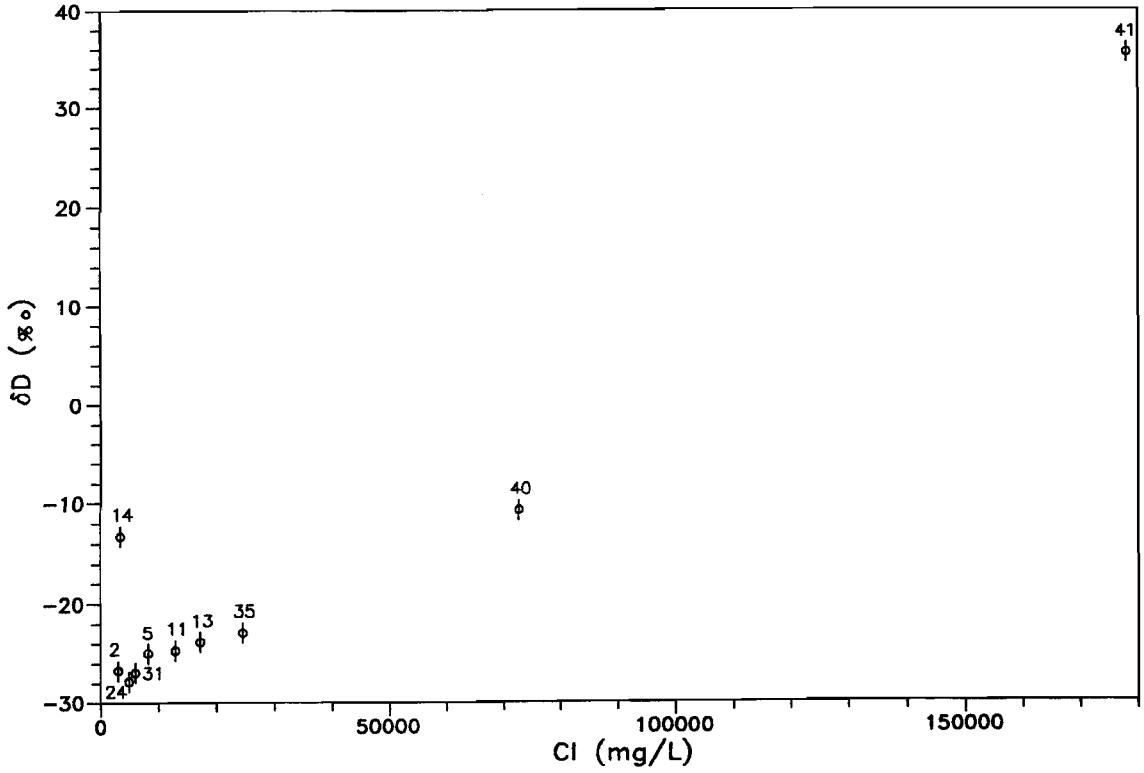

Figure 20. ‰δD (SMOW) vs. Cl for ten Mount Gibson Waters.

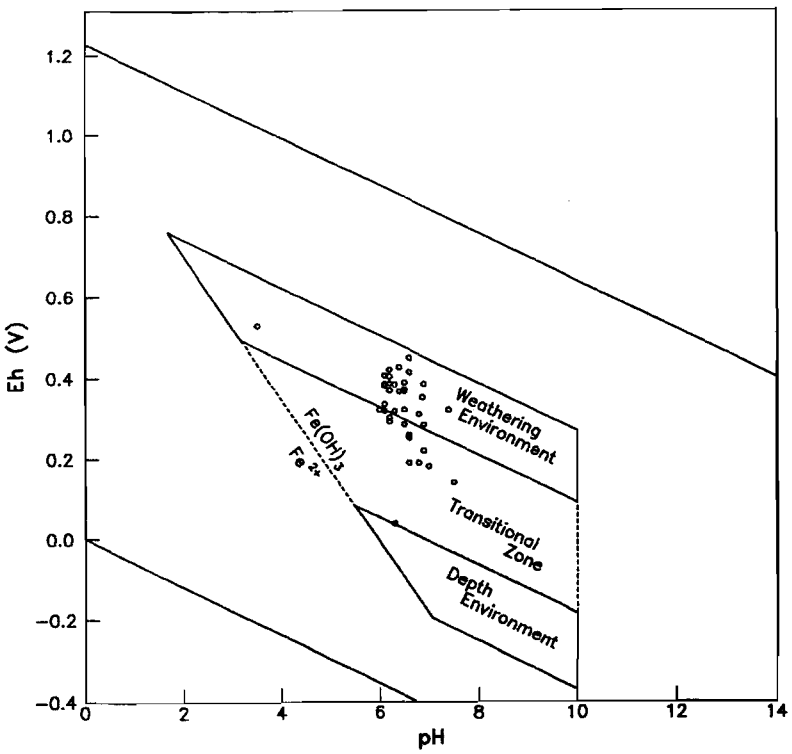

Figure 21. Eh vs. pH for Mount Gibson Waters, in context of pH/Eh Enviroments Postulated by Sato (1960).

(iii) a high salinity groundwater underlying the mine area at Midway (Group 8), possibly originating from the main north-south drainage system. It is not clear how far south this system goes into the mine area, though it appears to be absent at Tobias' Find;

(iv) the main north-south saline sump system south of the topographic Mount Gibson. This system is partially or wholly constrained between Mount Gibson and Mummaloo-Wye-Bubba Hill. Recirculating groundwaters increase in salinity with evaporation and mineral dissolution and form the saline sump system, as represented by Lake Karpa;

(v) The drainage system north of Mount Gibson, which tends to low salinities, particularly in the southern areas which are subject to recent recharge. Chemical data suggest this water to be of different origin to waters to the south of the topographic Mount Gibson.

4.6 pH/Eh Data

4.6.1 Explanation of parameters and general results

These two parameters describe important chemical attributes. The pH of a solution is the measure of the hydrogen ion (H^+) activity, which in aqueous solutions is primarily due to the hydronium ion (H_3O^+). Measured pH values below 7 indicate acid solutions, while solutions with pH values above 7 are alkaline. The redox potential (Eh) is an analogous measure of the electron (e^-) activity. High values of Eh denote oxidizing conditions, while low values denote reducing conditions. However, Eh differs from pH in that though water can adsorb or release H^+ to form H_3O^+ or OH^-, enabling easy and reproducible measurement of pH, the H_2O molecule does not react with electrons, making measurement and interpretation of Eh [6] more complicated than for pH.

Depending on the chemical environment, Eh may be controlled by reduction-oxidation couples such as Fe^{2+}/Fe^{3+}, O_2/H_2O_2, or SH^-/SO_4^{2-}. The Eh of solutions at depth, where pyrite is oxidizing, will be controlled by S couples such as SH^-/S or SO_3^{2-}/SO_4^{2-}, giving a low Eh. Closer to the surface, Fe^{2+} begins to oxidise to Fe^{3+}. This ion quickly hydrolyses and precipitates, and Eh is controlled by the $Fe^{2+}/Fe(OH)_{3(s)}$ couple. In oxidized solutions the O_2/H_2O_2 couple may dominate Eh, though more weakly than the $Fe^{2+}/Fe(OH)_{3(s)}$ couple, due to the slow kinetics of reaction.

Consideration of such reactions led to Sato's (1960) summary of groundwater pH/Eh controls, which is shown graphically in Fig. 21. He roughly divided groundwaters into three environments: the depth environment which is dominated by the chemistry of magnetite/hematite and SH^-/SO_4^{2-}; a transitional zone; and the upper weathering environment where groundwater Eh is dominated by the O_2/H_2O_2 couple. Additionally, pH is maintained below 10, under control of carbonate precipitation, and in acid conditions pH and Eh are controlled jointly by the $Fe^{2+}/Fe(OH)_3$ couple. A compilation of groundwater Eh and pH determinations by Baas Becking *et al.* (1960) agrees very well with this model.

Also shown in Fig. 21 are the superimposed pH/Eh values for the water samples. The Mt. Gibson and regional groundwaters show the pH/Eh characteristics of oxidizing groundwaters. Exceptions

[6] A description of Eh theory and the problems involved in measurement and interpretation is given in Hostettler (1984).

to this are the Midway waters, which are dominated by the $Fe^{2+}/Fe(OH)_3$ couple and MG35, which is an oxidized, acidic water. The results for these samples are discussed in Sections 4.6.2 and 4.6.3.

4.6.2 Midway waters

Solution Eh values were not obtained for the Midway samples MG13 and MG43 due to equipment problems. A number of chemical parameters suggest these samples to be considerably less oxidizing than the surrounding groundwaters:

(i) ferrous iron (Fe^{2+}) is high (> 50 mg/L; Fig. 22c);
(ii) dissolved oxygen (DO) is low (≤ 3.3 mg/L; Fig. 22b);
(iii) nitrate (formed by oxidation of ammonia) is low (< 2.4 mg/L; Fig. 22c).

In addition, these waters contained very low HCO_3, in comparison with other waters which contained higher levels of this anion (Fig. 22c). The chemistry of the Midway anomaly is illustrated in Figs. 23a and 23b, which show a line profile for various elements going from waters south of the Midway area (R < 4000), the two Midway pit holes MG13 (R = 4300) and MG43 (R = 4950), and MG35, which lies north of the Midway area (R = 5600). (The precise values of R were calculated by extending the line in Fig. 5 back to Tobias' Find, which was given an arbitrary R value of 0). The position of this line profile is shown in Fig. 5. The enrichment in Fe, and the depletion in dissolved oxygen, NO_3 and HCO_3 at Midway can be clearly observed.

The high Fe^{2+} in the Midway waters possibly originates via the oxidation of pyrite:

$$FeS_2 + {}^7/_2O_2 + H_2O \Rightarrow Fe^{2+} + 2SO_4^{2-} + 2H^+. \quad ...(1)$$

Unless neutralized this reaction may cause highly acid groundwaters. In many environments pyrite oxidation is buffered by carbonate (e.g. calcite, dolomite) dissolution:

$$CaCO_3 + H^+ \Rightarrow Ca^{2+} + HCO_3^-. \quad ...(2)$$

Under these conditions intermediate products of sulphur oxidation such as thiosulphate ($S_2O_3^{2-}$) and sulphite (SO_3^{2-}) are commonly formed:

$$FeS_2 + {}^3/_2O_2 \Rightarrow Fe^{2+} + S_2O_3^{2-} \quad ...(3)$$

(Listova *et al.*, 1968; Granger and Warren, 1969; Goldhaber, 1983; Webster, 1984). These compounds have a high stability in neutral and alkaline conditions (Rolla and Chakrabarti, 1982). They have a particular importance in Au hydrogeochemistry due to the very high solubility of the Au thio complexes (Sections 4.7.3, 4.8.4).

Carbonate buffering of pyrite oxidation will only be important in rocks with significant carbonate contents. Mann (1984b) has estimated that 400-800 g of $CaCO_3$ is required for every 240 g of FeS_2 in order to maintain alkaline conditions for thiosulphate production. Thus, there will be significant Au thiosulphate mobilization only where the carbonate/pyrite ratio is at or above this level.

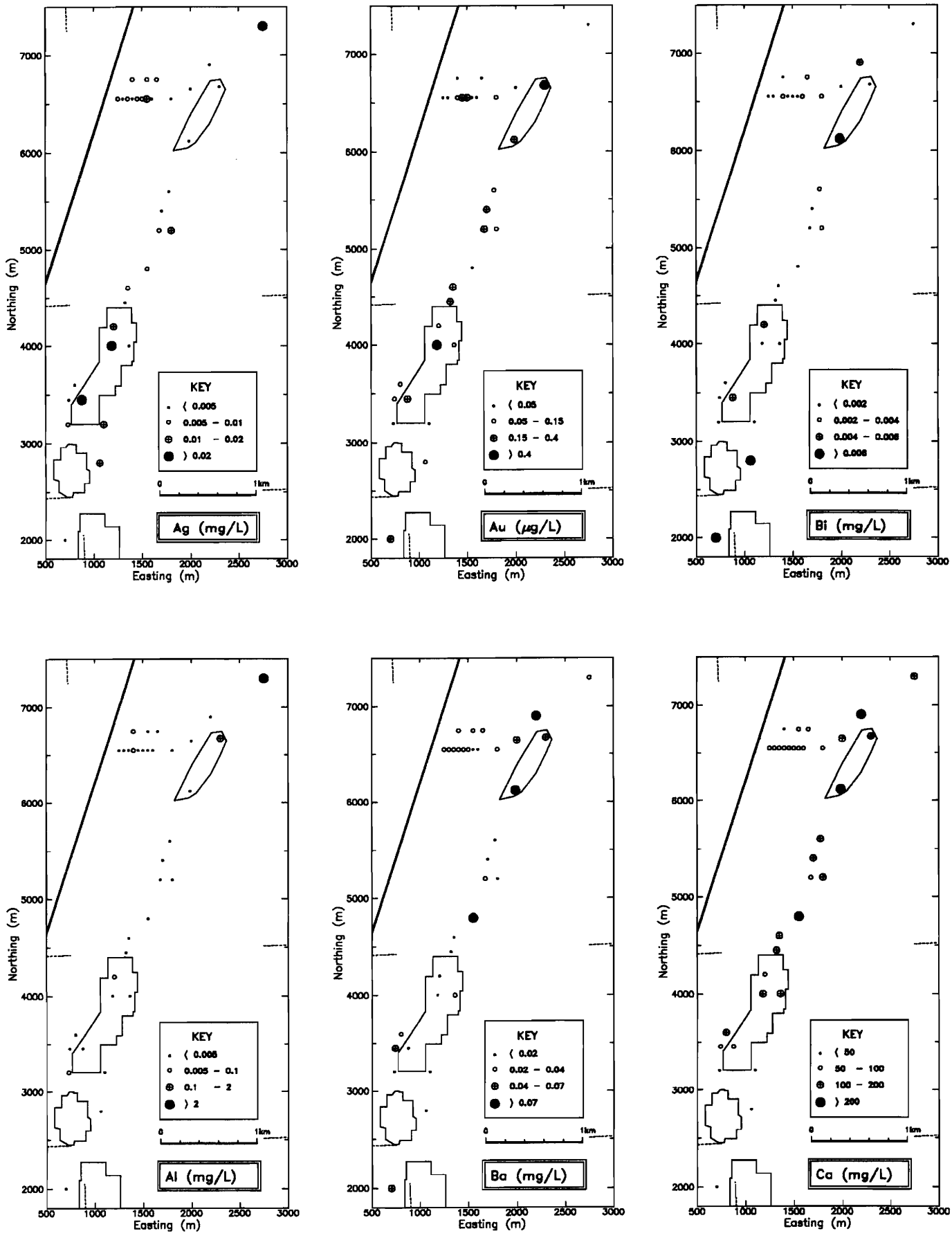

Figure 22a: Distributions of Ag, Al, Au, Ba, Bi and Ca within the Mt. Gibson Au Mine Area.

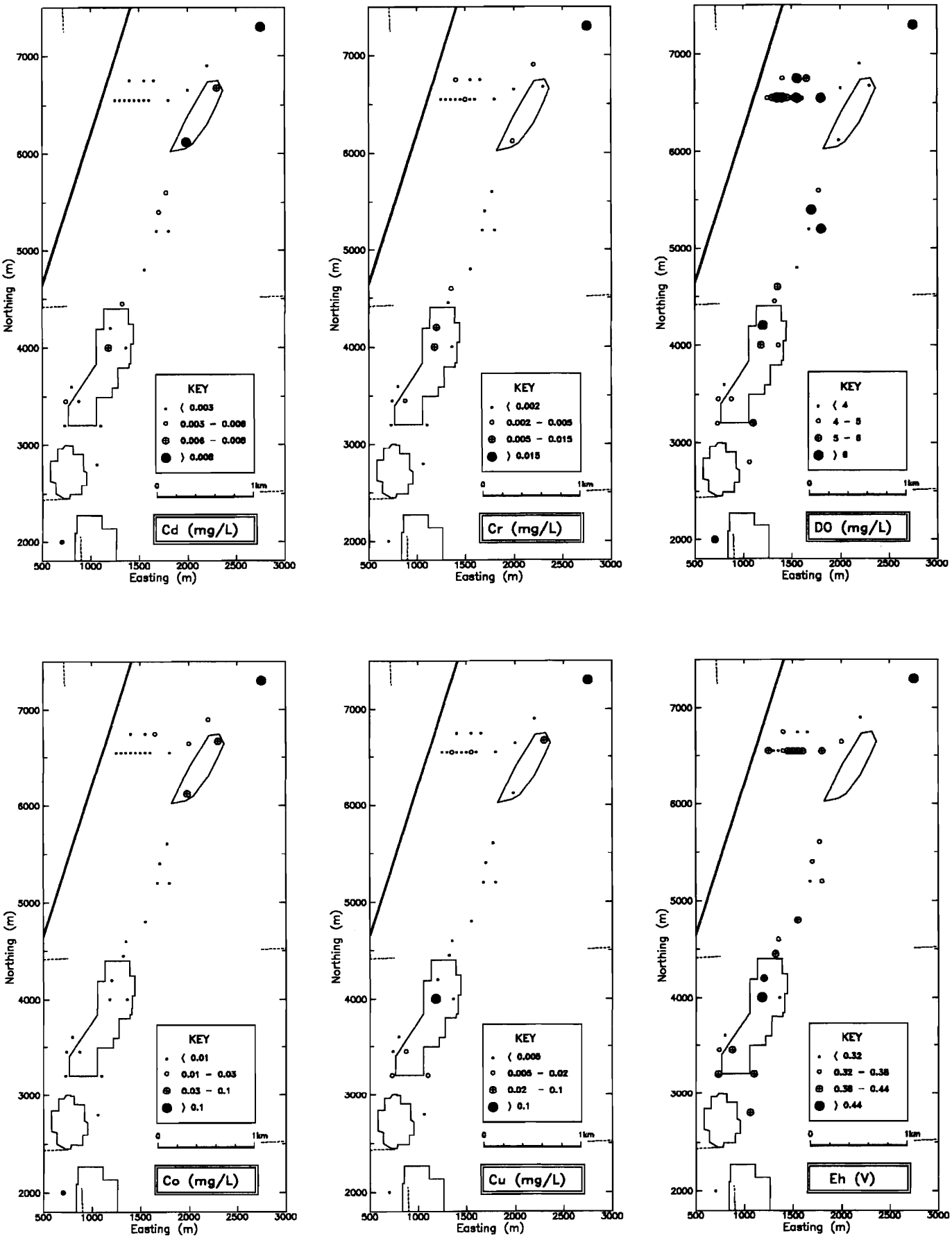

Figure 22b: Distributions of Cd, Co, Cr, Cu, DO (dissolved oxygen) and Eh within the Mt. Gibson Au Mine Area.

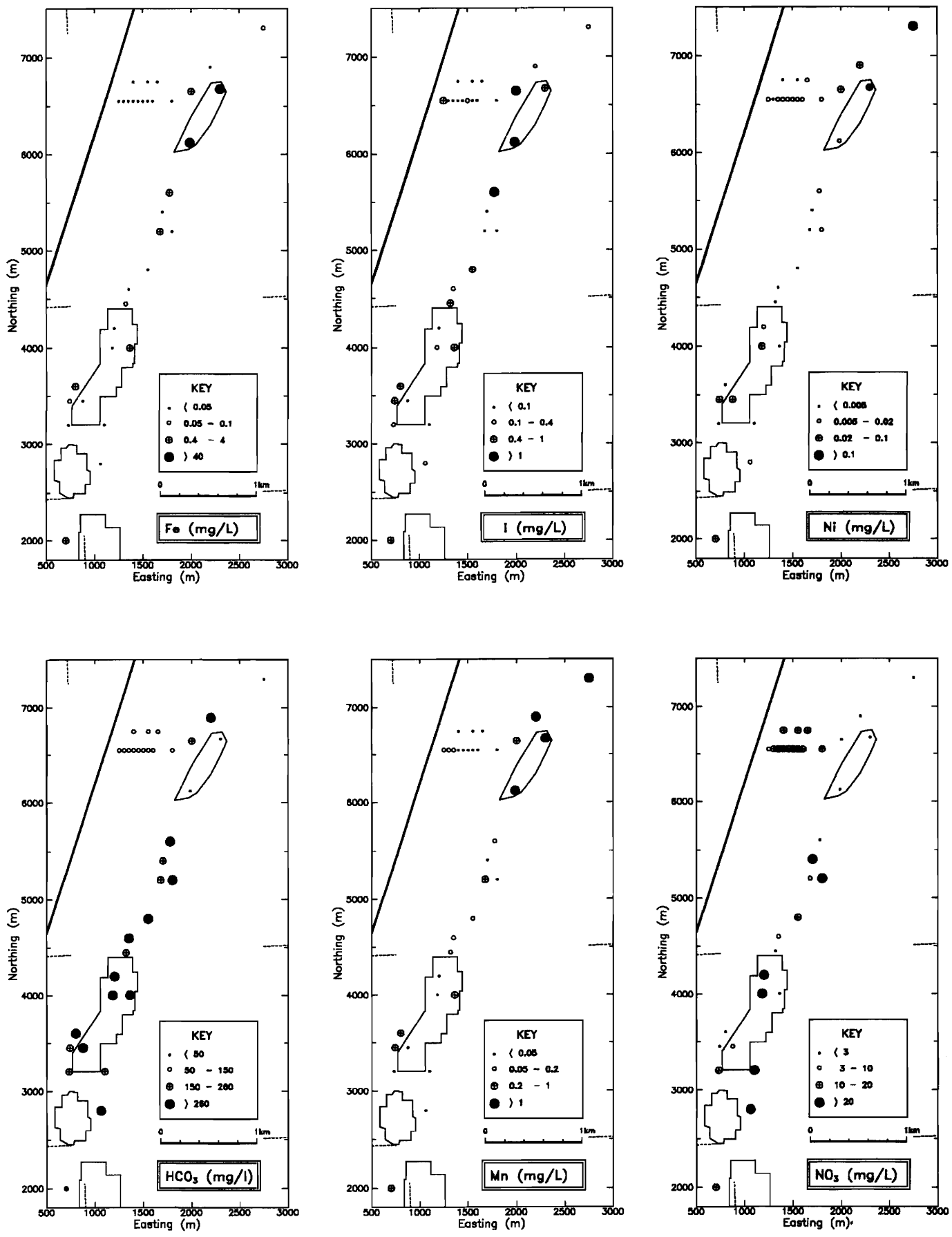

Figure 22c: Distributions of Fe, HCO_3, I, Mn, Ni and NO_3 within the Mt. Gibson Au Mine Area.

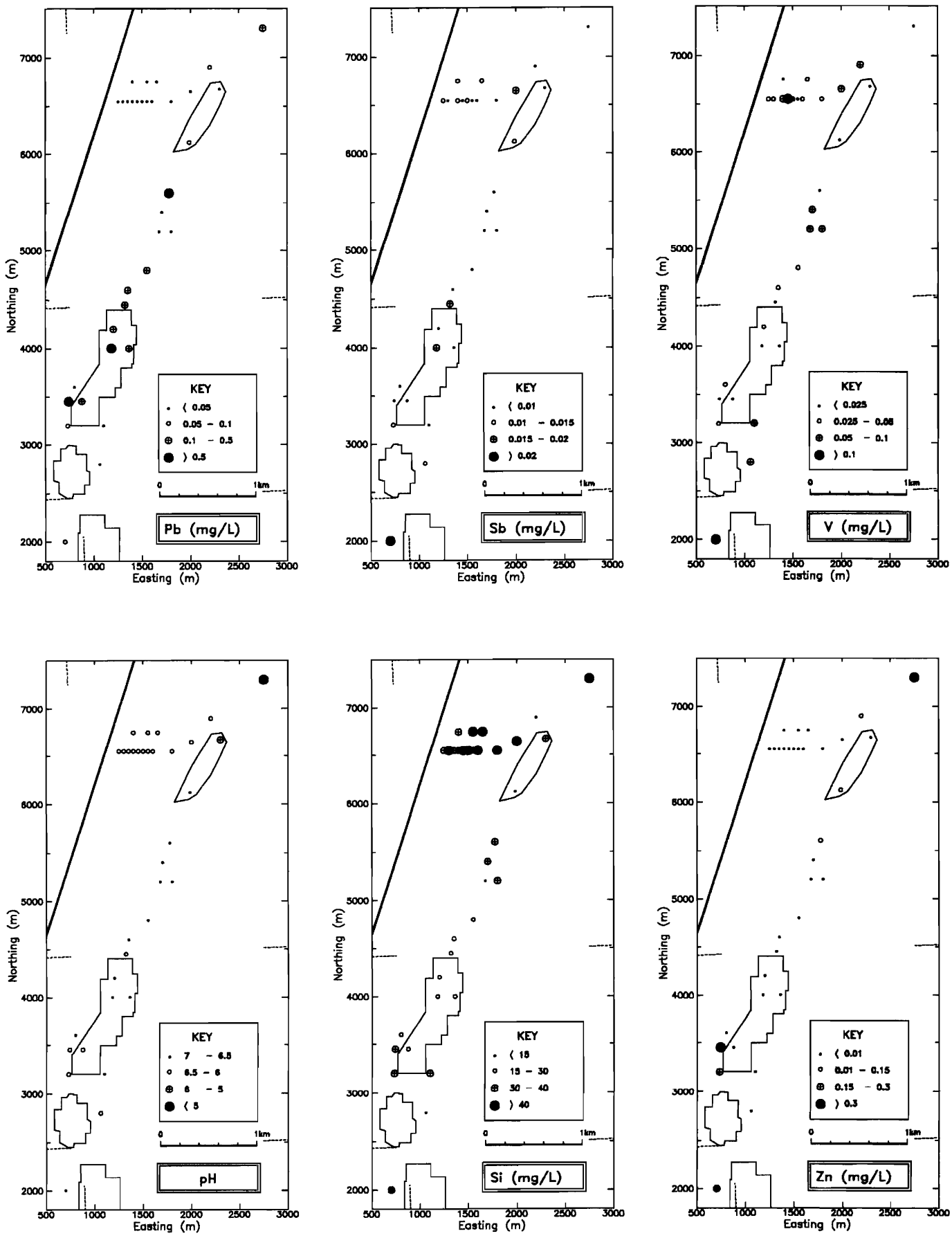

Figure 22d: Distributions of Pb, pH, Sb, Si, V and Zn within the Mt. Gibson Au Mine Area.

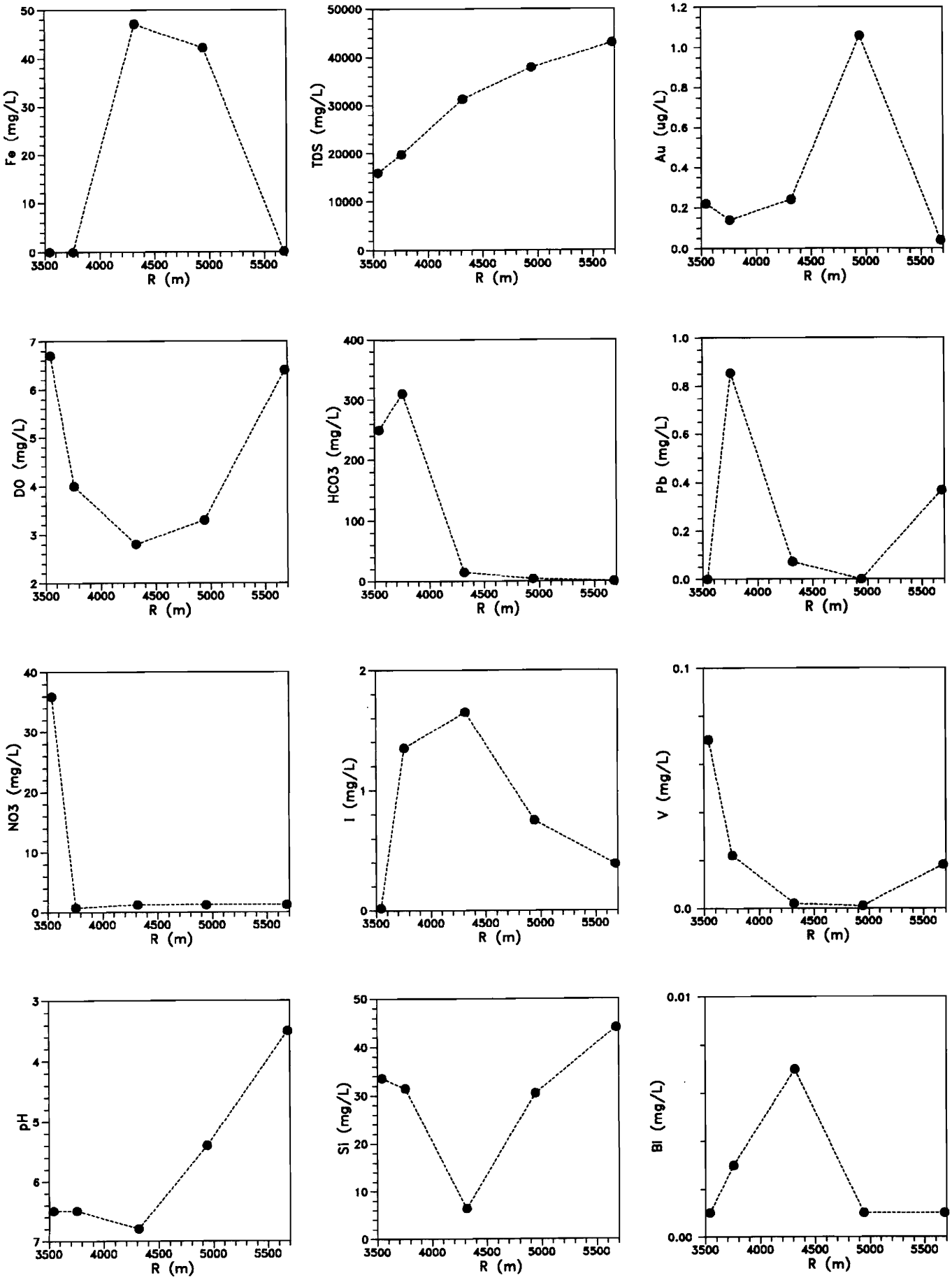

Figure 23a: Variations in Fe, DO (dissolved oxygen), NO3, pH, TDS, HCO3, I, Si, Au, Pb, V and Bi vs R (indicated in Fig. 5) across the Midway Transect (see Section 4.6.2 for details).

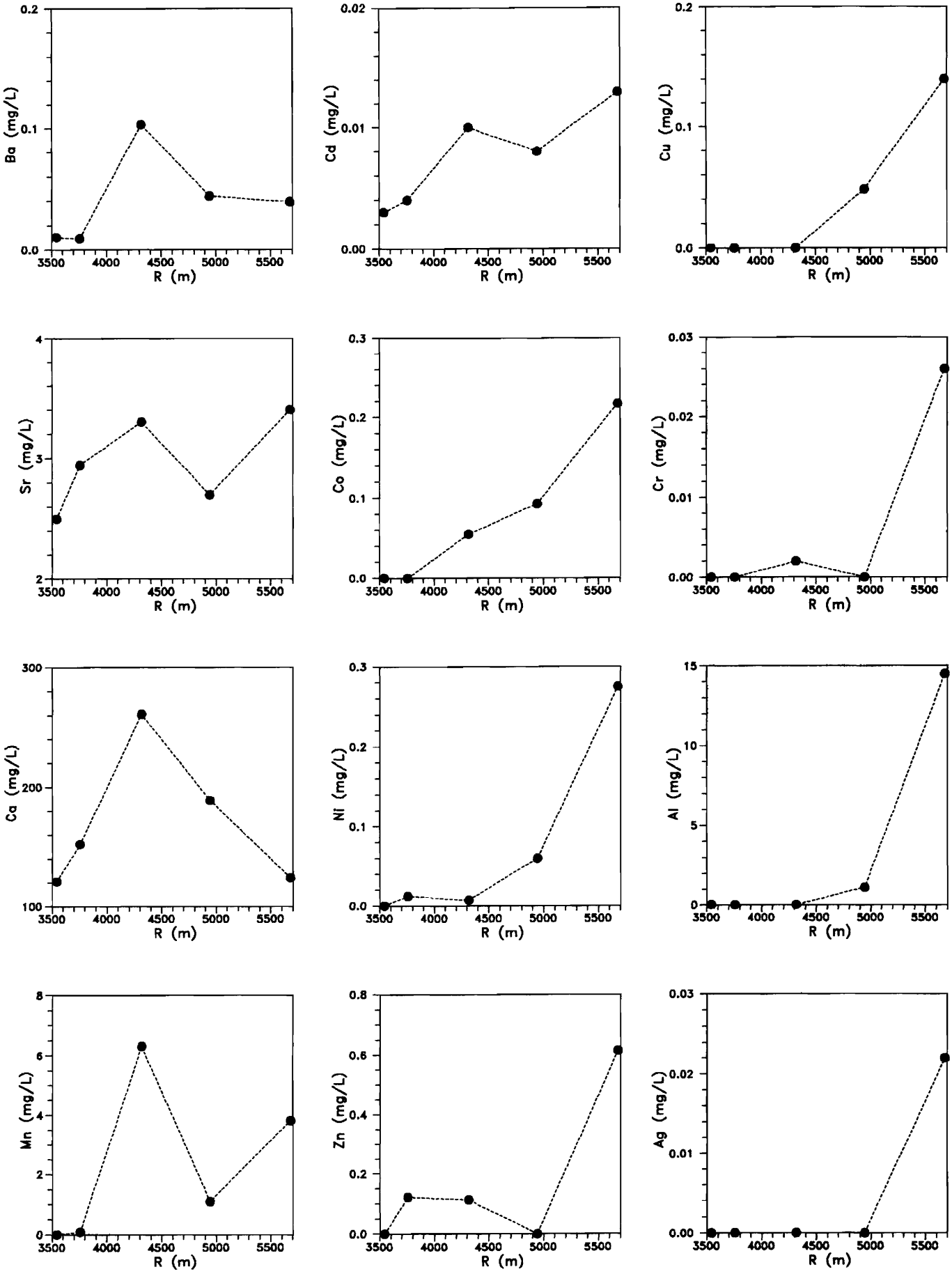

Figure 23b: Variations in Ba, Sr, Ca, Mn, Cd, Co, Ni, Zn, Cu, Cr, Al and Ag vs R (indicated in Fig. 5) across the Midway Transect (see Section 4.7.4 for details).

Both Ca and HCO_3 concentrations in the Midway groundwaters are highly variable, consistent with a complex and/or localized (temporally or spatially) series of reactions. These could include calcite precipitation under alkaline conditions:

$$Ca^{2+} + HCO_3^- \Rightarrow CaCO_{3(s)} + H^+ \quad ...(4)$$

or gypsum precipitation under saline conditions:

$$Ca^{2+} + SO_4^{2-} \Rightarrow CaSO_4 \cdot 2H_2O \quad ...(5)$$

with major variations in pH also occurring during weathering of minerals such as pyrite (eqn. 1; acid producing) or feldspar:

$$2NaAlSi_3O_8 + 3H_2O \Rightarrow Al_2Si_2O_5(OH)_4 + 4SiO_2 + 2Na^+ + 2OH^- \quad ...(6)$$

(acid consuming), and from CO_2 degassing:

$$HCO_3^- + H^+ \Rightarrow CO_2(g) + H_2O. \quad ...(7)$$

With the information available the precise arrangement of these reactions cannot be delineated. However, the generally neutral character of the deep waters (e.g. MG13) suggests that the first stage of pyrite weathering (eqn. 1) is occurring under neutral conditions and that appreciable $S_2O_3^{2-}$ may therefore be produced (eqn. 3), with important concequences for Au mobility (Sections 4.7.3, 4.8.4).

4.6.3 Ferrolysis effects

Groundwaters at the north end of Midway (e.g. MG43) and beyond (MG35) show an increase in acidity and Eh, consistent with control of the groundwater pH/Eh couple by Fe oxidation/hydrolysis:

$$2Fe^{2+} + \tfrac{1}{2}O_2 + 5H_2O \Rightarrow 2Fe(OH)_3 + 4H^+. \quad ...(8)$$

Such reactions are called ferrolysis (Brinkman, 1977). The measured pH and Eh values for samples MG13, MG43 and MG35 corresponded closely with ferrolysis solutions measured by Mann (1984a). Sample MG35, in particular, had a pH of 3.5 and an Eh of 0.53 V. Such a groundwater chemistry could be due to oxidation of the high levels of Fe in Midway-type waters. Oxidation of the MG13 and MG43 solutions was simulated by allowing collected solutions to oxidise in the laboratory and by computer simulation (using the computer program PHREEQE) of oxidation. Results are shown in Table 5.

As observed, the laboratory oxidized Midway solutions had similar pH values to MG35, consistent with MG35 water being a Ferrolysis water.

Thus, the groundwaters at Midway (MG13 and MG43) and just down-gradient (MG35) were seen to be particularly anomalous, with reducing conditions and high Fe^{2+} at Midway, and acid oxidizing conditions down gradient. As described below, various minor element anomalies were observed for these

waters, consistent with these effects. The acidic waters may have arisen from oxidation of Midway-type waters. The Midway waters may have flowed north until they hit a redox front AND/OR the difference may be temporal, i.e. waters in the MG35 area may have originally been similar to Midway and may have oxidized with time. At present, we have no site information that would allow us to distinguish between these two hypotheses.

Table 5. Oxidation of Midway Waters

Sample	Initial pH	Final pH	
		(observed)	(theory)
MG13	6.8	3.68	3.54
MG43	5.4	3.77	3.58
MG35	3.5	3.4	-

4.7 Minor Element Hydrogeochemistry

4.7.1 Representation of data

In addition to the major elements discussed above, the waters were analysed for a number of other elements: namely Ag, Al, Au, Ba, Bi, Cd, Co, Cr, Cu, Fe, I, Mn, Ni, Pb, $S_2O_3^{2-}$, Sb, V and Zn. Distribution of element concentrations within the mine area are plotted in Figs. 22a - 22d, while concentrations of selected elements vs. TDS are shown in Figs. 24 - 29.

A number of behaviours were observed. These are discussed below in terms of the anomalous regions in Sections 4.7.2 to 4.7.5.

4.7.2 Regional observations

A number of the elements had increased concentrations in the saline waters, particularly the Lake Karpa sample MG41 (Group 9). These elements included most of the transition metals: e.g. Cr, Mn, Co, Ni, Cu, Zn, Ag and Cd. This increase in concentration with salinity has been demonstrated for the heavy metals Cu, Pb and Zn (Mann and Deutscher, 1977, 1980) and is possibly due to Cl complexation in saline waters. When expressed relative to salinity, the concentration effect observed at this site is generally no greater than, and commonly less than, that expected from concentration of soluble constituents with evaporation (Figs. 25, 26, 27, 29). In this regard, this effect is minor, relative to other anomalies described below.

As observed in terms of the major element data, the mineralized (Groups 2, 3, 4, 5, 6 and 7) and unmineralized waters (Groups 11 and 12) had different trace element contents. The unmineralized waters were lower in Ag (Fig. 25), Au (Fig. 24), Cd (Fig. 26), Cu, Ni and Pb (Fig. 29). With the exception of the Karpa Bore, which lies near the mineralized area and has detectable Au, all of the unmineralized waters recorded Cu, Cd and Au levels below the detection limit. Unfortunately, the unmineralized water samples are not a good blank for comparison, as they represent a different aquifer type (Sections 4.2, 4.3), rather than being water from an unmineralized fractured rock aquifer, which could be directly comparable to the Mineralized waters.

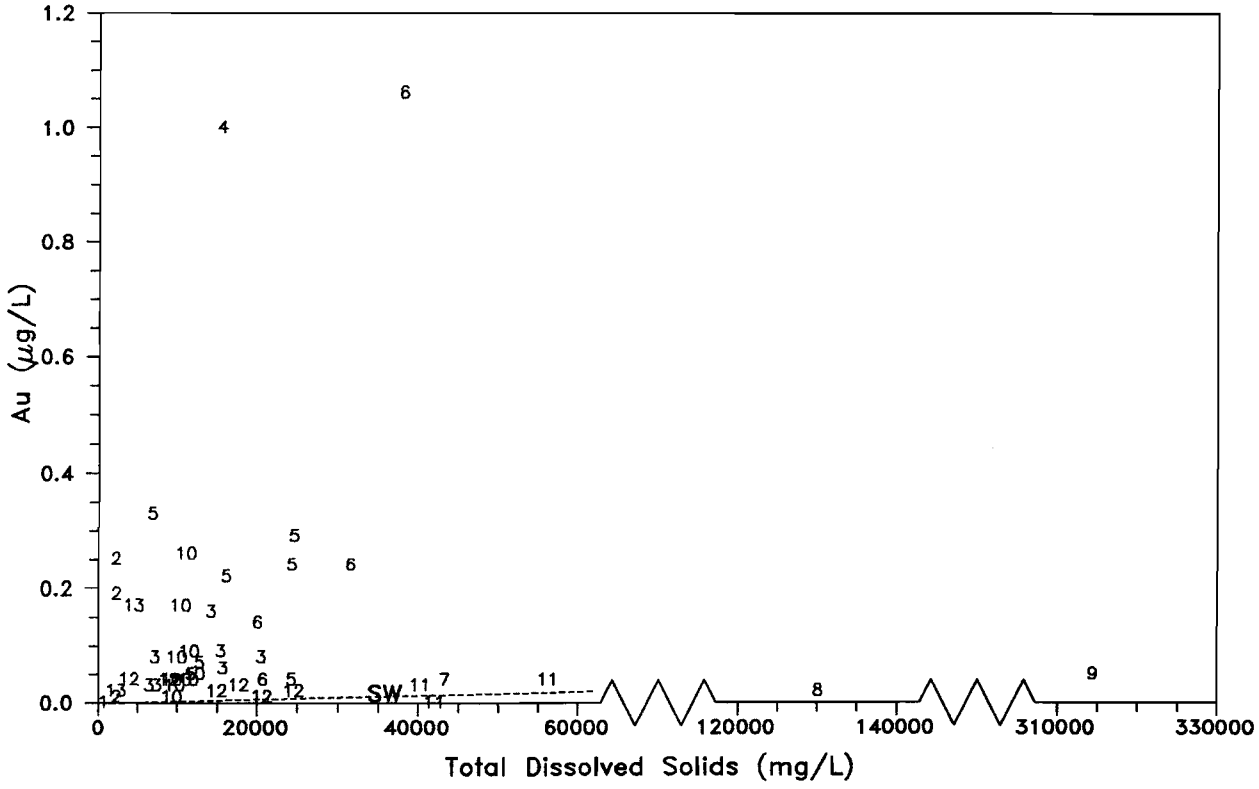

Figure 24. Au vs. TDS for Mount Gibson Waters.

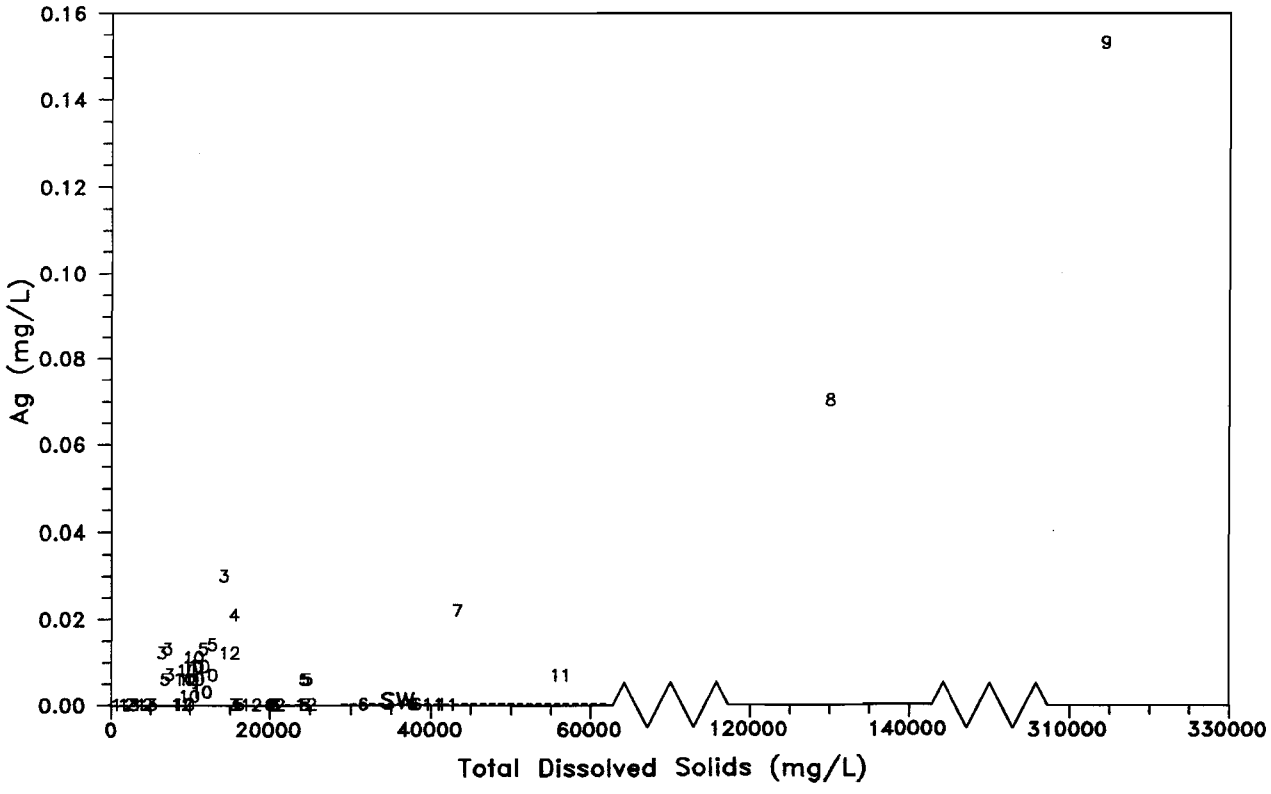

Figure 25. Ag vs. TDS for Mount Gibson Waters.

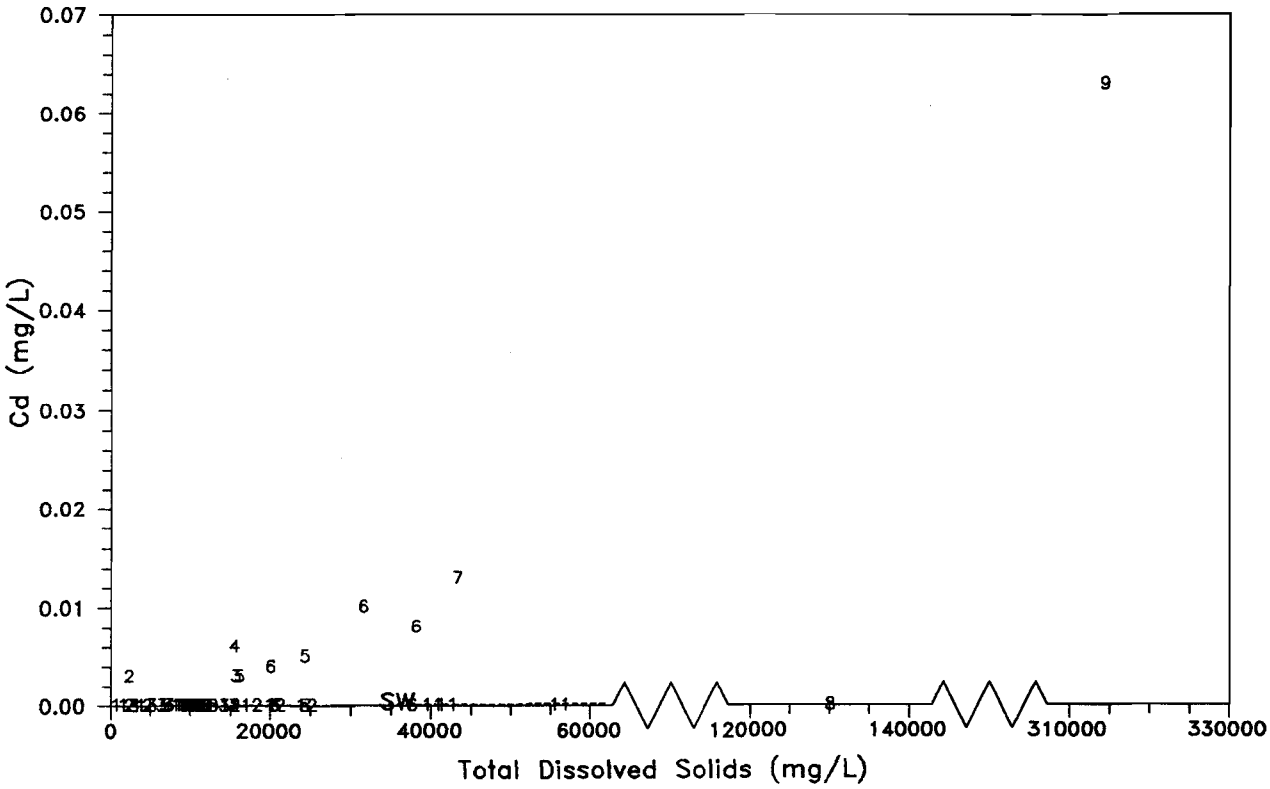

Figure 26. Cd vs. TDS for Mount Gibson Waters.

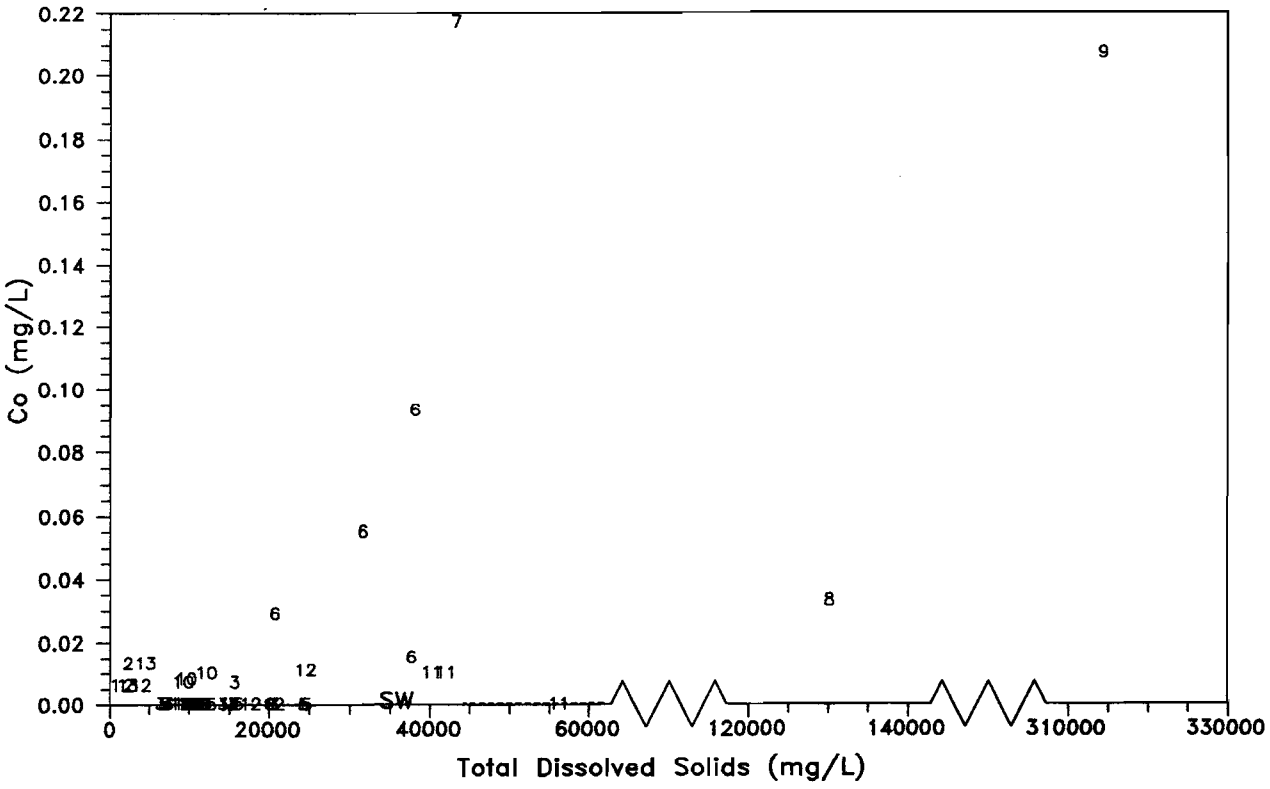

Figure 27. Co vs. TDS for Mount Gibson Waters.

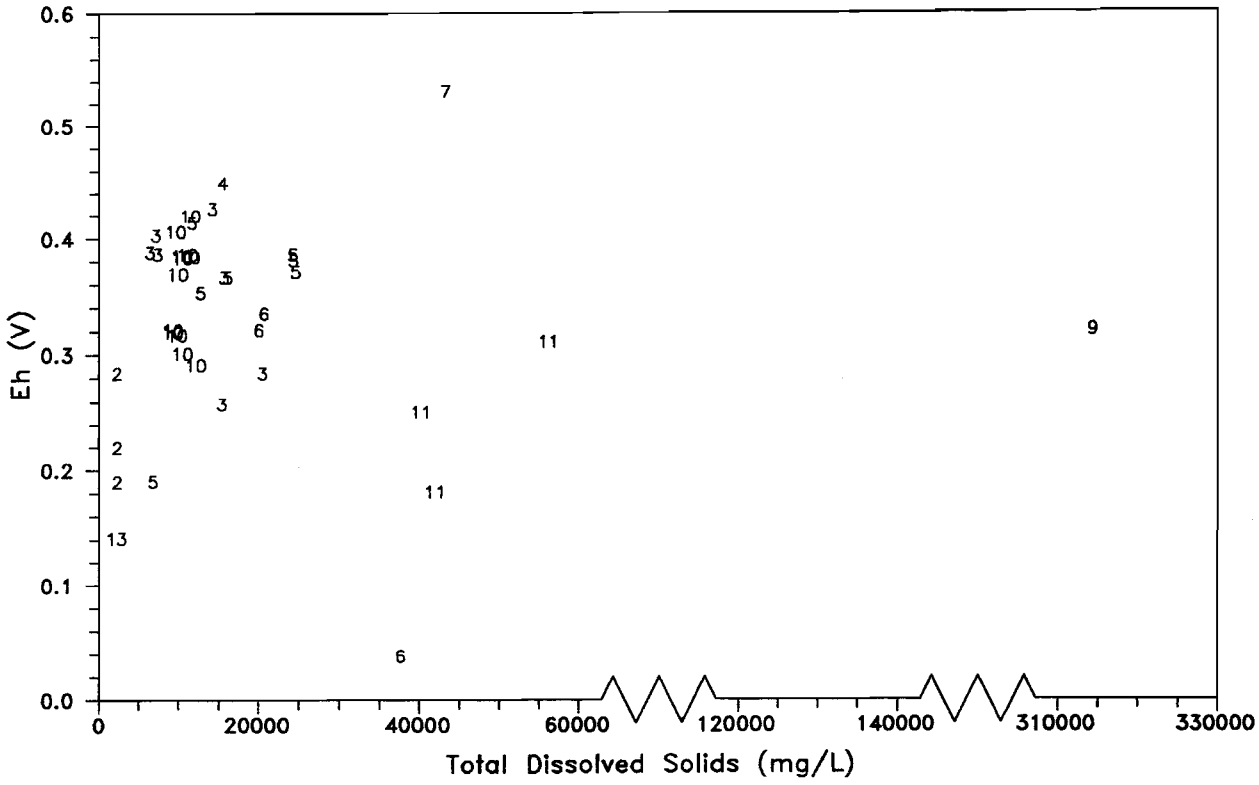

Figure 28. Eh vs. TDS for Mount Gibson Waters.

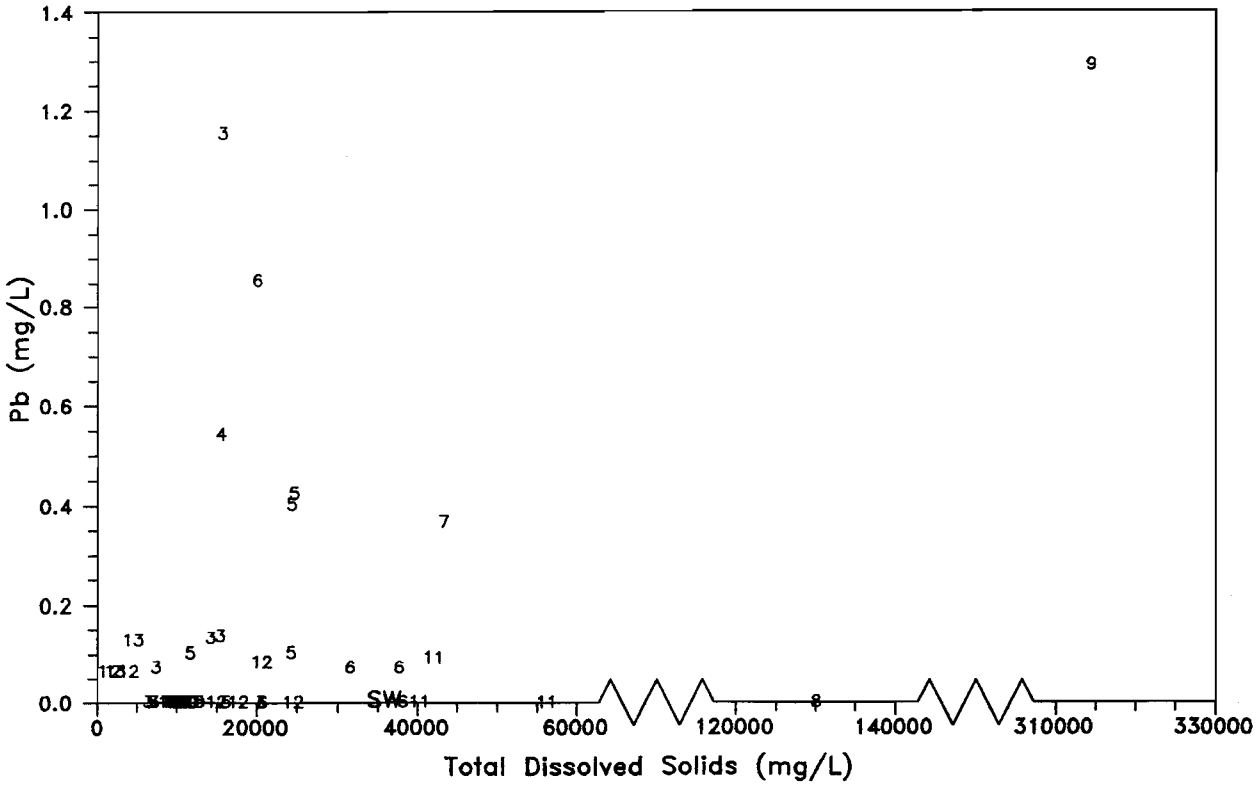

Figure 29. Pb vs. TDS for Mount Gibson Waters.

Within the mine area the Sterilization holes (Group 10) were clearly depleted in Pb (Fig. 29) and probably in Cd (Fig. 26), relative to the mineralized waters. The reason for this marked effect is not clear, but may be due to different geologies between the Sterilization area and the mineralized area. Lead has a marked anomalous behaviour, possibly due to its high mobility as the $PbCO_3^0$ complex (Section 4.8.3).

4.7.3 Midway waters

The Midway waters were highly anomalous, being enriched in Au, Fe, Mn, Co, Cd, Ba and I, relative to the other Mine waters (Figs. 22a - 22d).

The high dissolved Au values (up to 1 μg/L) can explain the supergene Au observed in this area. Due to the low levels of Au it is not possible to directly determine the chemical form of the dissolved Au. On the basis of previous work (Krauskopf, 1951; Cloke and Kelly, 1964; Goleva *et al.*, 1970; Miller and Fisher, 1973; Lakin *et al.*, 1974; Pitul'ko, 1976; Plyusnin *et al.*, 1981; Webster, 1984, 1986; Webster and Mann, 1984; Gray, 1989) the most likely forms are either as the chloride complex ($AuCl_2^-$) or the thiosulphate complex [$Au(S_2O_3)_2^{3-}$]. The presence of high levels of Fe^{2+} precludes the Au being present as $AuCl_2^-$, as this species would be readily reduced in such an environment (Mann, 1984b). Conversely, $Au(S_2O_3)_2^{3-}$ is much more stable in reducing environments and would not be reduced by Fe^{2+} in neutral waters. This hypothesis was tested by ion chromatography analysis for the $S_2O_3^{2-}$ ion in selected samples (Appendix 1), which indicated the $S_2O_3^{2-}$ concentration to be at or below the detection limit for most samples tested, with the exception of one of the Midway waters (MG34; 0.040 mg/L), Tobias' Find waters (MG19, MG20; 0.125, 0.135 mg/L), and Karpa Spring (MG42; 0.060 mg/L). This result is not inconsistent with the presence of $Au(S_2O_3)_2^{3-}$, as the Au complex could be formed at the interface where sulphides are weathering (and forming $S_2O_3^{2-}$) and Au is being dissolved. Because of the strength of the Au^+- $S_2O_3^{2-}$ bond the $Au(S_2O_3)_2^{3-}$ complex can then act to mobilise the Au and stabilise the $S_2O_3^{2-}$ ligand: i.e. $Au(S_2O_3)_2^{3-}$ is more stable than $S_2O_3^{2-}$ alone.

Thus, though Au is not present as $AuCl_2^-$, there is no positive evidence for $Au(S_2O_3)_2^{3-}$. Other species considered were the iodide complex (AuI_2^-) and colloidal Au. The presence of AuI_2^- was considered because of the relatively high levels of I^- in the Midway waters. Speciation analysis by PHREEQE (Section 4.8.4) indicated AuI_2^- would be thermodynamically preferred over $AuCl_2^-$ in the Midway area. However, it is expected that AuI_2^- would, like $AuCl_2^-$, be reduced by Fe^{2+}. Colloidal Au has not been observed in the natural environment (Boyle, 1979; Kolotov *et al.*, 1980). Laboratory syntheses have all involved organic suspensions (Goni *et al.*, 1967; Ong and Swanson, 1969; Ong *et al.*, 1970; Fedoseyeva *et al.*, 1986) suggesting that colloidal Au would only be important, if at all, in organic rich waters, such as soil solutions, rather than deeper groundwaters such as those studied here.

The other transition metals observed in anomalous concentrations at Midway were Fe, Mn, Co and Cd. The reason for this particular groundwater signature is not clear and may be related to the geochemistry of weathering, particularly of sulphide minerals. Both Ag and Cu had low solution levels in the Midway area (Figs. 22a and 22b), in comparison with the Group 8 water which was anomalous in Au, Ag and Cu (see below).

The Ba and I anomalies are of interest. The high Ba may indicate release from carbonate, which may be associated with the mineralization. Iodide is very strongly enriched (0.8 - 1.7 mg/L) in the Midway area. Two possible explanations are:

(i) iodide specifically arises from the source material in the Midway area,

AND/OR

(ii) groundwater conditions in the area of Midway protect iodide from oxidation whilst elsewhere more oxidizing conditions result in loss of iodide by volatilization.

The latter hypothesis is discounted by speciation analysis (Section 4.8.3) which indicates that iodine is present in all samples as I^- rather than I_2 or other oxidized iodine species, and therefore that volatilization as I_2 should not be a major process (Fuge, 1990). It is further refuted by the moderate level (0.4 mg/L) of iodide in MG35, down-gradient from Midway, despite it being the most oxidized water sampled in the Mount Gibson area. Use of the halides F, Cl and Br for detection of mineralization is well documented (Frick *et al.*, 1989 and references given therein). Work has suggested that I is a chalcophile element (Fuge and Johnson, 1984, 1986) extensively enriched in sulphide environments (Chitayeva *et al.*, 1971; Fuge *et al.*, 1988) and that it may be a useful pathfinder for mineralization (Xie Xuejing *et al.*, 1981; Andrews *et al.*, 1984; Fuge *et al.*, 1986). The Midway deposit may represent a general halide anomaly, with only the I enrichment being observed, due to the overriding salinity effect.

4.7.4 Ferrolysis effects

The Ferrolysis hole (Section 4.6.3) was enriched in Ag, Al, Cd, Co, Cr, Cu, Mn, Ni and Zn (Fig. 22a - 22d). Some of these enrichments were observed for the Midway region, with additional enrichments due to the acidification of this water. Fig. 23b shows the line profile for the various metals at Midway and MG35 (see Section 4.6.2 for explanation of the plot). The plots are ordered in inverse order of the pH required for dissolution of the corresponding solid hydroxide (pH_{sol}). That is, $Ba(OH)_{2(s)}$ is dissolved in waters of pH less than 10.2, giving this metal the highest pH_{sol} of the metals investigated. The pH_{sol} of Sr and Ca are only slightly lower [e.g. $pH_{sol}(Ca^{2+})$ = 9.4]. These three group II metals all showed similar behaviours, with no enrichment in the Ferrolysis sample (Fig. 23b).

The next group of similar metals is Mn and Cd, with $pH_{sol}(Mn^{2+})$ = 7.6 and $pH_{sol}(CdCl^+)$ [7] = 7.7 These two metals showed roughly similar behaviours, with a weak enrichment in the Ferrolysis water. The elements Co, Ni and Zn had similar pH_{sol} values [$pH_{sol}(Co^{2+})$ = 6.6; $pH_{sol}(Ni^{2+})$ = 6.4; $pH_{sol}(Zn^{2+})$ = 6.3] and showed very similar behaviours, with a marked enrichment going from Midway into the Ferrolysis region. The most acid metals are Cu, Cr and Al [$pH_{sol}(Cu^{2+})$ = 4.4; $pH_{sol}(Cr^{3+})$ = 4.0; $pH_{sol}(Al^{3+})$ = 3.5] and these metals were enriched only under very acid conditions.

In summary, a low pH_{sol} implies that the metal will be specifically enriched in the acidic waters only, whereas metals with high pH_{sol} values will have little enrichment in the acidic waters. In fact the

---

[7] $CdCl^+$ was used here as speciation analyses, described in Section 4.8.1, indicated this to be the dominant Cd solution species; in comparison $pH_{sol}(Cd^{2+})$ = 6.9, which is a minor change.

group II metals show depletion in the acid waters, particularly when related to the increase in TDS over the transect (Fig. 23a), possibly due to precipitation of sulphate salts [i.e. $BaSO_4$ (barite) or $CaSO_4 \cdot 2H_2O$ (gypsum)].

The sequence of dissolution of metals observed at this site correlates with other observations. Blowes and Jambor (1990) reported the concentrations and mobilities of metals during weathering of sulphide tailings to generally follow the order Fe = Mn ≥ Zn > Ni ≥ Co > Pb > Cu, which is similar to the order Co = Ni > Zn > Pb > Cu observed by Dubrovsky (1986) for a tailings impoundment. This compares with the sequence for mobilization of Ba,Sr,Ca > Mn,Cd > Co,Ni,Zn > Cu,Cr,Al suggested for this site.

This effect is sensible as dissolution of metals is related to competition between solution and solid phases, which can include sorbed or precipitated ions. These solid phases involve ion - oxygen bonding. Ions with low pH_{sol} values have a high affinity for oxygen and therefore require highly acid conditions for dissolution, while ions with high pH_{sol} values have lower oxygen affinities and are more readily dissolved. Thus, the order in which metals ions are sorbed onto ferrihydrite, goethite, hematite and magnetite (compiled in Gray, 1986; using references compiled from Grimme, 1968;, Kinniburgh *et al.*, 1976; Forbes *et al.*, 1976; Davis and Leckie, 1978; Venkataramini *et al.*, 1978; McKensie, 1980; Benjamin and Leckie, 1981; Kinniburgh and Jackson, 1982; Padmanabham, 1983a,b) is very similar to that discussed for pH_{sol}: Ba,Sr,Ca < Mn,Ca < Co,Ni,Zn < Cu. (Note that this order is for sorption, so is inverted from the order for mobilization of metals, given above.) This order of cations is therefore obtained from both theoretical (pH_{sol} values) and empirical (iron oxide sorption) investigations, and can explain the anomalous behaviour of most of the minor elements in Midway and Ferrolysis water samples.

Silver shows high solubility in the acidic water, and is included in Fig. 23b. However, the reason for this acid solubility is not clear. Silver is present in solution as the $AgCl_2^-$ and $AgCl_3^{2-}$ ions in saline waters (Section 4.8.1; Table 6). In the Midway waters the AgI_2^- ion may also be important, due to the high concentrations of I^- in these waters. This differs from the other metals discussed, which are generally present as the uncomplexed ion, or singly complexed in the case of Cd. Additionally, Ag is present at concentration levels close to that at which it will precipitate as $AgI_{(s)}$, unlike most of the other metals, which are present at concentrations well below that for precipitation of separate mineral phases (Section 4.8.3). The Ag behaviour may be due to a number of chemical factors such as salinity and iodide concentration, in addition to the pH effect which is observed to be the major control on concentration of other metals.

The other ions showing anomalous behaviour are Pb, V, Sb and Bi (Fig. 23a). Pb would commonly be expected to behave similarly to Cd, as both can form the mono-chloride complex, with similar chemistries. However, Pb can also speciate as the $PbCO_3^0$ complex (Section 4.8.1). It may be that the Pb is released at high concentrations (up to 1 mg/L) as the $PbCO_3^0$ complex in the initial region of Midway, as represented by MG16; while within the low carbonate region of Midway (MG13, MG43) solubility of this ion is strongly reduced; following which Pb is redissolved as the $PbCl^+$ ion in the acidic waters represented by MG35.

The behaviours of V, Sb and Bi are possibly a consequence of these elements being present as the oxides $H_2VO_4^-$ (VO^{2+} in MG35), $SbO(OH)^0$ and BiO^+, rather than as the unhydrolysed cations (e.g.

Fe^{2+}, Mn^{2+} etc.). Additionally, the concentrations of Pb, V, and Sb may all be controlled by solubility of phases not primarily affected by pH (Section 4.8.3), namely:

Pb	$Pb_3(VO_4)_2$, $Pb_2V_2O_7$
V	$Pb_3(VO_4)_2$, $Pb_2V_2O_7$, Fe-vanadate
Sb	$Sb(OH)_3$: (as the relevant solution species is $SbOOH^0$, solubility is independent of pH).

Thus, the elements that did not show behaviours correlated with the change in pH were influenced by additional factors such as carbonate complexing, formation of soluble oxides, and control of solution concentration by equilibration with a particular mineral phase.

The MG35 water (Group 7) had low soluble Au, in comparison with the relatively high levels at Midway (Figs. 22a, 23a and 24). This is consistent with Au mobilization at Midway being due to thiosulphate or other thio compounds, as such ligand complexes would be decomposed by acidification. Gold thus precipitated would not redissolve as $AuCl_2^-$, as oxidizing potentials at MG35, though high, are not sufficient for the reoxidation of Au metal. This implies that ferrolysis, by generating acidic conditions, can act to precipitate Au occurring as thio- (or other) complexes. Such a scheme can explain the common presence of secondary Au in laterite.

4.7.5 The MG8 anomaly

In addition to the Midway anomaly, a second, highly localized, Au anomaly was observed for the MG8 (Group 4) water (Figs. 22a and 24). This water showed several interesting characteristics when compared with the surrounding Group 3 and Group 5 waters, in that it:

(i) contained more HCO_3 than any of the other Orion or Yorktown waters (Fig. 10);

(ii) was strongly enriched in SO_4 (Fig. 14) and moderately enriched in Br, relative to salinity;

(iii) was strongly enriched in Mg (Fig. 17) and moderately enriched in Sr (Fig. 18), relative to salinity;

(iv) had the second highest redox potential of all of the waters analysed (Fig. 28), with the highest redox potential being measured for MG35 (the Ferrolysis water);

(v) was anomalously high in Ag, Au, Cd, Cr, Cu, Ni, Pb and Sb (Figs. 22a - 22d, 24, 25, 26, 29).

A possible explanation for this anomaly is that the drill hole is intersecting a localized Au/pyrite vein. Weathering within this vein would result in strong acid production and oxidizing conditions and the trace elements mentioned above would be dissolved. Waters flowing from the weathering pyrite would be neutralized by reactions with carbonates and other alkaline minerals. In such a neutralized water the anomalously high trace metal concentrations will be quickly reduced by sorption and precipitation reactions, explaining the localized nature of the anomaly. The only element to show any major dispersion from MG8 was Pb (Fig. 29), which commonly has a high mobility due to complexation by carbonate (see above; Section 4.8.1).

4.8 Speciation Analysis

4.8.1 Introduction

The speciation of the analysed elements, and their potential solid phases, was investigated using the speciation program PHREEQE (Parkhurst *et al.*, 1980). In this program the concentration of the elements is entered, along with other relevant parameters such as temperature (assumed to be 25 °C), pH, Eh and density (calculated from TDS). Using data for association constants for all the potential complexes, the program calculates, by a system of iterations, the activities and concentrations of all phases [8].

Additionally, the program calculates whether the solution is oversaturated with regards to specified solid phases. For a particular solid phase the Ion Activity Product (IAP) is calculated: e.g. for calcite, which precipitates according to:

$$Ca^{2+} + CO_3^{2-} \Rightarrow CaCO_{3(s)} \qquad ...(9)$$

the IAP is equal to $[Ca^{2+}] \times [CO_3^{2-}]$, where $[Ca^{2+}]$ denotes the activity of the free Ca^{2+} ion. This is related to the activity product of these ions for equilibrium (K_T) by calculation of the parameter $\log(IAP/K_T)$. In common with a number of other texts, this parameter is referred to here as the saturation index (SI). If the SI parameter equals zero then the water is in equilibrium with the solid phase, under the conditions specified. Where the SI is less than zero the solution is under-saturated with respect to the phase and the phase, if present, may dissolve. If the SI is greater than zero then the solution is super-saturated with respect to this phase and the phase can precipitate out of solution.

Note that this analysis only specifies POSSIBLE reactions. Kinetic constraints may rule out reactions that are thermodynamically allowed. Thus, for example, waters are commonly in equilibrium with calcite, though they can become over-saturated with respect to dolomite $[CaMg(CO_3)_2]$ due to the slow speed of equilibration of waters with this latter mineral (Drever, 1982). Additionally, waters tend to be in equilibrium with the first phase that precipitates from solution, rather than the final recrystallized form. Thus, for example, waters are commonly in equilibrium with amorphous forms of Fe such as ferrihydrite $[Fe(OH)_3 \cdot xH_2O]$ or $Fe_3(OH)_8$ rather than goethite (FeOOH) or hematite (Fe_2O_3; Schwab and Lindsay, 1983).

Finally, it should be noted that the mineral species controlling solubility of a particular element may not represent the dominant mineral for that element in the solid. The mineral need not be present in high levels in the solid - even concentrations below 1% may be sufficient to control solution levels. Additionally, phases controlling solubility are by definition the most active minerals in the solid. They tend to be amorphous or poorly crystalline, and may occur as disordered phases surrounding more crystalline phases. As a result, such minerals may not be detected by conventional analytical techniques such as X-ray diffraction or electron microprobe and the inability to observe the mineral under question should not necessarily be taken to disprove control of solution by this mineral.

---

[8] Generally, the activity of a phase is similar to its concentration; further details are available from a number of standard texts(e.g. Garrels and Christ, 1965).

The total output from the analysis of all of the groundwaters is voluminous and the output from only one sample water is shown in Appendix 2. The general speciation of elements is given in Table 6.

Data from this analysis have been utilized in earlier discussions. The non-metals C, Si, N, O, S, Cl, Br and I are present in their standard forms: namely HCO_3^-, $H_4SiO_4^0$, NO_3^-, H_2O, SO_4^{2-}, Cl^-, Br^- and I^-. Metals are commonly present in solution as the uncomplexed ions or as chloride complexes, with the exception of Cr^{3+}, which is complexed by OH^-, and Cu, Ni and Pb, which are in some cases complexed by HCO_3^- or CO_3^{2-}. V, Sb and Bi tend to be present in oxide forms, $H_2VO_4^-$, $SbO(OH)^0$ and BiO^+.

The SI values for a number of relevant phases are shown graphically in Figs. 30 - 42. Where the SI values tend to 0 this suggests that dissolution or precipitation of the mineral is occurring: i.e. the phase is tending to equilibrium with the solution. Interpretation of these results is given in Sections 4.8.2 to 4.8.4.

4.8.2 Major elements

The SI data for calcite ($CaCO_3$; Fig. 30) indicate that low salinity solutions (TDS < 30,000 mg/L) are generally under-saturated with respect to calcite. As TDS increases solutions become saturated with respect to calcite. Precipitation of this mineral commences and solutions are maintained at equilibria with calcite even at very high salinities.

Groundwaters also become saturated with respect to gypsum ($CaSO_4 \cdot 2H_2O$; Fig. 31), though at slightly higher salinities. Precipitation of calcite or gypsum will be controlled by $[Ca^{2+}]$, $[CO_3^{2-}]$ and $[SO_4^{2-}]$, which can lead to particular precipitation sequences (Jacobson *et al.*, 1988). Equilibration of the solutions with gypsum is particularly pronounced in the Group 8 (MG40) and 9 (MG41) waters (Fig. 12).

The SI data for dolomite (not shown) indicate little convergence to zero, with waters being up to 2 orders of magnitude over-saturated with respect to dolomite. This is in agreement with other observations (Drever, 1982), which have suggested that waters equilibrate with this mineral slowly.

Data for celestine ($SrSO_4$; Fig. 32) indicate that Sr concentrations (with the exception of MG41) are generally too low for saturation. However, most of the waters are at saturation for barite ($BaSO_4$; Fig. 33).

All solutions except MG41 are undersaturated with respect to halite (NaCl; Fig. 34). Sample MG41 is very close to halite saturation, which is hardly surprising given that this solution was collected from a saline sump containing halite crystals. This highly saline sample was at or near saturation for calcite (Fig. 30), gypsum (Fig. 31), celestine (Fig. 32), barite (Fig. 33), halite (Fig. 34), tenorite $[Cu(OH)_2 \cdot 2H_2O]$, iodyrite (AgI) and BiOCl (minor element minerals are discussed in Section 4.8.3)

All waters are oversaturated with respect to quartz (SiO_2; Fig. 35), and instead approach equilibrium with amorphous silica (Fig. 35), which is approximately 10 times more soluble than quartz. This is compatible with the common observation of hyalite cementing many of the surficial sediments to form hardpan, probably by evaporation of Si saturated groundwaters. The tendency of waters to be in equilibrium with amorphous phases was discussed in Section 4.8.1.

Table 6. Solution Speciation of Elements.

Element	Major Species	Extra Species
Na	Na^+	
K	K^+	
Mg	Mg^{2+}	
Ca	Ca^{2+}	
Sr	Sr^{2+}	
Ba	Ba^{2+}	$BaSO_4^0$ (TDS>50,000mg/L)
V	$H_2VO_4^-$	VO^{2+} (MG35)
Cr	$CrOH^{2+}$,$Cr(OH)_2^+$	[Cr^{3+},$CrSO_4^+$,$CrCl^{2+}$] (MG35)
Mn	Mn^{2+}	$MnCl^+$ (TDS>25,000mg/L), $MnCO_3^0$ (pH>8)
Fe	Fe^{2+}	
Co	Co^{2+}	$CoCl^+$ (TDS>100,000mg/L)
Ni	Ni^{2+}, $NiCO_3^0$	$NiCl_2^0$ (TDS>40,000mg/L)
Cu	Cu^{2+},$CuHCO_3^+$,$CuCl_2^-$	$CuCl^+$ (MG35)
Ag	$AgCl_2^-$	$AgCl_4^{3-}$ (TDS>100,000mg/L)
Au	AuI_2^-, $AuClOH^-$ (depending on I/Cl ratio)	$Au(S_2O_3)_2^{3-}$ (where $S_2O_3^{2-}$ is present)
Zn	Zn^{2+}	$ZnCl_x$ (TDS>50,000mg/L), $ZnCO_3^0$ (pH > 7.5)
Cd	$CdCl^+$, $CdCl_2^0$, $CdCl_3^-$ (depending on TDS)	
C	HCO_3^-	
Si	H_4SiO_4	
Pb	$PbHCO_3^+$, $PbCl^+$	[$PbCl_3^-$, $PbCl_4^{2-}$] (MG41)
N	NO_3^-	
Sb	$SbO(OH)^0$	
Bi	BiO^+	$Bi(OH)_3^0$ (pH>7.5)
O	H_2O	
S	SO_4^{2-}	
Cl	Cl^-	
Br	Br^-	
I	I^-	

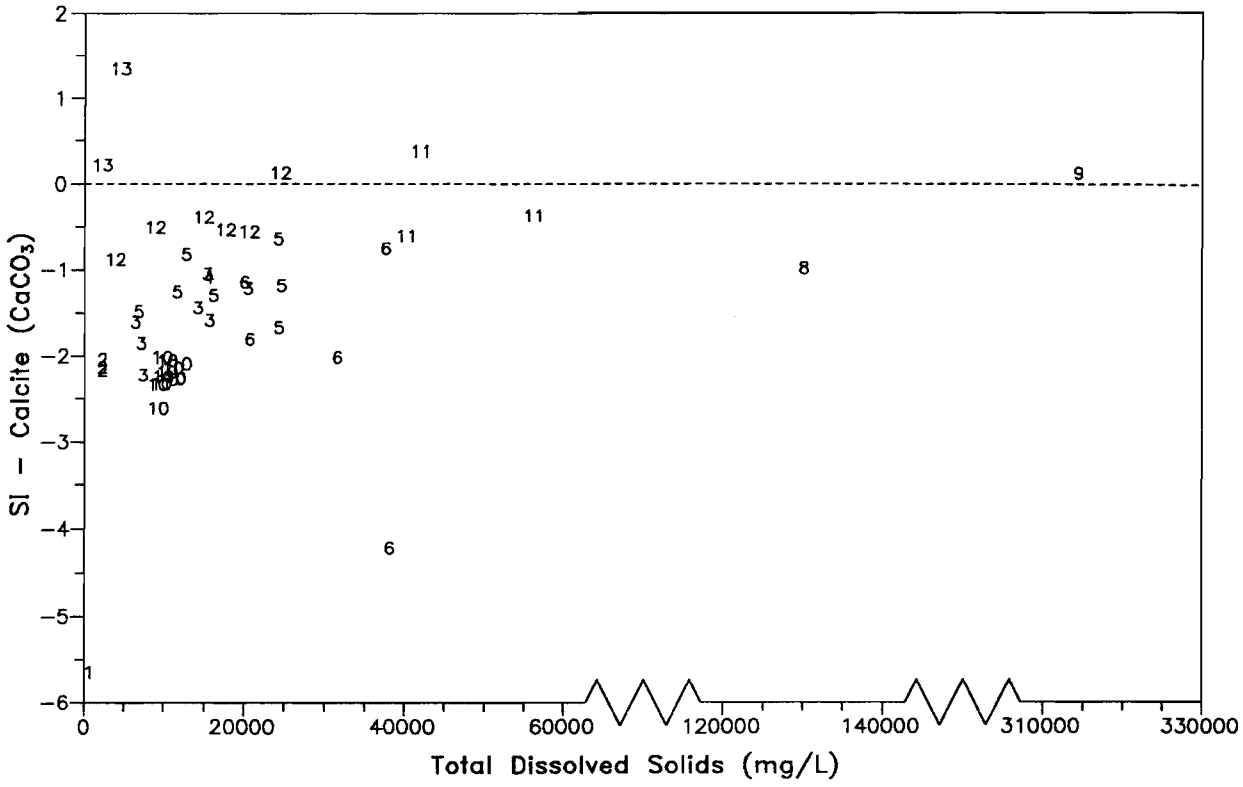

Figure 30. SI for Calcite ($CaCO_3$) vs. TDS for Mount Gibson Waters.

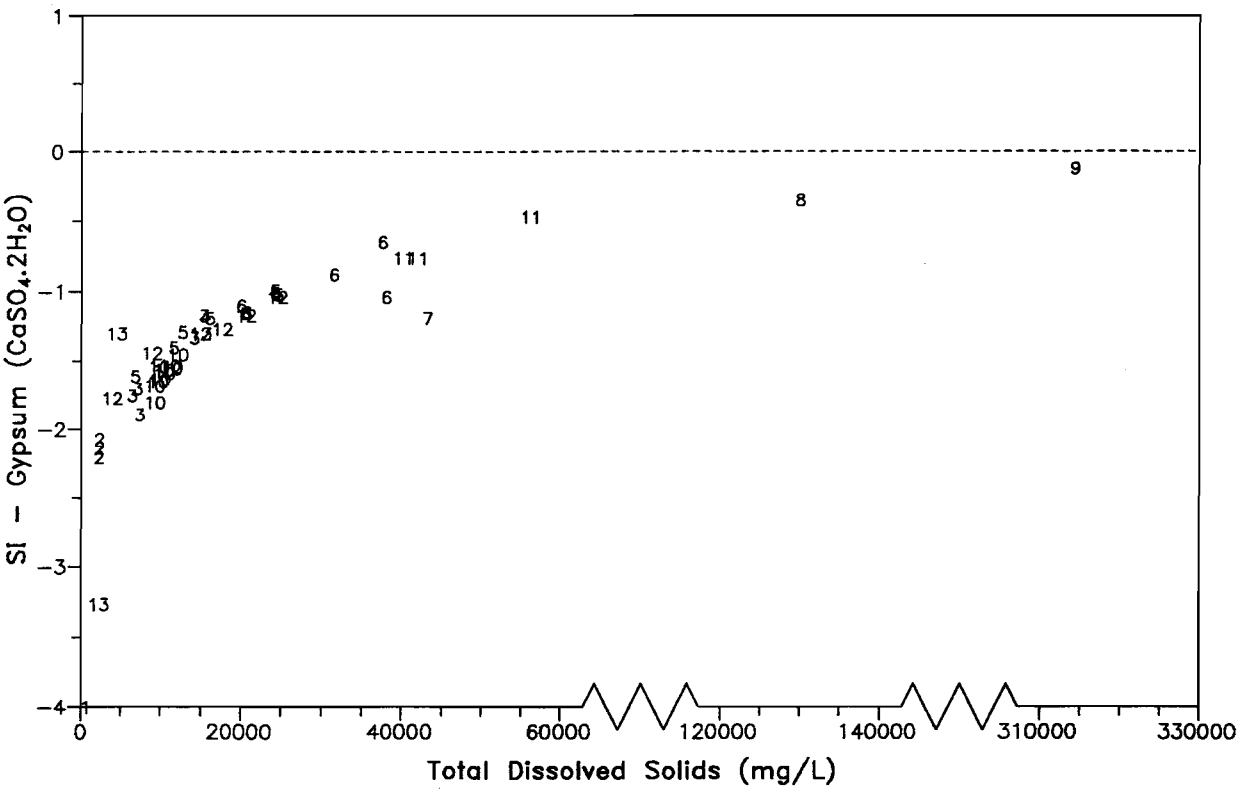

Figure 31. SI for Gypsum ($CaSO_4 \cdot 2H_2O$) vs. TDS for Mount Gibson Waters.

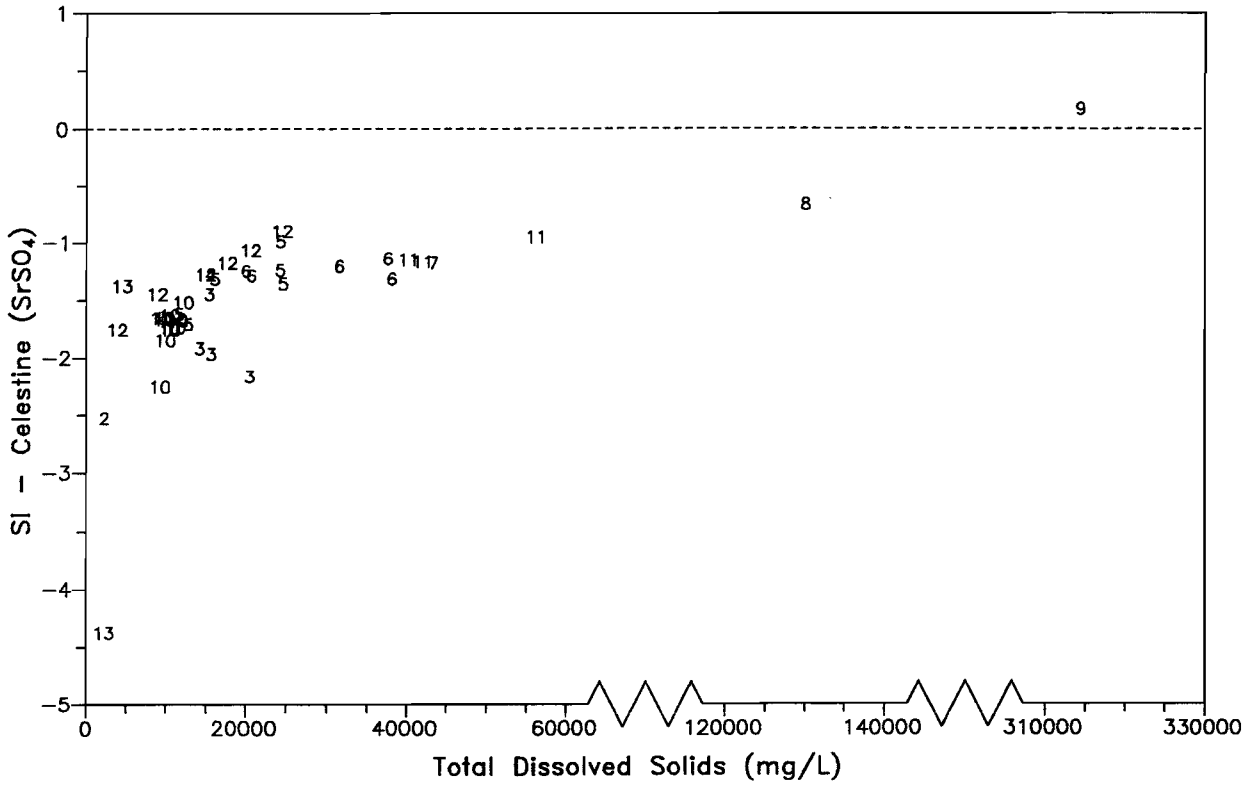

Figure 32. SI for Celestine ($SrSO_4$) vs. TDS for Mount Gibson Waters.

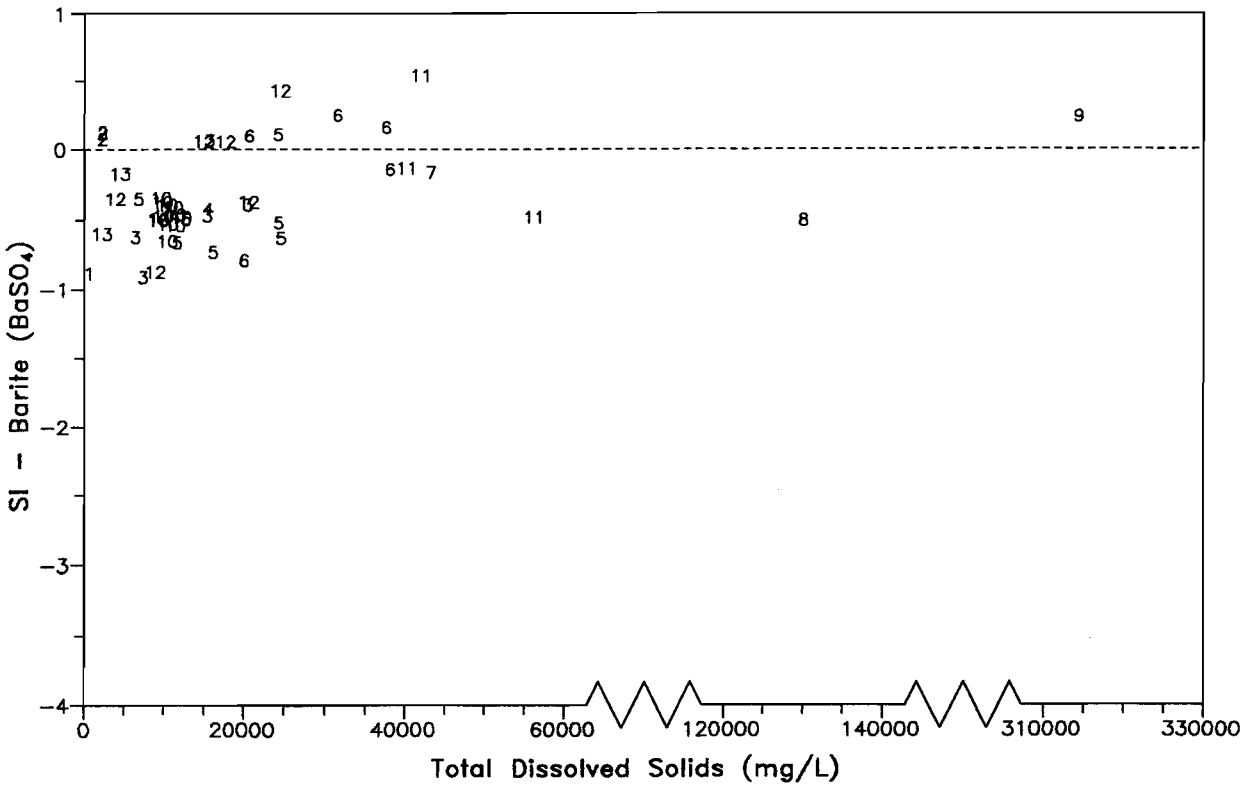

Figure 33. SI for Barite ($BaSO_4$) vs. TDS for Mount Gibson Waters.

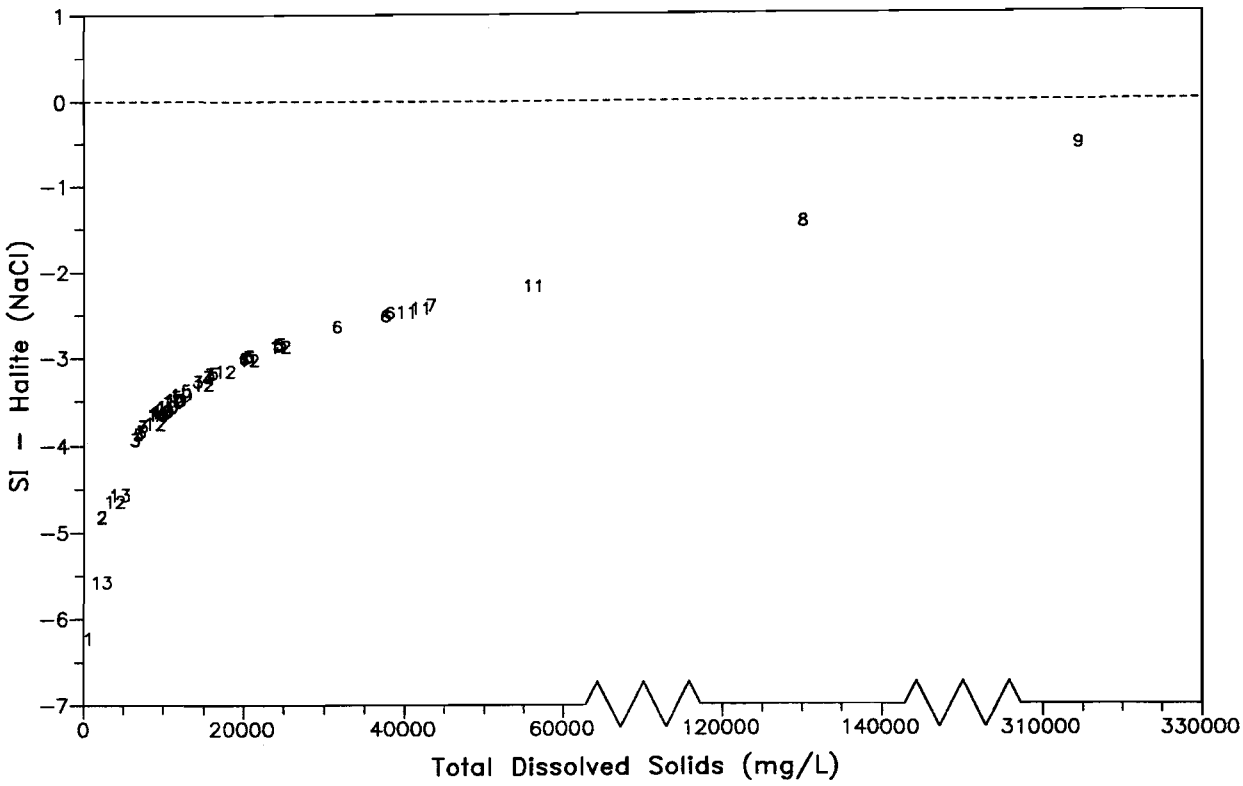

Figure 34. SI for Halite (NaCl) vs. TDS for Mount Gibson Waters.

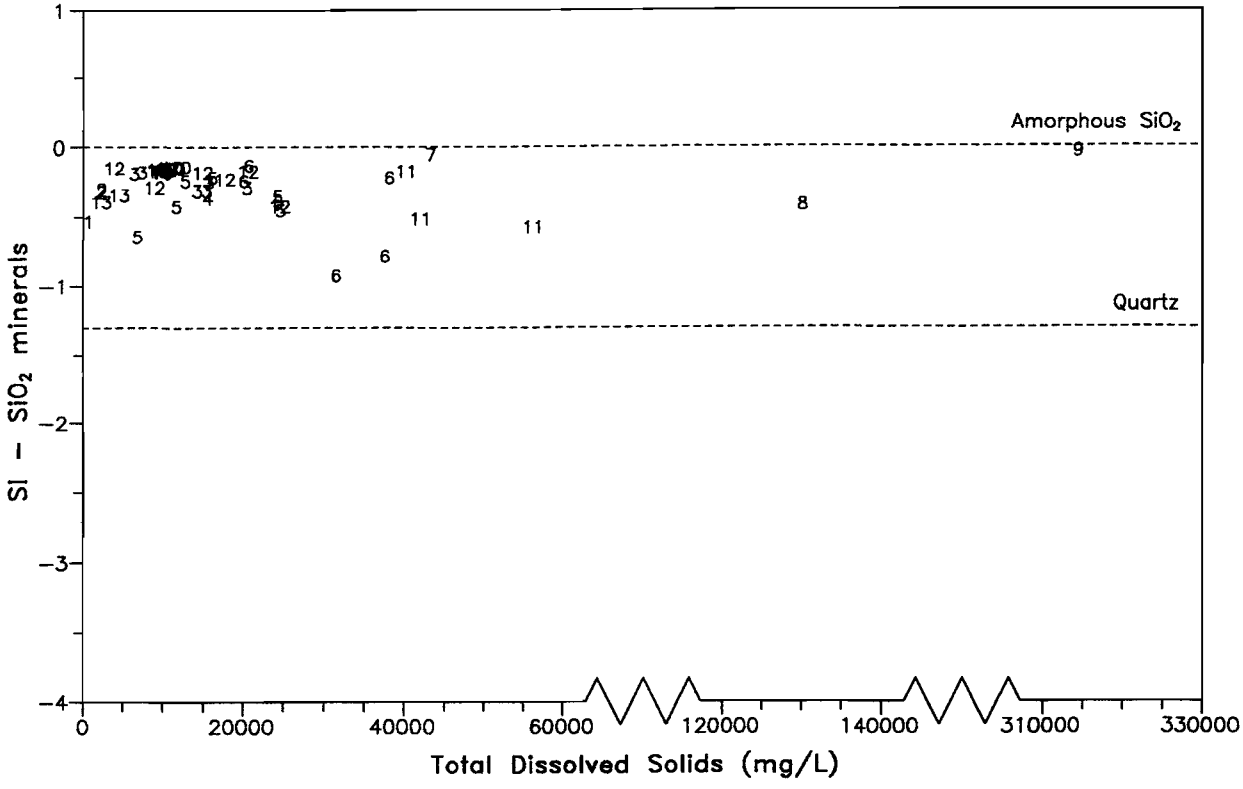

Figure 35. SI for SiO_2 Minerals vs. TDS for Mount Gibson Waters.

4.8.3 Minor elements

Data for Al and Fe (not shown) are highly variable, indicating that these elements are not controlled by single dissolution/precipitation processes. This is expected, given the presence of Al in clay minerals and the complex redox chemistry of Fe.

With regards to Mn solubility, waters show some tendency to reach saturation with respect to rhodochrosite ($MnCO_3$; Fig. 36), which is the least soluble Mn phase for these waters. Most of the other metals, namely Cu, Zn, Ni, Co and Cd, were undersaturated with respect to all solid phases. Waters were oversaturated with respect to Cr_2O_3 by 2 to 8 orders of magnitude, suggesting no equilibration with this solid phase. This evidence suggests that these metals are controlled by adsorption of co-precipitation type reactions, consistent with the strong pH effect on concentration for these metals in the Midway area (Section 4.7.4).

Silver can precipitate either as cerargyrite (AgCl) or iodyrite (AgI). Groundwaters in this investigation approached saturation with respect to iodyrite (Fig. 37), but were undersaturated with respect to cerargyrite. Other elements that may be controlled by precipitation reactions are: Pb, which appears to be at or above saturation with respect to cerrusite ($PbCO_3$; Fig. 38), $Pb_3(VO_4)_2$ (not shown) and $Pb_2V_2O_7$ (Fig. 39); V, which could be controlled by $Pb_3(VO_4)_2$, $Pb_2V_2O_7$ or Fe-vanadate (FeV_2O_6; not shown); and Sb, which is strongly oversaturated with respect to Sb_2O_4 (suggesting lack of equilibration with this phase), but is at equilibrium with respect to $Sb(OH)_3$ (Fig. 40). Bismuth is generally undersaturated with respect to the least soluble phase used (BiOCl; Fig. 41), though it may be under equilibrium control at high salinities.

4.8.4 Gold

The major solid phase of Au is expected to be as the metal. However, any determination of solubility of Au is questionable, given the major effect of ligands such as $S_2O_3^{2-}$ or CN^-, even when at concentrations below the detection limit. Preliminary SI values were determined without using $S_2O_3^{2-}$ values. In this case, the program only calculates for the effect of ligands such as Cl^- or I^- in solubilizing Au, with the resultant values plotted as the numbers in Fig. 42. Based on this data, the waters are significantly oversaturated (SI > > 1) with respect to Au metal.

The SI values were then recalculated, using the determined $S_2O_3^{2-}$ concentrations. Where the $S_2O_3^{2-}$ concentration was below detection, the concentration was assumed to be half of the detection limit [9]. The arrows in Fig. 42 represent the change in the SI value when using the $S_2O_3^{2-}$ values. Where the line is unbroken the $S_2O_3^{2-}$ value used was as analysed, whilst a broken line indicates that $S_2O_3^{2-}$ concentration was below detection and half the detection limit was used. The SI values are now significantly closer to zero. Clearly $S_2O_3^{2-}$, where present, is important for Au solubility, theoretically increasing it by up to six orders of magnitude in one instance. The magnitude in the changes of the calculated SI values for the broken lines in Fig. 42 indicate that even concentrations of $S_2O_3^{2-}$ below detection could have a major effect.

[9] As the final value is expressed as a log unit, then an order of magnitude error in the assumed $S_2O_3^{2-}$ concentration will change the final SI value by about one unit.

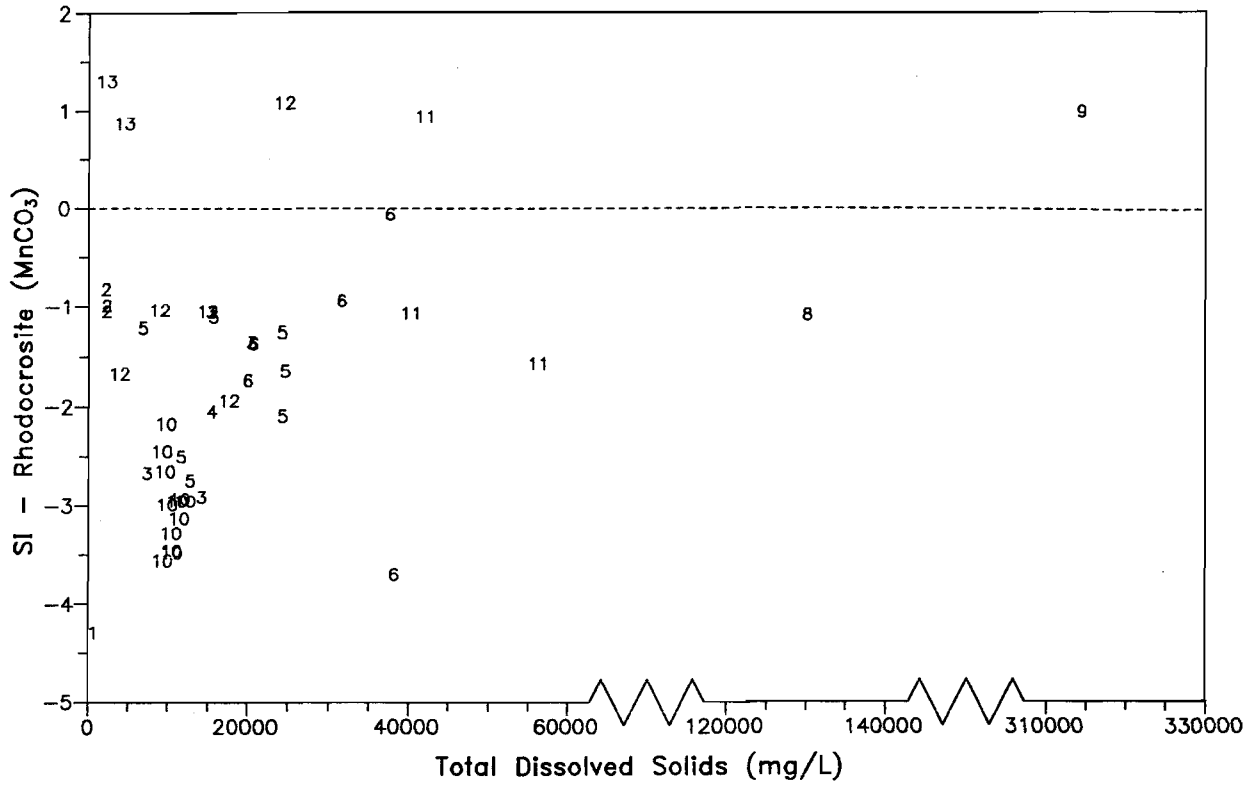

Figure 36. SI for Rhodocrosite ($MnCO_3$) vs. TDS for Mount Gibson Waters.

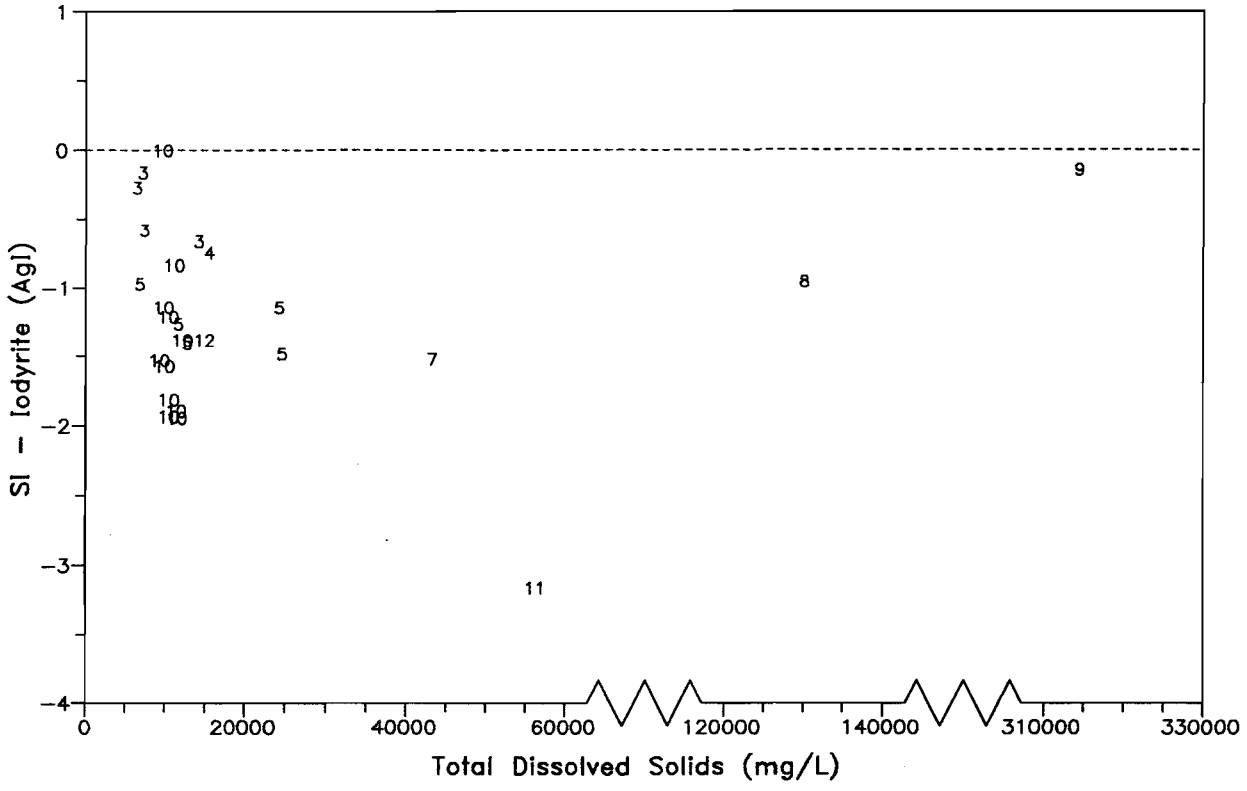

Figure 37. SI for Iodyrite (AgI) vs. TDS for Mount Gibson Waters.

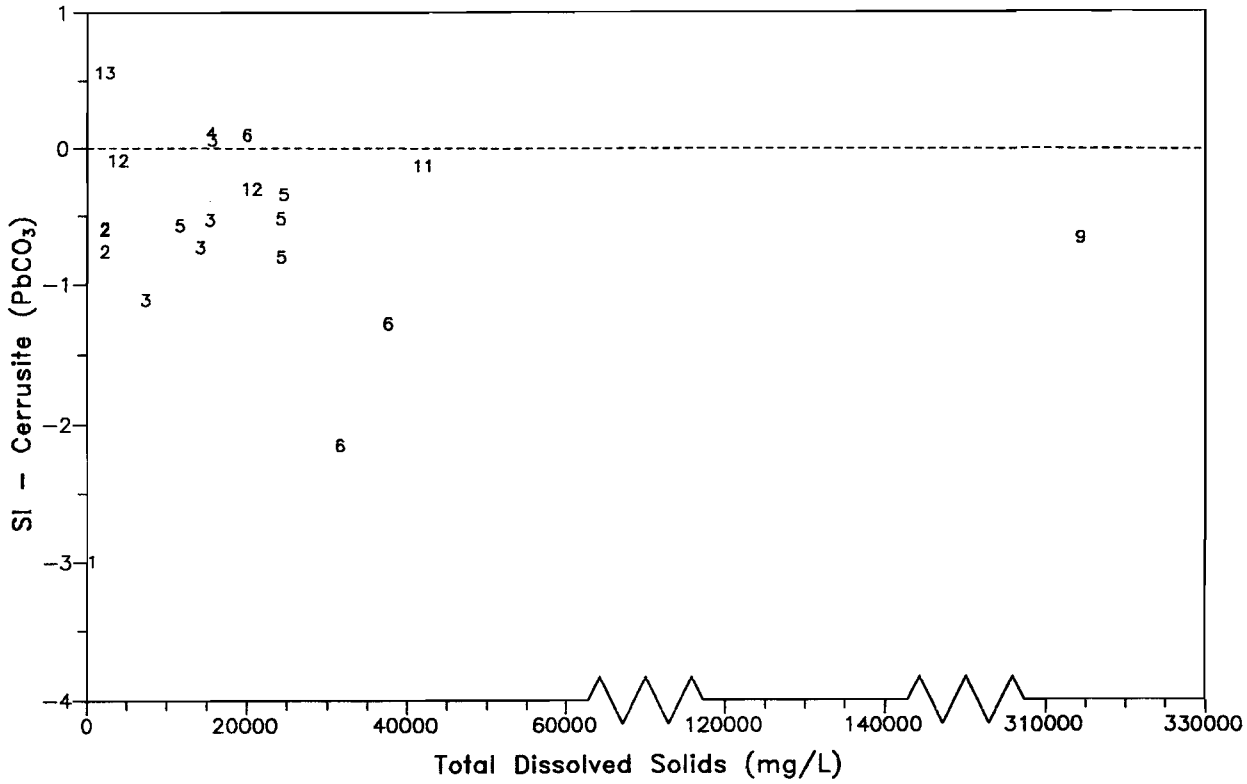

Figure 38. SI for Cerrusite ($PbCO_3$) vs. TDS for Mount Gibson Waters.

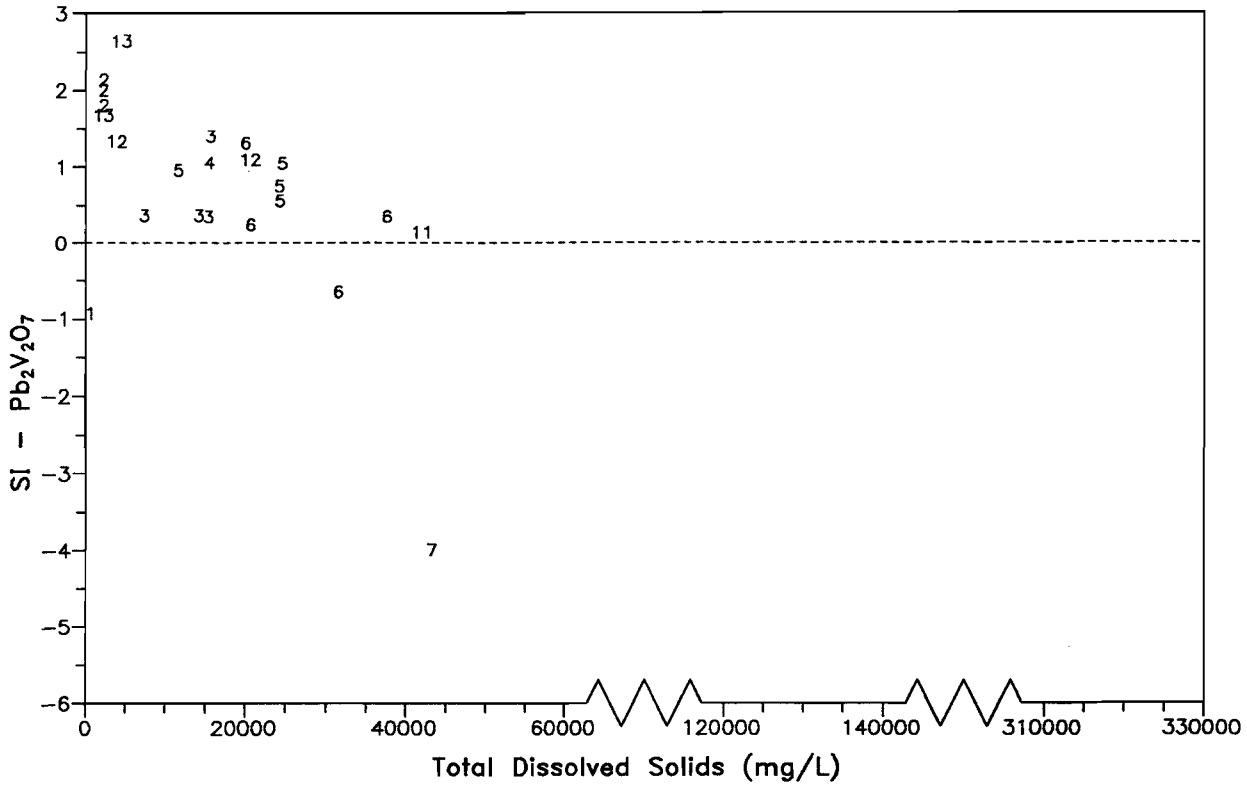

Figure 39. SI for $Pb_2V_2O_7$ vs. TDS for Mount Gibson Waters.

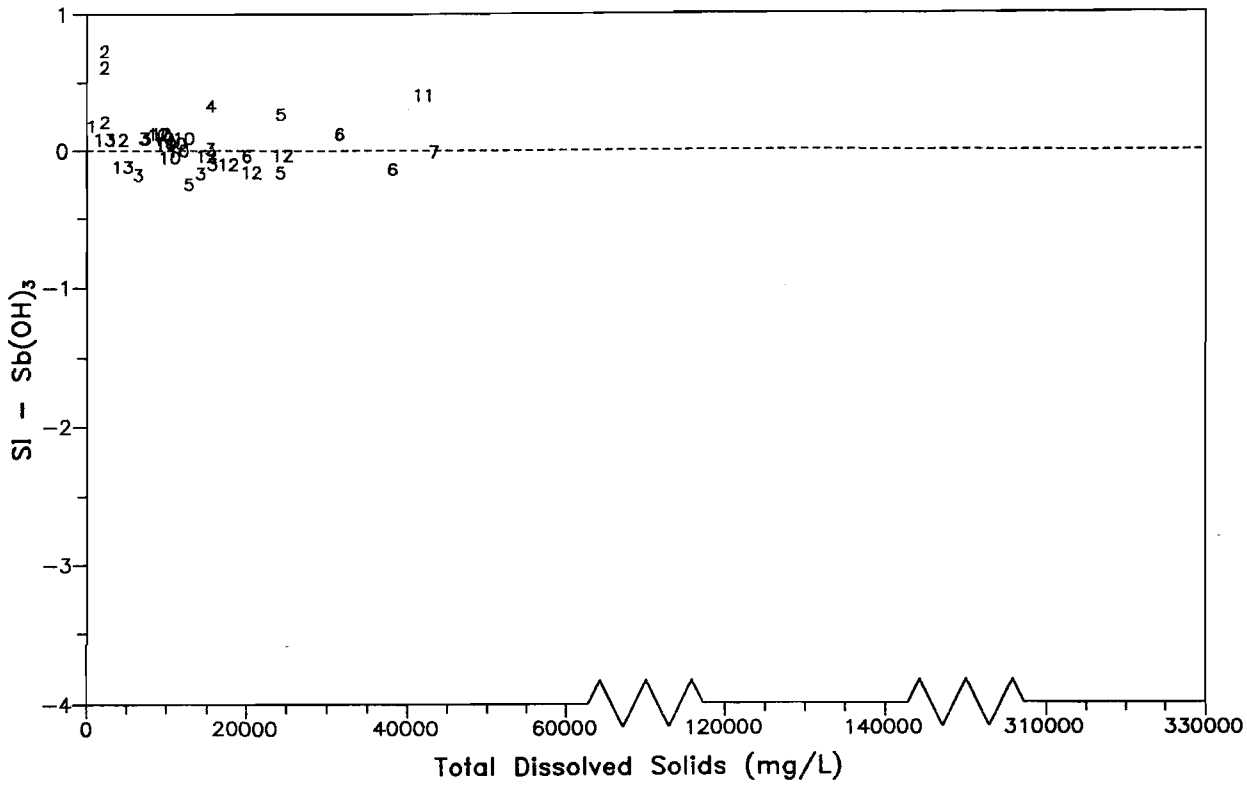

Figure 40. SI for $Sb(OH)_3$ vs. TDS for Mount Gibson Waters.

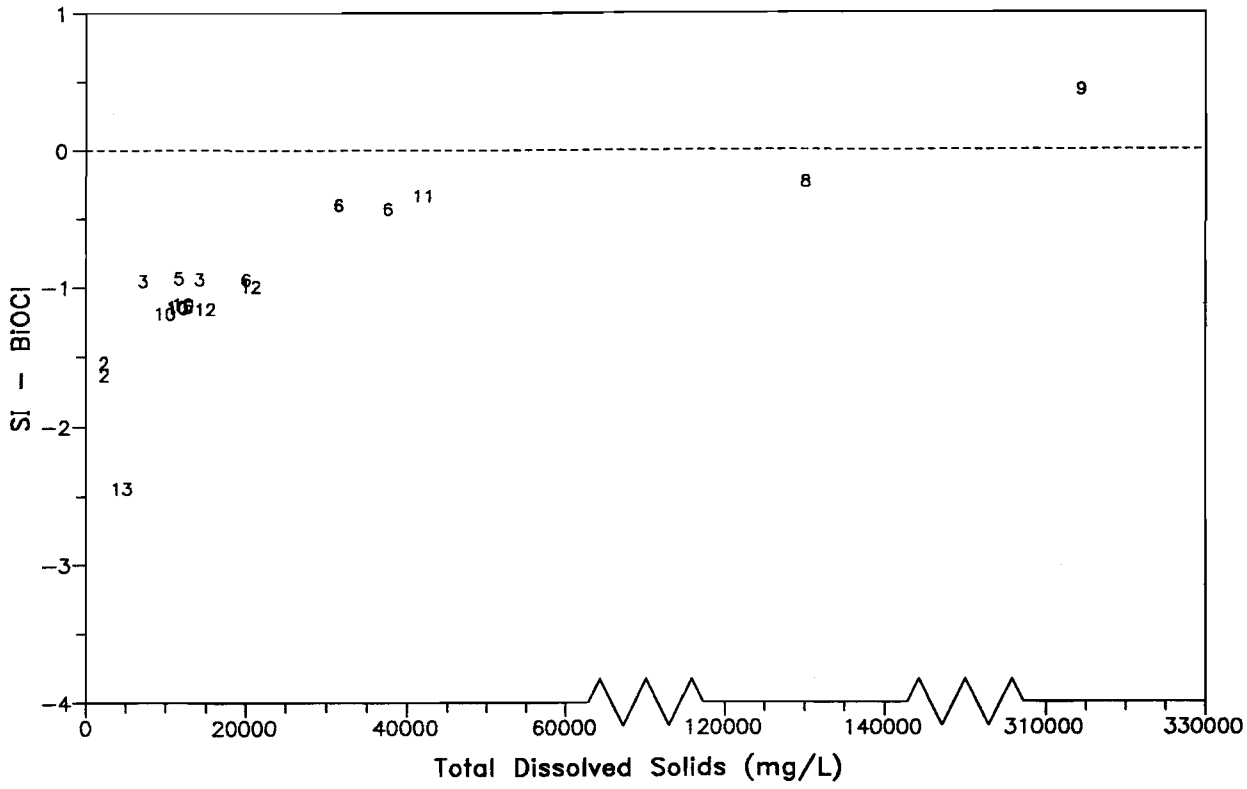

Figure 41. SI for BiOCl vs. TDS for Mount Gibson Waters.

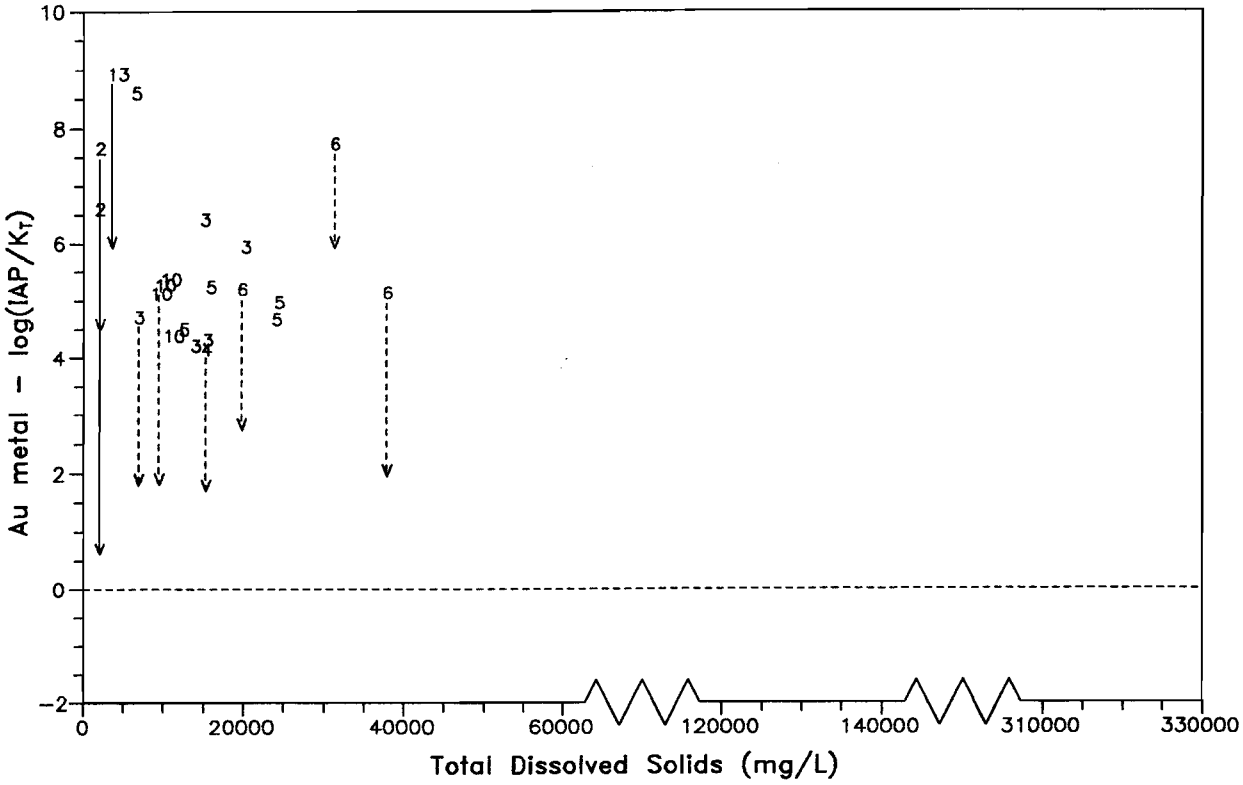

Figure 42. SI for Au Metal vs. TDS for Mount Gibson Waters.

This effect will be even more pronounced for CN^-. Calculations indicated that a free CN^- concentration of 1 μg/L, which is significantly below the detection limit, would result in all of the waters being at least three orders of magnitude undersaturated with respect to Au. In this respect, any determination of a SI value for Au metal can only be used as a maximum value, as various constituents below detection limits may be mobilizing Au.

Note that this effect is nowhere near as pronounced for the other elements investigated, as the strength of bonding with ligands such as $S_2O_3^{2-}$ or CN^- with the other metals analysed is much weaker than for Au, and major constituents such as Cl^-, HCO_3^- or OH^- will be more important for complexation and solubilization. That is, the conclusions on the other elements (apart from Au) would not be invalidated by assuming the presence of ligands such as CN^- at levels below detection.

In general, the speciation results support conclusions based on concentration data from previous sections. In particular, elements that behave in an anomalous, uncharacterized manner (e.g. Pb, V, Sb) are possibly controlled by precipitation of particular phases such as $Pb_2V_2O_7$. Most of the trace metals are not at equilibrium with their salts and appear to be controlled either by dissolution from source rocks or by adsorption.

4.9 Statistical Investigations

4.9.1 Introduction

The data were studied using statistical methods [10], in order to further investigate element associations in groundwaters, and see what additional information could be gained on relationships between groundwater masses.

The data were analysed using correlation co-efficient analysis and dynamic cluster analysis (DCA). This latter method was developed by Diday (1972) as an approach to non-hierarchical clustering. Lefebvre and David (1977) illustrated a geological application, although the technique has not been widely used. The procedure used here is a modification provided by E.G. Grunsky (CSIRO). An example of the method is given in Grunsky (1986). The DCA method will work most successfully with data sets with strong associations, representing uniquely defined groups. This method tries to find distinct groups based on the choice of random seeds and statistical uniqueness.

A sample correlation coefficient table for the data set of all 50 waters is shown in Appendix 3. This information was analysed by relating the correlation value for each variable pair to the probability that it represents a significant correlation. These data were then compiled, as shown in Table 7, which give significant correlations between variables where the entire data set was used. The correlations are divided into three groups: those significant at the > 99.9% significance level; those significant at the 99 - 99.9% significance level; and those significance at the 95 - 99 significance level. The elements are ordered from highest to lowest co-efficient.

[10] General statistical methods are discussed in various texts (e.g. Cooley and Lohnes, 1971).

4.9.2 Entire data set

Correlations for the entire set of waters (Table 7) are dominated by salinity effects, particularly from the Lake Karpa water, which is enriched in a large number of major and minor elements. Elements highly correlated within this "salinity" group included SO_4, Mg, Br, C, Na, K, Ag, Cd, Cr, Mn, Sr, Co, Ni and Pb. Calcium was correlated with this group, though less significantly, due to the levelling of Ca concentrations at high salinities (Sections 4.4, 4.8.2). The species HCO_3, pH and I were strongly correlated with each other, and less strongly correlated with the group II elements Ca, Sr and Ba. Elements within this "alkalinity" group (consisting of HCO_3, pH, I, Ca, Sr and Ba) also correlated weakly with Mn (which can be associated with group II elements) and Bi. Aluminium, Ni, Co and Cu correlated strongly positively with each other and strongly negatively with pH. This "acidity" group (consisting of Al, Ni, Co and Cu), represents those elements most strongly concentrated in the acidic MG35 water. Silicon correlated negatively with the "salinity" and "alkalinity" group elements, indicating that Si concentration is reduced with increased salinity or at higher pH values. The only other correlation of note was that between Au and Fe, due the high values of these two species in the Midway waters.

The samples were divided into statistically determined clusters by DCA. Most of the water samples divided into two clusters, with cluster 1 waters, on average, significantly higher in pH, I, Fe, Mn, Ba, Pb and Zn. The cluster may represent waters in contact with weakly mineralized sulphide or carbonate zones, which release these elements on weathering. Aside from the two major clusters there were ten outliers, i.e. samples that grouped alone:

(i) MG8 - the high Au water;
(ii) MG13 and MG43 - waters lying in the Midway Pit (Fig. 5);
(iii) MG35 - the acid water;
(iv) MG38, MG40 and MG41 - highly saline waters;
(v) MG39 and MG42 - surface samples;
(vi) MG44 - the low salinity run-off water at the southern end of the northern drainage (Section 4.2; Fig. 2).

The presence of these samples as outliers is reasonable.

4.9.3 Mine waters data set

Similar statistical work was done on the data set of the Mine waters (i.e. Groups 2, 3, 4, 5, 6, 7, 10) alone. Significant differences were observed, partially due to the absence of the highly saline waters MG38, MG40 and MG41. The correlation information (Table 8) showed some similarity to that from the previous analysis. Variables were divided into a "salinity" grouping, consisting of SO_4, Br, Na, K, Mg and Cl, and less strongly Sr and Ca; an "acidity" group consisting of Al, Ni, Co, Cr, Zn, Cu, and Cd; a weakly associated "alkalinity" group consisting of pH, HCO_3 and Ca (this lack of strong statistical correlation within this "alkalinity" group may be a consequence of the low number of alkaline samples in this data set); a "Midway" group consisting of Fe, Ba, I, and, more weakly, Au; a "lead" group consisting of Pb, Zn and Cd; and Si. Cluster analysis divided the samples into two major clusters:

(i) cluster 1 consisted of Tobias' Find waters, and some Orion and Yorktown waters with higher pH values and lower salinities;

Table 7. Significant Correlations - Entire Sample Set

No. of samples: 50

Element	Correlated at a Significance level of > 99.9%	99 - 99.9%	95 - 99%
pH	HCO_3, *Al, Cu*	*V, Ni, Co*	Ba, *Si*
HCO_3	pH, I	Ca	Ba, Sr, Bi, *Si*
SO_4	Mg, Br, Cl, Na, K, Ag, Cd, Cr, Mn, Sr, Co, Ni, Pb, Ca	*Si*	
Cl	Na, Mg, SO_4, Br, K, Ag, Mn, Cd, Cr, Sr, Co, Ni, Pb, Ca	*Si*	
Br	SO_4, Mg, K, Cl, Na, Cd, Ag, Mn, Cr, Sr, Co, Ni, Pb	Ca	*Si*
I	HCO_3	Sr, Ca, *NO_3, Si*	Mn, Ba, Bi
NO_3	*I*		
Na	Cl, Mg, SO_4, Br, K, Ag, Mn, Sr, Cd, Cr, Co, Ni, Ca, Pb	*Si*	*V*
K	Br, SO_4, Mg, Cl, Na, Cd, Cr, Mn, Ag, Sr, Co, Ni, Pb	Ca	*Si*
Mg	SO_4, Cl, Br, Na, K, Ag, Mn, Cd, Cr, Sr, Co, Ni, Pb, Ca	*Si*	
Ca	Sr, Na, Cl, Mg, SO_4, *Si*	Br, K, HCO_3, Ag, I	Mn, *Sb*
Al	Ni, Co, Cu, *pH*		
Ba			HCO_3, pH
Cr	Cd, K, Br, SO_4, Mn, Mg, Cl, Na, Ag, Ni, Co, Sr, Pb		Cu
Fe	Au		Bi, Co, *Si*
Mn	Cd, K, Br, SO_4, Mg, Cr, Cl, Na, Ag, Sr, Ni, Pb	*Si*	I, Ca
Ni	Co, Cd, Al, Cr, Mn, Br, Mg, K, SO_4, Cl, Na, Ag, Cu, Pb, Sr	*pH*	
Sr	Na, Cl, Mg, SO_4, Br, K, Mn, Ag, Ca, Cr, Cd, Co, Ni	Pb, I, *Si*	HCO_3
Ag	Mg, SO_4, K, Cl, Br, Na, Cr, Cd, Mn, Sr, Ni, Co, Pb	Ca	*Si*
Cd	K, Cr, Br, Mn, SO_4, Mg, Cl, Na, Ag, Co, Ni, Sr, Pb		Cu, *Si*
Co	Ni, Cd, Mn, Cr, Mg, Br, SO_4, Cl, K, Al, Na, Ag, Sr, Cu	Pb, *pH*	Fe
Cu	Al, Ni, Co, *pH*	Au	Cd, Pb
Pb	Cd, Cr, K, Br, SO_4, Mg, Mn, Cl, Na, Ni, Ag	Co, Sr	Cu
Zn			
Si	*Ca*	*Bi, Sr, Mn, Na, Cl, Mg, SO_4, I*	*Br, K, Fe, pH, HCO_3, Ag, Cd*
Au	Fe	Cu	
V		pH	*Na*
Bi		*Si*	Sb, HCO_3, Fe, I
Sb			Bi, *Ca*

Note: Fe measured as Fe^{2+} in the field
Elements are placed in order of significance
Elements in italics denote a negative correlation

Table 8. Significant Correlations - Mine Waters Sample Set

No. of samples: 36

Element	Correlated at a Significance level of > 99.9%	99 - 99.9%	95 - 99%
pH	*Al, Ni, Co, Cr, Cu, Mg, Cd, K, Cl*	*Zn, Br, Na, SO_4*	**HCO_3, NO_3**, *Si, Sr, Ag*
HCO_3		**Ca**, *Si, Co*	**pH**, *Fe, Ni*
SO_4	**Br, Na, K, Mg, Cl, Sr, Ca, Cd, Co, Mn**	**Ni, Cr, Al, I, Fe, Cu**, *NO_3, pH*	**Pb, Zn, Au, Ba**, *V, Si*
Cl	**Br, Mg, Na, K, SO_4, Ca, Sr, Mn, Cd, Co, Ni, Al**, *NO_3, pH*	**Cr, Fe, I, Cu**	**Ba, Zn**, *V*
Br	**Na, Cl, K, SO_4, Mg, Sr, Ca, Cd, Mn, Co**, *NO_3*	**Fe, Ni, Al, Cr, I, Cu**, *pH*	**Ba, Zn**, *V*
I	**Ba, Fe**, *NO_3*	**SO_4, Sr, Cd, Na, Br, K, Mg, Cl, Mn, Ca**, *Ag*	**Pb, Sb**
NO_3	*I, Na, Cl, Br*	*SO_4, K, Mg, Ca, Sr, Mn*	**V, pH**, *Pb, Ba, Co, Cd, Fe, Zn*
Na	**Br, Cl, K, Mg, SO_4, Sr, Ca, Cd, Mn, Co**, *NO_3*	**Fe, Ni, Al, Cr, I, Cu**, *pH*	**Ba, Au, Zn**, *V, Sb*
K	**Na, Br, Mg, Cl, SO_4, Sr, Ca, Cd, Co, Mn**, *pH*	**Ni, Al, Fe, Cr, I, Cu**, *NO_3, V*	**Au, Zn, Ba**, *Sb*
Mg	**Cl, Na, Br, K, SO_4, Sr, Ca, Cd, Co, Mn, Ni, Al, Cr**, *pH*	**Fe, Cu, I**, *NO_3*	**Ba, Zn, Au**, *V*
Ca	**Br, Cl, Na, SO_4, K, Mg, Sr, Mn**	**HCO_3, Ba, Fe, I**, *Si, NO_3*	**Cd**
Al	**Ni, Co, Cr, Zn, Cu, Cd, Mg, Cl**, *pH*	**K, SO_4, Br, Na, Mn**	**Ag**
Ba	**Mn, I**	**Fe, Ca**, *Ag*	**Cl, Sb, Mg, Na, Br, SO_4, Zn, K**, *NO_3*
Cr	**Cu, Al, Ni, Co, Cd, Ag, Zn, Mg**, *pH*	**SO_4, Cl, K, Br, Na, Mn**	**Sr**
Fe	**Mn, Cd, I**	**Mg, K, Na, Cl, Br, Ba, SO_4, Au, Ca**	**Co, Sr, Bi**, *Si, HCO_3, NO_3*
Mn	**Ca, Cl, Mg, Ba, Br, Na, K, SO_4, Fe, Cd, Co**	**Sr, I, Ni, Bi, Cr, Al**, *Si, NO_3*	**Zn**
Ni	**Al, Co, Cr, Zn, Cu, Cd, Mg, Cl**, *pH*	**K, SO_4, Br, Na, Mn**	**Ag**, *HCO_3*
Sr	**K, Br, SO_4, Na, Cl, Mg, Ca, Cd**	**Mn, I**, *NO_3*	**Co, Cr**, *pH*
Ag	**Cr, Cu**	*Ba, I*	**Al, Ni**
Cd	**Co, Mg, K, SO_4, Br, Na, Cl, Cu, Ni, Al, Cr, Mn, Fe, Zn, Sr**, *pH*	**I, Pb**	**Ca**, *V, NO_3*
Co	**Ni, Al, Cd, Cr, Mg, Cl, K, Cu, Na, Zn, SO_4, Br, Mn**, *pH*	*HCO_3*	**Fe, Sr**, *NO_3*
Cu	**Cr, Ni, Al, Cd, Co, Ag**, *pH*	**Au, Mg, SO_4, Zn, K, Cl, Br, Na**	**Pb**
Pb	**Zn**	**Cd**,	**SO_4, I, Cu**, *NO_3*
Zn	**Ni, Al, Co, Pb, Cd, Cr**	**Cu**, *pH*	**Mn, Mg, Cl, SO_4, Ba, Na, K, Br**, *NO_3*
Si	*Bi*	*Ca, HCO_3, Mn*	*pH, Fe, SO_4*
Au		**Cu, Fe, Cd**	**Mg, SO_4, K, Na, Br**
V		**Sb**, *K*	**NO_3, Bi**, *Na, SO_4, Br, Mg, Cl, Cd, Sr*
Bi	*Si*	**Mn**	**V**
Sb		**V**	**Ba, I**, *K, Na, Br*

Note: Fe measured as Fe^{2+} in the field
Elements are placed in order of significance
Elements in italics denote a negative correlation

(ii) cluster 2 consisted of the main bulk of the Orion and Yorktown waters and all of the Sterilization waters;

which were not obviously discrete. In addition there were six outliers:

(i) MG5 is an Orion water with high Pb, Zn, Ni and Mn concentrations;

(ii) MG8 is the high Au water (Table 2);

(iii) MG13, MG34 and MG43 are Midway waters;

(iv) MG35 is the Ferrolysis water.

4.9.4 Reduced data set

The outliers listed above (Section 4.9.3) were removed for an additional statistical run. The groups were determined, and any outliers removed. This process was continued until a sample set was produced that contained no outliers. This sample set contains all of the Tobias' Find (Group 2) and Sterilization (Group 10) waters and reduced subsets of the Orion and Yorktown (Groups 3 and 5) and Midway (Group 6) waters, and was used to observe some of the more subtle element associations for the 'normal' Mine waters. The correlation information is shown in Table 9. Interestingly, many of the observations of element correlations from the previous sample sets were still observed in this reduced sample set, suggesting that some of the major effects in the Midway area were still present, though in a less dramatic form than in the 'normal' Mine waters.

Variables were divided into similar groups as in analyses of the larger sample sets: a "salinity" group containing Na, K, Mg, Cl, Br and SO_4, and less strongly Ca, HCO_3 and Sr; an "iron" group containing Fe, Mn, pH and Ba; which is also associated with a "metalloid" group of Bi, Sb, V, Ni and Co; a "lead" group containing Pb, Cd and I; and Si. All of the samples clustered in one group. Interestingly this statistical method did not show any difference between the Sterilization waters and the other Mine waters.

A similar procedure to reduce the entire sample set (including the non-Mine waters) resulted in exactly the same sample set as that from reduction of the Mine waters set, described above. That is, none of the drainage waters were sufficiently similar to the Mine waters to cluster in the same multivariate normal group.

Table 9. Significant Correlations - Reduced Sample Set

No. of samples: 25

Group 2: MG18 MG19 MG20
Group 3: MG2 MG3 MG6 MG7
Group 5: MG10 MG12 MG14 MG15 MG17
Group 6: MG16
Group 10: MG21 MG22 MG23 MG24 MG25 MG26 MG27 MG28 MG29 MG31 MG32 MG33

Element	Correlated at a Significance level of		
	> 99.9%	99 - 99.9%	95 - 99%
pH	Mn, Ba, *Si*	Fe	V, Bi, Sb, Ni, I, *Al*
HCO_3	Ca, SO_4, Mg, Na, Br, Cl, K	*Ni, Co*	Pb, Sr, I, *Si, Sb*
SO_4	Br, Mg, Na, Cl, K, Ca, Sr, HCO_3	Cd, Pb, I, *Ni, Co*	*V, Si*
Cl	Na, Br, Mg, K, SO_4, Ca, Sr, HCO_3	Pb, *Ni, Co, V*	I, Cd, *Sb, Fe, Zn*
Br	Na, Cl, K, Mg, SO_4, Ca, Sr, HCO_3	Pb, Cd, *Ni, Co, V*	I, *Fe, Sb, Zn*
I	Pb	Cd, SO_4, Ca, Mg, *NO_3, Si, Ag*	Sr, Na, Cl, Br, Mn, K, HCO_3, Sb, Zn, pH
NO_3		*I*	V, Ag, *Pb, Cl, Na, Ca, Sr, Mn*
Na	Cl, Br, Mg, K, SO_4, Ca, Sr, HCO_3	Pb, *Ni, Co, V*	I, Cd, *Sb, Fe, NO_3, Zn*
K	Br, Na, Cl, Mg, SO_4, Ca, Sr, HCO_3	Pb, Cd, *Ni, Co, V*	I, *Fe, Sb, Zn*
Mg	Cl, Na, Br, SO_4, K, Ca, Sr, HCO_3	Pb, I, *Ni, Co*	Cd, *V, Sb, Zn*
Ca	Mg, Cl, Na, K, Br, SO_4, Sr, HCO_3	I, Pb	Cd, *Ni, Co, V, Si, Sb, Zn*
Al			*pH*
Ba	Mn, pH	Sb, Co, Ni, Fe	V, *Si*
Cr			
Fe	Mn	pH, Ba, *Si*	Sb, Zn, Co, V, Ni, *K, Br, Na, Cl, Ag*
Mn	Fe, Sb, Ba, pH, Co	Ni, *Si, Ag*	Zn, I, Bi, V, *K*
Ni	Sb, Co, Bi	V, Mn, Ba, Zn, *K, Br, Na, Cl, HCO_3, Mg, SO_4, Ca*	Fe, pH
Sr	K, Mg, Br, Na, Cl, SO_4, Ca	Cd, Pb	I, HCO_3, *V*
Ag	Cu	*Mn, I*	NO_3, Si, *Cd, Fe, Pb*
Cd	Pb	I, Sr, SO_4, K, Br	Mg, Na, Cl, Ca, *Ag, Si*
Co	Sb, Ni, Mn,	Ba, *K, Br, Na, HCO_3, Cl, Mg, SO_4*	Bi, Fe, V, Zn, *Ca*
Cu	Ag		
Pb	I, Cd	Sr, SO_4, K, Br, Mg, Na, Ca, Cl	HCO_3, *NO_3, Ag*
Zn		Sb, Ni	Mn, Fe, Co, I, *K, Mg, Cl, Br, Ca, Na*
Si	*pH*	*Fe, Mn, Au*	Ag, *I, HCO_3, Ca, Ba, Cd*
Au			*Si*, V
V		Ni, Bi, *K, Na, Br, Cl*	Sb, NO_3, Au, Ba, pH, Mn, Co, Fe, *Mg, SO_4, Ca, Sr*
Bi	Ni	V, Sb	Co, Mn, pH
Sb	Mn, Ni, Co	Ba, Zn, Bi, V	Fe, pH, I, *K, Na, Br, Cl, Mg, HCO_3, Ca*

Note: Fe measured as Fe^{2+} in the field
Elements are placed in order of significance
Elements in italics denote a negative correlation

5.0 GENERAL DISCUSSION

5.1 Key Observations

(i) The regional, northward-draining groundwater system shows a distinct difference in salinity and groundwater chemistry south and north of the topographic Mount Gibson (Section 4.2). The south section is a saline sump, with salt lake expressions and groundwater salinity levels of 4% and greater, whereas the north section is much less saline. This difference appears to be related to a major impediment to groundwater flow lying between the topographic Mount Gibson and Mummaloo-Wye-Bubba Hill.

(ii) The saline groundwater system described above appears to flow back, south into the Mine aquifer, at depth (Section 4.3). Thus, the north section, including Midway, has fresher waters (about 3% TDS) overlying hypersaline water (> 13%). This underlying saline system is not observed at Tobias' Find.

(iii) Sterilization waters were very similar to each other and showed a distinctly different hydrogeochemistry from the other Mine water samples (Sections 4.4, 4.5, 4.7.2), being lower in HCO_3 and SO_4, and higher in Si, suggesting that the Sterilization waters have resulted from contact with granitic rather than mafic rocks.

(iv) Waters sampled north of Tobias' Find up to the Orion area (Group 3 and 5) showed roughly similar chemistries (Sections 4.4, 4.5, 4.7.2). A single sample, MG8 (Group 4) was anomalous, with raised Eh, HCO_3, SO_4, Mg, Ag, Cd, Cr, Cu, Ni, Pb and Sb and highly anomalous Au (Section 4.7.5). Gold in this water may be present as $AuCl_2^-$. This sample may represent waters in contact with a local Au/pyrite vein, which has weathered under acid/oxidizing conditions.

(v) The Midway waters (Group 6) were highly enriched in Au, Fe, Mn, Co, Cd, Ba and I, relative to other Mine waters (Section 4.7.3). Gold is possibly present as the $Au(S_2O_3)_2^{3-}$ complex (Section 4.8.4).

(vi) Down gradient from Midway (Group 7), soluble Fe^{2+} has oxidized and precipitated, leading to acid solutions (Section 4.6.3). This has led to major dissolution of many metals, particularly (in order from least to most enriched) Cd, Co, Ni, Zn, Cu, Cr, Al and Ag. This enrichment is related to the base affinity of the metals.

(vii) Gold is not enriched in the acidified waters. This is consistent with Au occurring as the $Au(S_2O_3)_2^{3-}$ complex, which is unstable in acid solutions (Sections 4.6.2, 4.7.4).

(viii) Lead showed anomalous behaviour, possibly due the variety of soluble complexes in which it can occur (Sections 4.7.2 - 4.7.5, 4.8.1)

(ix) Speciation analysis (Section 4.8) suggested that groundwater concentrations of a number of elements were controlled by interaction with soluble phases, as listed below:

Ca	calcite/gypsum
Ba	barite

Si	amorphous silica
Ag	iodyrite
Pb	$PbCO_3$, $Pb_3(VO_4)_2$, $Pb_2V_2O_7$
V	$Pb_3(VO_4)_2$, $Pb_2V_2O_7$, Fe-vanadate
Sb	$Sb(OH)_3$
Au	Au metal

Concentrations of the other elements are possibly controlled by availability or by sorption or other solid/liquid interactions.

(x) Accurate calculation of speciation parameters for Au is not feasible, due to the influence of potential ligands such as $S_2O_3^{2-}$ or CN^-, even at concentrations below the detectable level (Section 4.8.4).

(xi) Correlation coefficient calculations for the Mine waters (Section 4.9.3) indicated that the variables could be roughly divided into 6 groups. The groups and the elements associated are given below:

salinity	SO_4, Br, Na, K, Mg and Cl	(dominated by TDS)
acidity	Al, Ni, Co, Cr, Zn, Cu and Cd	(enriched during ferrolysis)
alkalinity	pH, HCO_3 and Ca	(enriched in alkaline conditions)
Midway	Fe, Ba, I and (weakly) Au	(enriched in Midway waters)
lead	Pb, Zn, Cd	
silicon	Si	

These results are consistent with other observations described above [points (iii) - (ix)].

5.2 Outstanding Questions

Several points of interest are still unresolved. These include:

(i) How extensive is the lower saline aquifer in the mine area?

(ii) How do salinity and other hydrogeochemical parameters vary moving east or west of the line of water sampling bores?

(iii) What are the geochemical events that have lead to the Midway anomaly?

(iv) Does the strong I and Ba enrichment in the Midway waters indicate a usefulness for these elements as pathfinders for Au (or other minerals)?

(v) How extensive is the groundwater acidity down-gradient from Midway?

(vi) What is the relevance of the MG8 anomaly?

(vii) How are all the hydrogeochemical observations related to bedrock geology, as revealed by deep-drilling?

5.3 Implications for Exploration

The area of Au mineralization investigated in this report includes many interesting features, which may be relevant to exploration strategies:

(i) the mineralized area is upgradient to a saline sump system and brines have been refluxing underneath the area over long-time periods;

(ii) soluble gold values were only above detection within the mine area;

(iii) there appear to be two major soluble Au anomalies, one in N2 pit and the other in the region of the Midway pit, which roughly correlate to the two areas of economic Au in bedrock;

(iv) these two anomalies have distinct characteristics and may contain differing Au complexes, with $AuCl_2^-$ in the N2 anomaly and $Au(S_2O_3)_2^{3-}$ in the Midway anomaly.

The different forms of the soluble Au at the two anomalies may, at least, partially explain the difference in the supergene expression of Au at the two sites. Supergene mineralization at the N2 anomaly is restricted, consistent with a low mobility of $AuCl_2^-$ under all conditions except highly acid and oxidizing environments (Section 4.8; Gray, 1989). If the Midway Au is in the form of $Au(S_2O_3)_2^{3-}$ or as Au complexed by any other ligand(s) such as HS^- or CN^- then the Au may be more highly soluble and will form more extensive supergene deposits and associated depletion zones. Gold under these conditions will be strongly immobilized by acid or oxidizing conditions, such as those produced by ferrolysis type reactions, as observed at MG35, down gradient from Midway.

Further investigation of such an effect would be of value. Clearly, it would be advantageous to be able to decide on how Au is dispersed in weathered material, based on groundwater and/or other information. Unfortunately, though there is now a reasonable theoretical understanding of the aqueous chemistry of Au, little is known how this is related to geochemical dispersion patterns.

Based on the information obtained at this site, there may be some advantage in water sampling during drilling operations. Separate samples may be taken for Au analysis and for water quality measurements. The later sample could be sent for commercial analysis for Conductivity/TDS, pH, Fe^{2+}, and a limited suite of elements of interest, such as Mn, Co, Ni, Cu and Zn. Such a procedure could provide a low cost adjunct to petrological information. The observation of the two Au anomalies at this site suggests such a method could be successful in giving information on the location of buried mineralization in an area under investigation.

6.0 SUMMARY AND CONCLUSIONS

As a result of the groundwater survey, several conclusions may be drawn:

(i) the waters can be resolved into a number of (semi-)distinct groundwater masses (Section 4.5);

(ii) waters from the Midway area are anomalously high in Au, Fe, Mn, Co, Cd, Ba and I;

(iii) oxidation and acidification of a Midway type water in areas north of Midway (Section 4.6.3) have resulted in a Ferrolysis water of high acidity, anomalously high in Ag, Al, Cd, Co, Cr, Cu, Mn, Ni and Zn. This effect can be modelled as being due to de-adsorption of metals from oxide surfaces with acidification (Section 4.6);

(iv) speciation analyses (Section 4.8) indicated that elements with 'anomalous' behaviour (e.g. Ca, Pb, V, Sb, Bi) are controlled by precipitation reactions rather than mixing, acidification or mineral dissolution phenomena, as suggested for most of the elements analysed;

(v) observations detailed above were supported by statistical analysis (Section 4.9). In particular Au correlated weakly with the other elements, and the Fe/Mn/Ba correlation which was highly visible for the Midway region, was also observed for a reduced data set which did not include the Midway Pit waters;

(vi) soluble Au was only observed within the mineralized area (Section 4.7). Two major anomalies were recognized: the first, within the Midway area, may represent $Au(S_2O_3)_2^{3-}$ dissolution; while a second more localized anomaly at MG8 may represent $AuCl_2^-$ dissolution.

Implications for exploration are detailed in Section 5.3. In particular measurements of dissolved Au may represent a useful adjunct to drilling in Au exploration, particular with respect to buried mineralization.

ACKNOWLEDGEMENTS

I would like to thank CSIRO staff for their support in the preparation of this report. A. Giblin was involved in advice and in sample collection, while staff who assisted in the analysis of waters included G.D. Longman and M.J. Lintern, who were primarily involved in gold analysis, M.J. Willing, D.C. Wright and A.K. Howe, who provided AAS and Ion Chromatography analyses, and J.W. Wildman who provided ICP analyses. Some of the statistical programs were provided by E.C. Grunsky. Drafting support was provided by C.R. Steel and A.D. Vartesi. Thanks also go to R.E. Smith and R.R. Anand for critical comments and to J.L. Perdrix for support in the Manuscript preparation.

In addition, I would like to thank the staff of Reynolds Australia Mines Pty Ltd and Forsyth (Gibson) Ltd for their assistance during the sample collection period, with particular mention of Simon Coxhell who put significant time into guiding us around the Mount Gibson area.

REFERENCES

Andrews, M.J., Bibby, J.M., Fuge, R. and Johnson, C.C., 1984. The distribution of iodine and chlorine in soils over lead-zinc mineralisation, east of Glogfawr, mid-Wales. *J. Geochem. Explor.*, **20**:19-32.

Anand, R.R., Smith, R.E., Innes, J. and Churchward, H.M., 1989. Exploration geochemistry about the Mt. Gibson gold deposits, Western Australia: Progress to 31 March 1989. CSIRO/AMIRA Laterite Geochemistry Project P240, Report 20R.

Baas Becking, L.G.M., Kaplan, I.R. and Moore, D., 1960. Limits of the natural environment in terms of pH and oxidation-reduction potentials. *J. Geol.*, **68**:243-84.

Benjamin, M.M. and Leckie, J.O., 1981. Multiple site adsorption of Cd, Cu, Zn and Pb on amorphous iron oxyhydroxide. *J. Colliod Interface Sci.*, **79**:209-21.

Blowes, D.W. and Jambor, J.L., 1990. The pore-water geochemistry and the mineralogy of the vadose zone of sulfide tailings, Waite Amulet, Quebec, Canada. *App. Geochem.*, 5:327-46.

Boyle, R.W., 1979. The geochemistry of gold and its deposits. *Geol. Surv. Can., Bull.*, 280, 584 pp.

Brinkman, R., 1977. Surface-water gley soils in Bangladesh: Genesis. *Geoderma*, **17**:111-44.

Chitayeva, N.A., Miller, A.D., Grosse, Yu.I. and Christyakova, N.I., 1971. Iodine distribution in the supergene zone of the Gay chalcopyrite deposit. *Geochem. Int.*, **8(3)**:426-36.

Cloke, P.L. and Kelly, W.C., 1964. Solubility of gold under inorganic supergene conditions. *Econ. Geol.*, **59**:259-70.

Cooley, W.W and Lohnes, P.R., 1971. "Multivariate Data Analysis." (John Wiley & Sons, New York). 364 pp.

Craig, H., 1961. Isotopic variations in meteoric waters. *Science*, **133**:1702-3.

Davis, J.A. and Leckie, J.O., 1978. Effect of adsorbed complexing ligands on trace metal uptake by hydrous oxides. *Environ. Sci. Technol.*, **12**:1309-15.

Diday, E., 1972. The dynamic clusters method in nonhierarchical. Intern. *J. Comp. Inform. Sci.*, 2:61-88.

Dionex, 1985. Technical Note 16. (PO Box 3603 Sunnyvale, California, USA).

Drever, J.I., 1982. "The Geochemistry of Natural Waters." (Prentice-Hall, Inc., Englewood Cliffs, N.J. U.S.A.). 388 pp.

Dubrovsky, N.M., 1986. Geochemical evolution of inactive pyritic tailings in the Elliot Lake Uranium District. (PhD Dissertation: University of Waterloo, Waterloo, Ontario, Canada.)
(Reported in Blowes and Jambor, 1990.)

Eugster, H.P. and Jones, B.F., 1979. Behaviour of major solutes during closed-basin brine evolution. *Amer J. Sci.*, **279**:609-31.

Fedoseyeva, V.I., Fedoseyev, N.F. and Zvonareva, G.V., 1986. Interaction of some gold complexes with humic and fulvic acids. *Geochem. Int.*, **23(3)**:106-10.

Forbes, E.A., Posner, A.M. and Quirk, J.P., 1976. The specific adsorption of divalent Cd, Co, Cu, Pb and Zn on goethite. *J. Soil Sci.*, **27**:154-66.

Frick, C., Strauss, S.W. and Dixon, R., 1989. The use of chlorine, bromine and fluorine in detecting a buried Cu-Zn orebody along the zinc-line in the Murchison Range, South Africa. *J. Geochem. Explor.*, **34**:83-102.

Fuge, R., 1990. The role of volatility in the distribution of iodine in the secondary environment. *Appl. Geochem.*, **5**:357-360.

Fuge, R. and Johnson, C.C., 1984. Evidence for the chalcophile nature of iodine. *Chem. Geol.*, **43**:347-52.

Fuge, R. and Johnson, C.C., 1986. The geochemistry of iodine - a review. *Environ. geochem. Hlth.*, **8**:31-54.

Fuge, R., Andrews, M.J. and Johnson, C.C., 1986. Chlorine and iodine, potential pathfinder elements in exploration geochemistry. *Appl. Geochem.*, **1**:111-6.

Fuge, R., Andrews, M.J., Clevenger, T.E., Davies, B.E., Gale, N.L., Pavely, C.F. and Wixson, B.G., 1988. The distribution of chlorine and iodine in soil in the vicinity of lead mining and smelting operations, Bixby area, S.E. Missouri, U.S.A. *Appl. Geochem.*, **3**:517-21.

Garrels, R.M. and Christ, C.L., 1965. "Solutions, Minerals and Equilibria." (Harper and Row, New York). 450 pp.

Gat, J.R. and Gonfiantini, R., 1981. "Stable Isotope Hydrology. Deuterium and Oxygen-18 in the Water Cycle." (Technical Reports Series No. 210, IAEA, Vienna 1981, ISBN 92-0-145281-0).

Gold Gazette, 1988. May Mellor bullish on Forsayth NL. 10 Oct., p.71.

Goldhaber, M.B., 1983. Experimental study of metastable sulfur oxyanion formation during pyrite oxidation at pH 6-9 and 30°C. *Amer. J. Sci.*, **283**:193-217.

Goleva, G.A., Krivenko, V.A. and Gutz, Z.G., 1970. Geochemical trends in the occurrence and migration forms of gold in natural waters. *Geochem. Int.*, **7**:518-29.

Goni, J., Guillemin, C. and Sarcia, C., 1967. Geochemie de l'or exogene. Etude experimentale de la formation des dispersions colloidales d'or et de leur stabilite. *Miner. Deposita*, **1**:259-68.

Granger, H.C. and Warren, C.G., 1969. Unstable sulfur compounds and the origin of roll-type uranium deposits. *Econ. Geol.*, **64**:160-71.

Gray, D.J., 1986. The geochemistry of uranium and thorium during weathering of chloritic schists at the Alligator Rivers Uranium Province, N.T., Australia. (PhD Dissertation: University of Sydney, Sydney, NSW, Australia.)

Gray, D.J., 1989. "The Aqueous Chemistry of Gold in the Weathering Environment." CSIRO/AMIRA Projects 240/241. Exploration Geoscience Restricted Report EG 4R.

Grimme, H., 1968. Die adsorption von Mn, Co, Cu und Zn durch Goethit aus verdünnten Lösungen. *Zeit. Pflanzen. Bodenkunde*, **121**:58-65.

Grunsky, E.C., 1986. Recognition of alteration in volcanic rocks using statistical analysis of lithochemical data. *J. Geochem. Explor.*, **25**:157-83.

Hostettler, J.D., 1984. Electrode electrons, aqueous electrons, and redox potentials in natural waters. *Amer. J. Sci*, **284**:734-59.

Jacobson, G., Arakel, A.V. and Chen Yijian, 1988. The central Australian groundwater discharge zone: Evolution of associated calcrete and gypcrete deposits. *Aust. J. Earth Sci.*, **35**:549-65.

Kinniburgh, D.G. and Jackson, M.L., 1982. Concentration and pH dependence of calcium and zinc adsorption by iron hydrous oxide gel. *Soil Sci. Soc. Amer. J.*, **46**:56-61.

Kinniburgh, D.G., Jackson, M.L. and Syers, J.K., 1976. Adsorption of alkaline earth, transition, and heavy metal cations by hydrous oxide gels of iron and aluminum. *Soil Sci. Soc. Amer. J.*, **40**:796-99.

Kolotov, B.A., Spasskaya, T.S., Vagner, B.B. and Minacheva, L.I., 1980. The relationship between colloidal and other forms of migration of gold in water in the supergene zones of ore deposits *Geochem. Int.*, **17**:80-2.

Krauskopf, K.B., 1951. The solubility of gold. *Econ. Geol.*, **46**:858-70.

Lakin, H.W., Curtin, G.C. and Hubert, A.E., 1974. Geochemistry of gold in the weathering cycle. U.S. Geol. Surv. Bull. 1330, 80 pp.

Lefebvre, D. and David, M., 1977. Dynamic clustering and strong patterns recognition: new tools in automatic classification. *Can. J. Earth Sci.*, **14**:2232-45.

Lipple, S.L., Baxter, L.J. and Marston, R.J., 1983. Ninghan, Western Australia, Geol. Surv. West. Aust. 1:250 000 Geol. Series Explan. Notes, 23 pp.

Listova, L.P., Vainshtein, A.Z. and Ryabinina, A.A., 1968. Dissolution of gold in media forming during oxidation of some sulphides. Metallogeniya Osad. Osad.-Metamorf. Porad, Akad. Nauk SSSR, Lab. Osad. Polez. Iskop. pp 189-199. (In Russian, obtained from Chemical Abstracts 68: 88967h).

Mann, A.W., 1984a. Mobility of gold and silver in lateritic weathering profiles: some observations from Western Australia. *Econ. Geol.*, **79**:38-49.

Mann, A.W., 1984b. Redistribution of gold in the oxidized zone of some Western Australian deposits. A.I.M.M. Perth and Kalgoorlie Branches, Regional Conf. on "Gold Mining, Metallurgy and Geology", Oct 1984.

Mann, A.W. and Deutscher, R.L., 1977. Solution geochemistry of copper in water containing carbonate, sulphate and chloride ions. *Chem. Geol.*, **19**:253-65.

Mann, A.W. and Deutscher, R.L., 1980. Solution geochemistry of lead and zinc in water containing carbonate. *Chem. Geol.*, **29**:293-311.

Marston, R.J., 1979. Copper mineralization in Western Australia. Geol. Surv. West. Aust. Min. Resources Bull., 13, 208 pp.

McKensie, R.M., 1980. The adsorption of lead and other heavy metals on oxides of manganese and iron. *Aust. J. Soil Res.*, **18**:61-73.

Miller, A.D. and Fisher, E.I., 1973. Dissolution of gold during oxidation by MnO_2. *Geochem. Int.*, **10**:656-63.

Ong, H.L. and Swanson, V.E., 1969. Natural organic acids in the transportation, deposition and concentration of gold. *Colo. Sch. Mines*, **Q., 64(1)**:395-425.

Ong, H.L., Swanson, V.E. and Bisque, R.E., 1970. Natural organic acids as agents of chemical weathering. U.S. Geol. Surv., Prof. Pap. 700C: 130-137.

Padmanabham, M., 1983a. Adsorption-desorption behaviour of copper(II) at the goethite-solution interface. *Aust. J. Soil Res.*, **21**:309-320.

Padmanabham, M., 1983b. Competitive study of the adsorption-desorption behaviour of copper(II), zinc(II), cobalt(II) and lead(II) at the goethite-solution interface. *Aust. J. Soil Res.*, **21**:515-525.

Parkhurst, D.L., Thorstenson, D.C. and Plummer, L.N., 1980. PHREEQE, a computer program for geochemical calculations. U.S. Geol. Surv. Water Resources Investigations 80-96, 210 pp.

Pitul'ko, V.M., 1976. The behaviour of gold in the oxidation zones of deposits in the far north. *Geochem. Int.*, **13**:157-63.

Plyusnin, A.M., Pogrelnyak, Yu.F., Mironov, A.G. and Zhmodik, S.M., 1981. The behaviour of gold in the oxidation of gold bearing sulphides. *Geochem. Int.*, **18**:116-23.

Rolla, E. and Chakrabarti, C.L., 1982. Kinetics of decomposition of tetrathionate, trithionate and thiosulphate in alkaline media. *Environ. Sci. Technol.*, **16**:852-7.

Sato, M., 1960. Oxidation of sulfide ore bodies, 1. Geochemical environments in terms of Eh and pH. *Econ. Geol.*, **55**:928-61.

Schwab, A.P. and Lindsay, W.L., 1983. Effect of redox on the solubility and availability of iron. *Soil Sci. Soc. Am. J.*, **47**:201-5.

Smith, R.E., 1987. Patterns in laterite geochemistry, Mt. Gibson, Western Australia. Geochemex Australia Progress report to Forsayth NL, 37 pp.

Venkataramini, B., Venkateswarlu, K.S. and Shankar, J., 1978. Sorption properties of oxides. III. Iron oxides. *J. Colliod Interface Sci.*, **67**:187-94.

Weast, R.C., Astle, M.J. and Beyer, W.H., 1984. "CRC Handbook of Chemistry and Physics." F-154 Elements in Sea Water. (64th Edition; CRC Press Inc., Florida, USA).

Webster, J.G., 1984. Thiosulphate complexing of gold and silver during the oxidation of a sulphide-bearing carbonate lode system, Upper Ridges Mine, P.N.G. A.I.M.M. Perth and Kalgoorlie Branches, Regional Conf. on "Gold Mining, Metallurgy and Geology", Oct 1984.

Webster, J.G., 1986. The solubility of gold and silver in the system Au-Ag-S-O_2-H_2O at 25°C and 1 atm. *Geochim. Cosmochim. Acta*, **50**:1837-45.

Webster, J.G. and Mann, A.W., 1984. The influence of climate, geomorphology and primary geology on the supergene migration of gold and silver. *J. Geochem. Explor.*, **22**:21-42.

Xie Xuejing, Sun Huanzhen and Li Shanfang, 1981. Geochemical exploration in China. *J. Geochem. Explor.*, **15**:489-506.

Appendix 1. Mount Gibson Groundwaters - Analytical Data

Sample No.	Hole Name	Class	Easting (m)	Northing (m)	RL (m)	R (m)	Incline (deg.)	WT (m)	SD (m)	WT (mRL)	SD (mRL)
MG1	1581	3	1060	2800	347	873	60	39	43	313	310
MG2	1473	3	1100	3200	341	1265	60	34	39	312	307
MG3	1566	3	730	3200	346	1146	60	39	43	313	310
MG4	1605	3	875	3450	340	1429	60	31	32	314	313
MG5	1611	3	740	3450	347	1385	60	38	43	314	310
MG6	1472	3	800	3600	345	1547	60	nd	nd	nd	nd
MG7	1456	3	1360	4000	336	2106	60	28	33	312	308
MG8	1460	4	1180	4000	337	2048	60	30	35	311	307
MG9	1617	5	1200	4200	335	2244	60	25	31	313	308
MG10	1554	5	1320	4450	332	2519	60	24	29	312	308
MG11	1612	5	1350	4600	331	2671	60	22	24	312	311
MG12	1530	5	1550	4800	327	2924	60	18	23	312	307
MG13	PB6	6	1985	6120	321	4314	90	12	17	309	304
MG14	1491	5	1675	5200	326	3343	60	18	22	311	307
MG15	1590	5	1700	5400	324	3541	60	17	22	310	305
MG16	1478	6	1775	5600	322	3754	60	16	21	309	305
MG17	1489	5	1800	5200	324	3384	60	17	20	310	307
MG18	1591	2	700	2000	361	0	60	50	80	318	292
MG19	1591	2	700	2000	361	0	60	50	68	318	303
MG20	1591	2	700	2000	361	0	60	50	55	318	314
MG21	44	10	1250	6550	318	na	90	11	16	308	303
MG22	45	10	1300	6550	318	na	90	10	15	308	303
MG23	46	10	1350	6550	318	na	60	12	17	308	303
MG24	47	10	1400	6550	318	na	90	11	16	308	303
MG25	48	10	1450	6550	318	na	90	10	15	309	304
MG26	49	10	1500	6550	318	na	90	10	15	309	304
MG27	50	10	1550	6550	318	na	90	11	16	308	303
MG28	51	10	1600	6550	318	na	90	10	15	309	304
MG29	MGH510	10	1800	6550	319	na	90	10	15	309	304
MG30	M2	6	2000	6650	319	4820	90	10	15	309	304
MG31	41	10	1650	6750	318	na	90	10	15	309	304
MG32	39	10	1550	6750	318	na	90	10	15	309	304
MG33	36	10	1400	6750	318	na	90	11	16	308	303
MG34	M3	6	2200	6900	nd	5122	90	9	12	nd	nd
MG35	MGR003	7	2750	7300	317	5678	60	11	13	308	306
MG36	M4	11	3630	14440	nd	na	90	6	8	nd	nd
MG37	M5	11	3610	15682	nd	na	90	5	10	nd	nd
MG38	M6	11	2564	15600	nd	na	90	4	9	nd	nd
MG39	SC Wind.	13	1950	9480	nd	na	90	13	18	nd	nd
MG40	M dewater	8	2265	6590	nd	4849	nd	nd	nd	nd	nd
MG41	Lake Karpa	9	5060	7735	nd	na	na	nd	nd	nd	nd
MG42	Karpa Bore	13	5435	8885	nd	na	90	nd	nd	nd	nd
MG43	M7	6	2300	6675	319	4941	90	17	22	302	297
MG44	PB1	12	4309	19925	nd	na	90	nd	nd	nd	nd
MG45	OB7	12	5739	17725	nd	na	90	14	19	nd	nd
MG46	OB11	12	3279	22155	nd	na	90	20	25	nd	nd
MG47	OB10	12	3159	23355	nd	na	90	19	24	nd	nd
MG48	OB6	12	3609	23925	nd	na	90	21	26	nd	nd
MG49	OB9	12	5059	16975	nd	na	90	9	14	nd	nd
MG50	M9	1	3300	-750	nd	na	90	28	33	nd	nd

na : not applicable
nd : not determined

WT: Watertable
SD: Sampling Depth

	Eh (V)	pH	Fe^{2+} (mg/L)	DO # (mg/L)	HCO_3 (mg/L)	SO_4 (mg/L)	Cl (mg/L)	Br (mg/L)	I (mg/L)	NO_3 (mg/L)	S_2O_3 (mg/L)
MG1	0.40	6.2	0	4.4	275	580	3480	12.9	0.14	22	<0.004
MG2	0.39	6.5	0	5.3	253	525	3040	11.8	0.086	25	<0.002
MG3	0.39	6.2	0	4.4	187	575	3630	12.5	0.11	12	nd
MG4	0.43	6.4	0	4.9	275	1060	7200	24.4	0.095	6.6	nd
MG5	0.37	6.4	0.1	4.5	203	1230	8200	26.3	0.45	<0.9	nd
MG6	0.28	6.5	0	3.7	304	1600	10900	35	0.47	<1.5	nd
MG7	0.26	6.6	1	4.1	296	1130	8040	25.5	0.47	<0.9	nd
MG8	0.45	6.6	0	5	335	1390	7900	27.6	0.15	21	<0.008
MG9	0.41	6.6	0	7	287	940	5950	20.7	0.035	28	nd
MG10	0.38	6.1	0.1	4	240	2110	12800	43.7	0.87	0.69	nd
MG11	0.37	6.5	0	5.3	272	1920	12900	41.3	0.32	3.1	nd
MG12	0.39	6.9	0	3.7	302	1710	13000	37.8	0.72	11	nd
MG13	nd	6.8	52	2.8	15	2360	17300	53	1.7	<2.4	<0.02
MG14	0.19	6.6	1.5	3.6	178	495	3460	11.5	0.045	9.2	nd
MG15	0.37	6.5	0	6.7	250	1310	8290	28.4	0.018	36	nd
MG16	0.32	6.5	0.4	4	311	1560	10400	34.3	1.4	<1.5	<0.008
MG17	0.35	6.87	0	6	316	950	6650	21.9	0.031	35	nd
MG18	0.22	6.9	1.5	3.8	55	205	985	3.8	0.48	18	0.005
MG19	0.19	6.8	1.8	4.5	45	205	985	3.8	0.49	17	0.13
MG20	0.28	6.9	0.5	5.1	54	210	985	3.7	0.57	15.9	0.14
MG21	0.41	6.1	0	4.1	96	580	4680	15.3	0.61	3.33	nd
MG22	0.32	6.1	0	5.7	97	545	4480	14.9	0.038	14.2	nd
MG23	0.32	6.3	0	6.3	104	620	4670	16.2	0.058	12	nd
MG24	0.37	6.2	0	6.4	91	595	4870	16	0.072	14.7	nd
MG25	0.38	6.2	0	5.2	93	645	5090	17.1	0.04	18.1	<0.008
MG26	0.39	6.2	0	4.9	102	685	5520	17.9	0.115	13.4	nd
MG27	0.38	6.3	0	6.2	107	695	5030	16.9	0.006	14.1	nd
MG28	0.38	6.1	0	4.6	107	745	5640	18.3	0.032	12.9	nd
MG29	0.42	6.2	0	6.8	89	800	5630	18.6	0.028	13.7	nd
MG30	0.33	6.1	4	3.4	205	1650	10900	36.5	1.4	<1.5	0.02
MG31	0.29	6.2	0	5.2	99	760	6000	19.8	0.051	11.4	nd
MG32	0.30	6.2	0	6.6	80	645	5070	17.3	0.015	14.4	nd
MG33	0.32	6	0	4.9	87	545	4510	15	0.022	10.1	nd
MG34	0.04	6.3	5	2.5	496	2490	21400	62	0.21	<2.4	0.04
MG35	0.53	3.5	0	6.4	0	3180	24600	70	0.39	<2.4	<0.024
MG36	0.25	6.6	0	4.4	463	2700	21700	54	0.39	6.2	nd
MG37	0.18	7	5	2.6	1430	2230	22100	58	4.4	<2.4	nd
MG38	0.31	6.8	0	6.3	282	3530	30800	74	0.04	41.2	nd
MG39	0.14	7.5	1	3.4	440	2.4	410	1.6	0.50	0.2	<0.002
MG40	nd	6.5	5	5.7	150	8790	72700	170	0.95	<7	<0.072
MG41	0.32	7.4	0	2.1	287	26000	178000	600	1	<24	<0.2
MG42	nd	8.4	0	4.1	565	190	1600	4.8	0.25	3.2	0.06
MG43	nd	5.4	44	3.3	4	2660	20900	62	0.75	<2.4	<0.014
MG44	nd	7.1	4	6.3	435	640	3890	12.5	0.7	36	<0.002
MG45	nd	6.9	0	7.4	348	220	1280	4.8	<0.001	60	<0.002
MG46	nd	7.1	0	6.8	596	1130	7010	22.1	0.043	56	nd
MG47	nd	7	0	6.9	539	1340	8730	26.9	0.032	49	nd
MG48	nd	6.9	0	4.8	571	1580	10100	31.6	0.024	42	nd
MG49	nd	7.4	0.4	3.9	579	1580	12600	38.1	4.5	<1.5	nd
MG50	nd	5	0	6	6	11.4	195	0.8	0.013	12	nd
SW			0.01		142	2210	19000	65	0.06	2.2	

: Dissolved Oxygen

nd : not determined

	Na (mg/L)	K (mg/L)	Mg (mg/L)	Ca (mg/L)	TDS (mg/L)	Anions (meq/L)	Cations (meq/L)	Cat-An/ /Anions	Al (mg/L)	Ba (mg/L)
MG1	2209	81	212	41	6914	115	118	0.02	0	0
MG2	1998	73	195	37	6195	101	107	0.05	0	0.014
MG3	2429	78	150	26	7139	118	121	0.03	0.006	0.007
MG4	4676	152	457	97	13977	230	250	0.09	0	0
MG5	5032	152	460	95	15434	261	265	0.02	0	0.064
MG6	6417	186	631	130	20235	346	342	-0.01	0	0.022
MG7	4843	157	521	141	15185	256	265	0.04	0	0.020
MG8	4737	169	564	116	15288	258	263	0.02	0	0.019
MG9	3594	131	355	77	11407	193	193	0.00	0.009	0.012
MG10	7559	271	844	168	24065	410	414	0.01	0	0.015
MG11	7945	258	831	180	24373	409	430	0.05	0	0.013
MG12	7642	241	836	214	24023	408	418	0.02	0	0.078
MG13	9761	330	1148	261	31296	538	543	0.01	0	0.103
MG14	2058	76	219	57	6578	111	112	0.01	0	0.029
MG15	5115	178	526	121	15890	266	276	0.04	0	0.010
MG16	6409	216	660	152	19781	331	346	0.04	0	0.009
MG17	3874	144	409	106	12540	213	211	-0.01	0	0.019
MG18	666	26.5	28	14.0	2032	33	33	-0.02	0	0.061
MG19	673	26.7	29	16.1	2030	33	33	0.00	0	0.067
MG20	662	26.3	28	11.5	2027	33	32	-0.03	0	0.066
MG21	2853	106	247	55	8676	146	150	0.03	0	0.031
MG22	2724	99	227	52	8294	140	142	0.02	0	0.022
MG23	2928	106	259	67	8822	147	155	0.05	0	0.028
MG24	2898	104	249	57	8935	152	152	0.00	0.007	0.023
MG25	3065	115	279	65	9429	159	162	0.02	0	0.027
MG26	3284	120	299	69	10154	172	174	0.01	0	0.026
MG27	3133	112	285	61	9495	159	166	0.04	0	0.014
MG28	3360	123	321	63	10432	177	179	0.01	0	0.018
MG29	3420	111	349	62	10536	177	183	0.03	0	0.021
MG30	6583	199	667	133	20421	346	353	0.02	0	0.068
MG31	3685	127	369	85	11200	187	198	0.06	0	0.022
MG32	3178	123	281	62	9512	158	168	0.06	0	0.020
MG33	2769	106	209	39	8332	140	142	0.01	0.007	0.022
MG34	10820	330	1295	472	37387	664	610	-0.08	0	0.089
MG35	12864	432	1719	124	43059	761	718	-0.06	15	0.039
MG36	12031	373	1562	367	39295	677	680	0.00	0.035	0.046
MG37	13015	284	1473	444	41065	694	717	0.03	0	0.254
MG38	17631	453	1693	720	55243	949	954	0.01	0	0.021
MG39	265	8.4	51	70	1277	19	20	0.04	0	0.862
MG40	41239	1109	4891	747	129829	2239	2262	0.01	0	0.017
MG41	90045	5174	13623	331	314142	5575	5187	-0.07	0	0.027
MG42	810	28.7	172	153	3559	58	58	-0.01	0	0.053
MG43	12107	381	1469	189	37853	646	668	0.03	1.1	0.044
MG44	2482	82	272	76	7967	131	136	0.04	0	0.008
MG45	840	33.4	99	37	2966	47	47	0.00	0	0.026
MG46	4381	144	502	97	13980	232	240	0.04	0	0.063
MG47	5198	191	518	100	16728	284	279	-0.02	0	0.061
MG48	6280	199	678	127	19651	328	340	0.04	0	0.023
MG49	7567	233	736	199	23571	398	406	0.02	0	0.165
MG50	110	5.7	13	1.7	375	6	6	0.02	0.26	0.060
SW	10500	380	1350	400.0	34061	585	598	0.02	0.01	0.030

	Cr (mg/L)	Fe (mg/L)	Mn (mg/L)	Ni (mg/L)	Sr (mg/L)	Ag (mg/L)	Cd (mg/L)	Co (mg/L)	Cu (mg/L)	Pb (mg/L)
MG1	0	0	0	0.01	0	0.013	0	0	0.004	0
MG2	0	0	0	0	0	0.012	0	0	0.008	0
MG3	0	0	0.02	0	0	0.007	0	0	0.011	0.07
MG4	0.004	0	0.01	0.02	0.7	0.030	0	0	0.013	0.13
MG5	0	0	0.61	0.04	0.6	0	0.003	0.01	0.004	1.15
MG6	0	0.77	0.21	0	0.3	0	0	0	0	0
MG7	0	0	0.31	0	2.1	0	0	0	0	0.14
MG8	0.013	0	0.03	0.02	2.5	0.021	0.006	0	0.140	0.54
MG9	0.006	0	0.01	0.01	1.3	0.013	0	0	0.003	0.10
MG10	0	0	0.13	0	4.8	0	0.005	0	0	0.40
MG11	0.003	0	0.13	0	2.3	0.006	nd	0	0	0.43
MG12	0	0	0.12	0	3.3	0.006	0	0	0	0.10
MG13	0.002	47	6.3	0.01	3.3	0	0.010	0.06	0	0.07
MG14	0	0.11	0.23	0	0	0.006	0	0	0	0
MG15	0	0	0	0	2.5	0	0.003	0	0	0
MG16	0	0	0.08	0.01	2.9	0	0.004	0	0	0.85
MG17	0	0	0	0.01	1.1	0.014	0	0	0.003	0
MG18	0	0	0.36	0.02	0	0	0	0.01	0	0.06
MG19	0	0.20	0.47	0.03	0	0	0.003	0.01	0	0.06
MG20	0	0	0.54	0.03	0.1	0	0	0.01	0	0.06
MG21	0	0	0.05	0.01	1.4	0.008	0	0.01	0.002	0
MG22	0	0	0.08	0	0.4	0	0	0.01	0	0
MG23	0	0	0.10	0	1.5	0.006	0	0	0.005	0
MG24	0	0	0.02	0	0.9	0.002	0	0	0	0
MG25	0	0	0.01	0.01	1.2	0.009	0	0	0.002	0
MG26	0.003	0	0.02	0.01	1.2	0.009	0	0	0.003	0
MG27	0	0	0.01	0.01	1.4	0.011	0	0	0.009	0
MG28	0	0	0.02	0.01	1.3	0.003	0	0	0	0
MG29	0	0	0.03	0.01	1.2	0.003	0	0	0	0
MG30	0	0	0.76	0.04	2.6	0	0	0.03	0	0
MG31	0	0	0.02	0.02	2.0	0.007	0	0.01	0	0
MG32	0	0	0.01	0	1.1	0.006	0	0	0	0
MG33	0.002	0	0.01	0	1.5	0.006	0	0	0	0
MG34	0.004	0	5.4	0.02	4.1	0	0	0.02	0	0.07
MG35	0.026	0.07	3.8	0.28	3.4	0.022	0.013	0.22	0.140	0.37
MG36	0	0	0.28	0.01	4.1	0	0	0.01	0	0
MG37	0.005	0	4.5	0.01	4.7	0	0	0.01	0	0.09
MG38	0	0	0.10	0.01	6.5	0.007	0	0	0	0
MG39	0	0.07	2.9	0.01	0.1	0	0	0.01	0	0.06
MG40	0	0	1.4	0.03	9.6	0.070	0	0.03	0	0
MG41	0.15	0	26.7	0.24	15.2	0.15	0.063	0.21	0.036	1.29
MG42	0	0	0.37	0.02	3.4	0	0	0.01	0	0.13
MG43	0	42	1.1	0.06	2.7	0	0.008	0.09	0.048	0
MG44	0	0	0.06	0.01	2.1	0	0	0	0	0
MG45	0.003	0	0.02	0.01	1.0	0	0	0.01	0	0.06
MG46	0	1.1	0.05	0	2.8	0.012	0	0	0	0
MG47	0.009	0	0.01	0	3.4	0	0	0	0	0
MG48	0.035	0.07	0	0	4.4	0	0	0	0	0.08
MG49	0	0	4.7	0	7.5	0	0	0.01	0	0
MG50	0	0.07	0.07	0.02	0	0	0	0.01	0.109	0.06
SW	0.00005	0.01	0.002	0.01	8.1	0.0003	0.00011	0.00027	0.003	0.00003

nd: not determined

	Zn (mg/L)	Si (mg/L)	Au (μg/L)	V (mg/L)	Bi (mg/L)	Sb (mg/L)
MG1	0	nd	0.10	0.055	0.007	0.011
MG2	0	38	<0.05	0.06	<0.002	0.006
MG3	0.23	39	<0.05	0.026	<0.002	0.011
MG4	0	28	0.15	0.015	0.004	0.006
MG5	0.51	31	0.05	0.02	<0.002	0.007
MG6	0	28	0.10	0.026	<0.002	<0.005
MG7	0	28	0.10	0.01	<0.002	0.009
MG8	0	25	1.00	0.013	<0.002	0.019
MG9	0	22	0.05	0.045	0.005	<0.005
MG10	0	22	0.25	0.022	<0.002	0.016
MG11	0	19	0.30	0.027	<0.002	<0.005
MG12	0	24	<0.05	0.025	<0.002	0.006
MG13	0.11	6	0.25	0.002	0.007	0.011
MG14	0	14	0.35	0.053	<0.002	<0.005
MG15	0	34	0.20	0.07	<0.002	<0.005
MG16	0.12	32	0.15	0.022	0.003	0.008
MG17	0	33	0.05	0.061	0.003	0.005
MG18	0.10	30	0.20	0.153	0.005	0.015
MG19	0.17	28	<0.05	0.083	<0.002	0.037
MG20	0.12	29	0.25	0.112	0.006	0.049
MG21	0	39	<0.05	0.03	<0.002	0.011
MG22	0	41	<0.05	0.029	<0.002	<0.005
MG23	0	38	nd	nd	nd	nd
MG24	0	39	0.10	0.06	0.003	0.01
MG25	0.01	41	0.15	0.142	<0.002	0.008
MG26	0	42	0.25	0.049	<0.002	0.01
MG27	0	40	<0.05	0.023	<0.002	<0.005
MG28	0	41	<0.05	0.048	0.003	<0.005
MG29	0	41	0.10	0.048	0.003	0.009
MG30	0	41	<0.05	0.079	<0.002	0.015
MG31	0	42	<0.05	0.04	0.003	0.011
MG32	0	41	nd	nd	nd	nd
MG33	0	40	<0.05	0.022	<0.002	0.012
MG34	0.06	8	nd	0.088	0.005	<0.005
MG35	0.61	44	<0.05	0.018	<0.002	0.008
MG36	0.31	34	<0.05	0.08	<0.002	<0.005
MG37	0.057	15	<0.05	0.011	0.007	0.021
MG38	0.11	13	<0.05	0.006	<0.002	<0.005
MG39	0.064	24	<0.05	0.037	<0.002	0.011
MG40	0	13	<0.05	<0.002	0.002	<0.005
MG41	0.90	13	<0.05	<0.002	0.002	<0.005
MG42	0.12	29	0.15	0.362	0.003	0.007
MG43	0	30	1.05	<0.002	<0.002	0.006
MG44	8.74	30	<0.05	0.058	<0.002	0.012
MG45	0.19	43	<0.05	0.048	<0.002	0.011
MG46	0	37	<0.05	0.073	0.003	0.008
MG47	0.026	33	<0.05	0.053	<0.002	0.007
MG48	0	37	<0.05	0.067	0.003	0.006
MG49	0	21	<0.05	0.011	<0.002	0.008
MG50	0.13	18	<0.05	0.004	<0.002	0.014
SW	0.01	3		0.002	0.00002	0.0003

nd: not determined

Appendix 2. Sample PHREEQE Output

(see Section 4.8 for details)

```
MG1           Hole No. 1581
0000000000 0 0          .00000
SOLUTION 1
Class 3       1060 East   2800 North
17 10 2     6.20      6.80      25.0      1.01
  10  2.750D+02  29  5.800D+02  13  3.480D+03   9  1.290D+01  18  1.350D-01
  23  2.160D+01  24  2.209D+03  19  8.100D+01  21  2.120D+02  11  4.110D+01
  25  9.000D-03   4  1.300D-02  15  4.000D-03  38  8.000D-05  33  5.500D-02
  40  7.000D-03  35  1.100D-02
SOLUTION NUMBER 1          Class 3       1060 East   2800 North
```

TOTAL MOLALITIES OF ELEMENTS

ELEMENT	MOLALITY	LOG MOLALITY
Ag	1.198242D-07	-6.9215
Br	1.605148D-04	-3.7945
TOT ALK	4.481001D-03	-2.3486
Ca	1.019549D-03	-2.9916
Cl	9.759335D-02	-1.0106
Cu	6.258434D-08	-7.2035
I	1.057672D-06	-5.9756
K	2.059586D-03	-2.6862
Mg	8.669801D-03	-2.0620
N	3.463552D-04	-3.4605
Na	9.553323D-02	-1.0198
Ni	1.524138D-07	-6.8170
SO4	6.003052D-03	-2.2216
V	1.073458D-06	-5.9692
Sb	8.982923D-08	-7.0466
Au	4.038235D-10	-9.3938
Bi	3.330324D-08	-7.4775

----DESCRIPTION OF SOLUTION----

PH =	6.20
PE =	6.7951
ACTIVITY H2O =	.9963
IONIC STRENGTH =	.1255
TEMPERATURE =	25.0000
ELECTRICAL BALANCE =	2.7847D-03
THOR =	7.1391D-02
TOTAL ALKALINITY =	4.4810D-03
ITERATIONS =	12
TOTAL CARBON =	8.8826D-03

DISTRIBUTION OF SPECIES

I	SPECIES	Z	MOLALITY	LOG MOLALITY	ACTIVITY	LOG ACTIVITY
1	H+	1.0	9.57D-07	-6.02	6.31D-07	-6.20
2	E-	-1.0	1.60D-07	-6.80	1.60D-07	-6.80
3	H2O	.0	9.96D-01	.00	9.96D-01	.00
4	Ag+	1.0	9.20D-11	-10.04	7.07D-11	-10.15
9	Br-	-1.0	1.61D-04	-3.79	1.23D-04	-3.91
10	CO3 2-	-2.0	6.84D-07	-6.16	2.39D-07	-6.62
11	Ca 2+	2.0	9.10D-04	-3.04	3.58D-04	-3.45
13	Cl-	-1.0	9.76D-02	-1.01	7.20D-02	-1.14
15	Cu 2+	2.0	3.46D-08	-7.46	1.21D-08	-7.92
18	I-	-1.0	1.06D-06	-5.98	8.12D-07	-6.09
19	K+	1.0	2.04D-03	-2.69	1.51D-03	-2.82
21	Mg 2+	2.0	7.56D-03	-2.12	3.10D-03	-2.51
23	NO3 -	-1.0	3.81D-07	-6.42	2.93D-07	-6.53
24	Na+	1.0	9.48D-02	-1.02	7.29D-02	-1.14
25	Ni 2+	2.0	1.22D-07	-6.91	4.27D-08	-7.37
29	SO4 2-	-2.0	4.28D-03	-2.37	1.36D-03	-2.87
33	VO2 1+	1.0	5.13D-12	-11.29	3.94D-12	-11.40
35	SbO +	1.0	1.16D-12	-11.94	8.88D-13	-12.05
38	Au+	1.0	2.93D-17	-16.53	2.25D-17	-16.65
40	Bi 3+	3.0	2.59D-18	-17.59	2.42D-19	-18.62
52	Cu+	1.0	1.32D-12	-11.88	1.02D-12	-11.99
55	NH4 +	1.0	2.01D-04	-3.70	1.54D-04	-3.81
56	NO2 -	-1.0	1.45D-04	-3.84	1.12D-04	-3.95
64	VO 2+	2.0	6.16D-14	-13.21	2.15D-14	-13.67
65	OH-	-1.0	2.05D-08	-7.69	1.58D-08	-7.80
78	MgCO3 0	.0	6.86D-07	-6.16	7.06D-07	-6.15
79	MgHCO3 +	1.0	1.51D-04	-3.82	1.16D-04	-3.94
80	MgSO4 0	.0	9.60D-04	-3.02	9.88D-04	-3.01
85	CaHCO3 +	1.0	1.55D-05	-4.81	1.19D-05	-4.92
86	CaCO3 0	.0	1.18D-07	-6.93	1.21D-07	-6.92
87	CaSO4 0	.0	9.42D-05	-4.03	9.70D-05	-4.01
93	NaCO3 -	-1.0	4.21D-07	-6.38	3.24D-07	-6.49
94	NaHCO3 0	.0	1.28D-04	-3.89	1.32D-04	-3.88
95	NaSO4 -	-1.0	6.46D-04	-3.19	4.96D-04	-3.30
99	KSO4 -	-1.0	1.87D-05	-4.73	1.44D-05	-4.84
151	CuCl2 -	-1.0	2.17D-09	-8.66	1.67D-09	-8.78
152	CuCl3 2-	-2.0	5.45D-10	-9.26	1.90D-10	-9.72
153	CuCO3 0	.0	1.50D-08	-7.82	1.55D-08	-7.81
154	Cu(CO3)2	-2.0	3.12D-11	-10.51	1.09D-11	-10.96
155	CuCl +	1.0	3.05D-09	-8.52	2.34D-09	-8.63
156	CuCl2 0	.0	8.79D-11	-10.06	9.05D-11	-10.04
160	CuOH +	1.0	7.85D-10	-9.11	6.03D-10	-9.22
161	Cu(OH)2	.0	1.85D-12	-11.73	1.90D-12	-11.72
165	CuSO4 0	.0	3.26D-09	-8.49	3.35D-09	-8.47
167	CuHCO3 +	1.0	2.98D-09	-8.53	2.29D-09	-8.64
243	NiOH +	1.0	1.21D-11	-10.92	9.31D-12	-11.03
244	Ni(OH)2	.0	1.03D-14	-13.99	1.06D-14	-13.97
245	NiHCO3 +	1.0	6.95D-09	-8.16	5.34D-09	-8.27
246	NiCO3 0	.0	3.68D-11	-10.43	3.78D-11	-10.42
248	NiCl +	1.0	1.00D-08	-8.00	7.70D-09	-8.11
249	NiCl2 0	.0	1.96D-09	-8.71	2.02D-09	-8.70
250	NiSO4 0	.0	1.10D-08	-7.96	1.13D-08	-7.95

252	AgBr 0	.0	1.47D-10	-9.83	1.52D-10	-9.82
253	AgBr2 -	-1.0	2.67D-11	-10.57	2.05D-11	-10.69
254	AgCl 0	.0	9.21D-09	-8.04	9.48D-09	-8.02
255	AgCl2 -	-1.0	8.88D-08	-7.05	6.82D-08	-7.17
256	AgCl3 2-	-2.0	1.47D-08	-7.83	5.14D-09	-8.29
257	AgCl4 3-	-3.0	6.57D-09	-8.18	6.14D-10	-9.21
261	AgI 0	.0	2.22D-10	-9.65	2.29D-10	-9.64
262	AgI2 -	-1.0	2.91D-12	-11.54	2.23D-12	-11.65
265	AgSO4 -	-1.0	2.44D-12	-11.61	1.87D-12	-11.73
278	HCO3 -	-1.0	4.18D-03	-2.38	3.21D-03	-2.49
279	H2CO3 0	.0	4.40D-03	-2.36	4.53D-03	-2.34
329	V(OH)3 0	.0	2.40D-20	-19.62	2.47D-20	-19.61
330	VSO4 +1	1.0	3.21D-29	-28.49	2.46D-29	-28.61
333	V(OH)3 +	1.0	9.40D-14	-13.03	7.22D-14	-13.14
339	VOSO4 0	.0	7.99D-15	-14.10	8.22D-15	-14.09
340	VOCl +1	1.0	2.11D-15	-14.68	1.62D-15	-14.79
341	H3VO4 0	.0	3.02D-09	-8.52	3.11D-09	-8.51
342	H2VO4 -	-1.0	1.04D-06	-5.98	7.98D-07	-6.10
343	HVO4 2-	-2.0	3.16D-08	-7.50	1.10D-08	-7.96
345	V2O7 -4	-4.0	1.37D-13	-12.86	2.02D-15	-14.69
357	VO2SO4 -	-1.0	3.57D-13	-12.45	2.74D-13	-12.56
374	AgNH3+	1.0	2.29D-14	-13.64	1.76D-14	-13.75
375	Ag(NH3)2	1.0	2.86D-17	-16.54	2.19D-17	-16.66
387	AuCl 0	.0	7.89D-14	-13.10	8.12D-14	-13.09
388	AuCl2 -	-1.0	1.52D-10	-9.82	1.17D-10	-9.93
397	AuOH 0	.0	2.75D-13	-12.56	2.84D-13	-12.55
398	Au(OH)2-	-1.0	5.85D-11	-10.23	4.50D-11	-10.35
410	AuI2 -	-1.0	1.93D-10	-9.71	1.48D-10	-9.83
449	SbO2 -	-1.0	3.08D-13	-12.51	2.37D-13	-12.63
450	SbOOH 0	.0	8.98D-08	-7.05	9.25D-08	-7.03
459	BiO +	1.0	3.21D-08	-7.49	2.47D-08	-7.61
461	Bi(OH)3	.0	1.16D-09	-8.93	1.20D-09	-8.92

---- LOOK MIN IAP ----

PHASE	LOG IAP	LOG KT	LOG IAP/KT
Calcite	-10.0690	-8.4749	-1.59
Gypsum	-6.3167	-4.5800	-1.74
Dolo-ord	-19.1999	-17.0900	-2.11
Magnesit	-9.1309	-8.0300	-1.10
Epsomite	-5.3867	-2.1400	-3.25
Halite	-2.2802	1.5800	-3.86
Tenorite	4.4805	7.6200	-3.14
NiCO3	-13.9921	-6.8400	-7.15
Ni(OH)2	5.0271	10.8000	-5.77
Cerargyr	-11.2932	-9.7500	-1.54
Iodyrite	-16.2407	-16.0700	-.17
Au_Metal	-23.4428	-28.6000	5.16
Sb(OH)3	-5.8547	-5.9300	.08
Sb2O4	14.2841	5.7400	8.54
BiOCl	-7.3612	-6.4000	-.96
CO2(gas)	-19.0209	-18.1500	-.87
O2(gas)	51.9772	83.1200	-31.14
CH4(GAS)	-122.9784	-41.0800	-81.90

Title: Mt. Gibson Waters

Correlation Matrix

No. of samples: 50

	pH	HCO_3	SO_4	Cl	Br	I	NO_3	Na	K	Mg	Ca	Al	Ba	Cr	Fe^{2+}	Mn	Ni	Sr	Ag	Cd	Co	Cu	Pb	Zn	Si	Au	V	Bi	Sb
pH	1																												
HCO_3	0.51	1																											
SO_4	0.13	0.05	1																										
Cl	0.12	0.07	1.00	1																									
Br	0.13	0.06	1.00	0.99	1																								
I	0.23	0.54	0.16	0.19	0.17	1																							
NO_3	0.24	0.15	-0.09	-0.11	-0.10	-0.37	1																						
Na	0.12	0.08	0.99	1.00	0.99	0.20	-0.11	1																					
K	0.15	0.03	0.99	0.98	1.00	0.14	-0.07	0.97	1																				
Mg	0.13	0.07	1.00	1.00	1.00	0.18	-0.10	0.99	0.99	1																			
Ca	0.15	0.34	0.46	0.53	0.43	0.33	-0.13	0.56	0.36	0.48	1																		
Al	-0.65	-0.17	0.05	0.07	0.05	-0.02	-0.14	0.06	0.03	0.06	-0.02	1																	
Ba	0.28	0.31	-0.07	-0.06	-0.06	0.28	-0.21	-0.06	-0.06	-0.05	0.03	-0.02	1																
Cr	0.11	0.07	0.91	0.88	0.92	0.06	0.03	0.86	0.94	0.90	0.17	0.13	-0.05	1															
Fe^{2+}	-0.08	-0.16	0.05	0.07	0.05	0.23	-0.21	0.08	0.03	0.06	0.18	0.01	0.06	-0.05	1														
Mn	0.17	0.13	0.91	0.89	0.92	0.32	-0.18	0.87	0.93	0.91	0.31	0.09	0.13	0.90	0.15	1													
Ni	-0.38	-0.15	0.66	0.65	0.67	0.06	-0.18	0.64	0.66	0.66	0.13	0.73	-0.03	0.71	0.04	0.68	1												
Sr	0.23	0.29	0.85	0.87	0.83	0.42	-0.07	0.88	0.80	0.85	0.71	0.05	-0.04	0.69	0.08	0.74	0.48	1											
Ag	0.09	-0.05	0.93	0.93	0.93	0.02	-0.04	0.92	0.93	0.93	0.33	0.07	-0.11	0.85	-0.07	0.80	0.64	0.72	1										
Cd	0.04	-0.06	0.92	0.89	0.93	0.11	-0.10	0.87	0.95	0.91	0.18	0.17	-0.05	0.94	0.13	0.93	0.76	0.68	0.84	1									
Co	-0.35	-0.16	0.69	0.69	0.70	0.14	-0.22	0.68	0.69	0.70	0.20	0.69	-0.01	0.70	0.27	0.72	0.96	0.54	0.63	0.78	1								
Cu	-0.56	-0.19	0.14	0.13	0.13	-0.08	-0.09	0.12	0.13	0.14	-0.08	0.61	-0.06	0.24	0.05	0.14	0.56	0.06	0.20	0.28	0.51	1							
Pb	0.04	0.03	0.58	0.55	0.59	0.11	-0.23	0.54	0.59	0.56	0.09	0.12	-0.05	0.61	-0.08	0.56	0.53	0.42	0.52	0.68	0.45	0.28	1						
Zn	0.11	0.10	0.05	0.04	0.05	0.04	0.18	0.04	0.06	0.05	-0.04	0.04	-0.06	0.07	0.02	0.06	0.07	0.05	0.03	0.07	0.06	0.00	0.03	1					
Si	-0.27	-0.26	-0.33	-0.35	-0.32	-0.33	0.20	-0.36	-0.29	-0.34	-0.53	0.19	-0.16	-0.18	-0.28	-0.37	-0.02	-0.38	-0.26	-0.24	-0.09	-0.02	-0.19	-0.01	1				
Au	-0.10	-0.17	-0.02	-0.03	-0.03	-0.04	-0.12	-0.03	-0.03	-0.03	-0.05	-0.01	-0.10	-0.03	0.47	-0.06	0.04	-0.05	-0.03	0.10	0.11	0.43	0.13	-0.08	-0.11	1			
V	0.42	0.13	-0.21	-0.22	-0.21	-0.17	0.10	-0.24	-0.18	-0.20	-0.16	-0.09	-0.02	-0.13	-0.16	-0.16	-0.10	-0.16	-0.20	-0.18	-0.15	-0.21	-0.17	0.02	0.12	-0.03	1		
Bi	0.19	0.28	0.00	0.01	0.01	0.25	-0.02	0.01	-0.01	0.01	0.12	-0.10	0.04	0.01	0.27	0.14	-0.04	0.00	0.00	0.00	-0.01	-0.17	-0.04	-0.10	-0.45	-0.04	0.20	1	
Sb	0.07	-0.02	-0.20	-0.21	-0.19	0.21	-0.03	-0.21	-0.18	-0.19	-0.25	-0.02	0.14	-0.12	0.02	-0.08	-0.01	-0.23	-0.19	-0.08	-0.05	0.09	-0.02	0.05	-0.02	0.13	0.17	0.30	1